AN EXPERIMENTAL INVESTIGATION INTO PERFORMANCE OF A NANOREFRIGERANT (R134a+CuO) BASED DOMESTIC VAPOUR COMPRESSION REFRIGERATION SYSTEM

Submitted in partial fulfillment of requirement for the award

Degree of

Master of Engineering

In

M.E Thermal

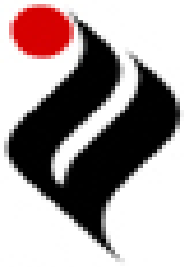

Submitted By:

Qasim Kadhim Salman

(ROLL NO.801283022)

Under the supervision of:

Mr. Kundan Lal, Assistant Professor

DEPARTMENT OF MECHANICAL ENGINEERING

THAPAR UNIVERSITY

Patiala-147004 (Punjab) India, July 2014

Established under section 3 of UGC Act, 1956 vide notification # F-12/84-U-.3

Government of India

DECLARATION

I hereby declare that thesis entitled **"An Experimental Investigation into Performance of Nanorefrigerant (R134a+CuO) Based Domestic Vapour Compression Refrigeration System"** is an authentic record of my study carried out as requirements for award of degree of **M.E. (Thermal Engineering)** at **Thapar University, Patiala,** under the guidance of **Mr. Kundan Lal,** Assistant Professor Department of Mechanical Engineering, Thapar University, Patiala during **August 2013 to July 2014.** The matter embodied in this thesis has not been submitted in part or full to any other university or institute for award of any degree.

(QASIM KADHIM SALMAN)

This is to certify that above declaration made by the student concerned is correct to best of my knowledge and belief.

(Mr. KUNDAN LAL)
Assistant Professor, MED
Thapar University
Patiala-147004

Countersigned by

(Dr. AJAY BATISH)
Professor and Head
Department of Mechanical Engineering
Thapar University
Patiala-147004

(Dr. S.K. MOHAPATRA)
Senior Professor, MED
Dean of Academic Affairs
Thapar University
Patiala-147004

ABSTRACT

The performance of the refrigeration system depends upon the heat transfer characteristics of the refrigerant being used. The present study on an experimental investigation into the performance of a nanorefrigerant (R134a + CuO) based refrigeration system is conducted at the Mechanical Engineering Department, Thapar University, Patiala. Refrigerant, R134a is one of the commonly used refrigerants in many refrigeration applications but it has been observed that its heat transfer characteristics are poor which thereby limits its performance. In our experimental study an attempt has been made to improve its performance by mixing nanoparticles (CuO) into the refrigerant R134a. Copper oxide (CuO) nanoparticles are used to enhancing the heat transfer capacity of R134a refrigerant in the refrigeration system because of its improved thermal conductivity. In these experiment investigations nanofluids are prepared by using CuO as nanoparticles (size 20 nm) in the base fluids which is R134a refrigerant at various concentrations (0.25 % to 2 %) with an increase of 0.25% of volume fraction in each step. Effect of various parameters like heat flux, cooling load in evaporator, mass flow rate of nanorefrigerant (R134a+CuO) with varied volume fraction of CuO nanoparticles in base refrigerantR134a have been investigated. The performance enhancement of a domestic refrigerator is investigated by using CuO nanorefrigerants. It has been observed that the addition CuO of nanoparticles to the R134a refrigerant results in improvements in the thermo-physical properties and heat transfer characteristics of the refrigerant, thereby improving the performance of the refrigeration system. Stable nanorefrigerant (R134a+CuO) has been prepared for the study and the experimental studies indicate that the refrigeration system with nanorefrigerant works normal. The results show that there is a marginal increase in pressure drop up to 2 kpa in both condenser and evaporator. But, there is a significant increase in temperature drop (19%) with increase in volume fraction (1.25%) in condenser side and it is found to be 14 % in evaporator side at same volume fraction at constant heat flux in the evaporator at 35°C. It has been also observed that the freezing capacity of the system is increased by 18.27 % at 1.25 % of volume fraction for 10 LPH of mass flow rate and a 22 % increase is observed at 1.25 % volume fraction at mass flow rate of 15 LHP. Power consumption of the system is found to be reduced by 13 % at volume fraction of 1.25 % and an improvement in COP is by 20 % in comparison to COP of a pure R134a

refrigerant. Suitable concentration range of nanoparticles (CuO) for the conducted experimental investigation s is found to be 1-1.25 % for the best results.

Keywords:

Copper oxide nanoparticle, nanorefrigerant, thermo-physical properties, freezing capacity, pressure and temperature drop, condenser and evaporator, COP, energy consumption and optimum CuO concentration.

ACKNOWLEDGEMENT

At first, I would like to thank our God for all good deeds, second thanks to the people of India, Govt of India and Govt of Iraq almighty for his abundant blessing showered on me throughout this endeavour to complete this work successfully.

My honorable guide **Mr. Kundan Lal**, Assistant Professor, Department of Mechanical Engineering, is a person to whom I shall always remain grateful for his excellent guidance, valuable discussions, encouragement, constructive criticism and his insights have strengthened this study significantly. He gave me a complete freedom to use my opinion, correcting whenever necessary in my dissertation.

I would like to thank our Head of the Department, **Dr. Ajay Batish**, and **Dr. S.K Mohapatra** Dean of Academic Affairs, also **Mr. Gurpinder singh** Deputy/ asstt. Registrar of Thapar University Patiala, who has been supportive at all times and accommodative.

I would like to thank to all faculty members and employees of Mechanical Engineering Department, Thapar University, and Patiala for everlasting support.

My heartfelt thanks are due to all the Faculty and staff members specially **Mr. Charanjeet Singh**, **Mr. Kuldeep Singh** (Technicians) of the Mechanical Engineering Department, Thapar University Patiala for providing the necessary instrumentation facility for carrying out the research work.

I would also like to thank **TEQIP- II** for providing me grant and funds for carrying out research work.

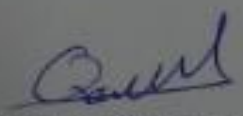

Qasim Kadhim Salman

CONTENTS

LIST OF FIGURES **PAGE NO.**

LIST OF TABLES **PAGE NO.**

NOMENCLATURE

Symbol	Description	Unit
A	Cross sectional area	m^2
Cp	Specific heat	J/Kg k
D	Diameter	m
h	Enthalpy	KJ/Kg
hfg	Latent heat of vaporization	w/m k
K	Thermal conductivity	w/m k
m	Mass flow rate	Kg/s
T	Temperature	°C
v	Velocity	m/s
Greek symbols		
σ	Surface tension	N/m
ρ	Density	Kg/m^3
μ	Dynamic viscosity	Kg/ms
ω	Nanoparticle concentration in the nanoparticle oil suspension	
Ψ	Volume fraction of nanoparticle in the nanoparticle/oil volume fraction suspension	
Subscripts		
F	liquid	
g	gas	
n	nanoparticle	
o	oil	
r	refrigerant	
n,o	nanoparticle and oil	

r,o	refrigerant and oil
r,n,o	refrigerant, nanoparticle and oil

Abbreviation

CuO	Copper oxide
HTC	Heat transfer coefficient
TR	Ton of refrigeration
COP	Coefficient of performance
HRF	Heat rejection factor
MWCNT	Multi-walled carbon nanotubes
PCS	Photon correlation spectroscopy
PLC	Programmable logic controller
SANS	Small angle neutron scattering
SAXS	Small angle x-ray scattering
SEM	Scanning electron microscopy
SPM	Scanning probe microscopy
TEM	Transmission electron microscopy
TiO_2	Titanium oxide
XRD	X-Ray diffraction
XPCS	X-ray photon correlation spectroscopy

CHAPTER-1

INTRODUCTION

It is true that quick industrialization has led to unparallel growth, development and technological progression across the globe. It has also given rise to a number of new concerns. Today' global warming and ozone layer depletion on the one hand and spiraling oil prices on the other hand have become main challenges. Excessive use of fossil fuels is leading to their sharp diminution and nuclear energy is not out of harm's way. In the face of imminent energy resource crunch there is need for developing thermal systems which are energy efficient. Thermal systems like refrigerators and air conditioners consume large amount of electric power. So avenues of developing energy efficient refrigeration and air conditioning systems with nature friendly refrigerants need to be explored The rapid advances in nanotechnology have lead to emerging of new generation heat transfer fluids called nanofluids. Nanofluids are prepared by suspending nanoparticles sized (1-100nm) in conventional fluids and have higher thermal conductivity than the base fluids. Nanofluids have the following characteristics compared to the normal solid liquid suspensions.

(i) Higher heat transfer between the particles and fluids because of the high surface area of the particle

(ii) Better diffusion stability with predominant Brownian motion

(iii) Reduces particle obstruction

(iv) Reduced pumping power as compared to base fluid to obtain correspondent heat transfer.

Based on the applications, nanoparticles are currently made out of a very extensive variety of materials, the most common of the new generation of nanoparticles being ceramics. Which are better split into metal oxide ceramics, such as titanium, zinc, aluminum and iron oxides, to name a prominent few and silicate nanoparticles, generally in the appearance of nanoscale flakes of clay. Addition of nanoparticles transforms the boiling characteristics of the base fluids. Nanoparticles can be used in refrigeration systems because of its significant improvement in

thermo physical and heat transfer potentials to enhance the performance of refrigeration systems. In a vapour compression refrigeration system the nanoparticles can be added to the lubricant (compressor oil). When the refrigerant is circulated through the compressor it carries tinges of lubricant + nanoparticles mixture call nanolubricants so that the other components of the system will have nanolubricant-refrigerant mixture or mixture with the refrigerant openly and injection to system by charge to compressor this call nanorefrigerant.

1.1 Nanofluids

Nanofluids (nanoparticle fluid postponements) is the term coined by (Choi et al.,1995) to describe this new class of nanotechnology based heat transfer fluids that exhibit thermal properties superior to those of their host fluids or conventional particle fluid suspension. When a small amount of nanoparticles, are added in the base fluids, can provide a dramatic change in the properties of base fluids. Nanofluids are engineered by suspending nanoparticles with the average size below 100 nm in conventional heat transfer fluids such as water, oil, ethylene glycol and refrigerant. Nanofluid technology is a new inter field of great important, where nanotechnology, nanoscience and thermal engineering was meeting. The aspire of the nanofluids is to achieve the highest possible thermal properties at smallest possible volume fractions by uniform dispersion and stable suspension of nanoparticles in the base fluids. These nanoparticles can possess properties that are significantly different from their parent materials like CuO possesses different properties from Cu. There are three methods of generating these nanofluids are available: creating them from chemical precipitation, buying the nanoparticles in powder form and mix them with the base fluid, and direct buying of prepared nanofluids.

1.2 Importance of nanosize in nanofluid

The mean problem with the use of large particles is the slow settling of these particles in fluids. Other problems are scrape and clogging to the pipes through which they are made to flow. These problems are highly undesirable for many practical cooling and heating applications. The nanofluids are leaders in overcoming these problems because nanoparticles get stabled at nanoscale quite than the millimeter or micrometer sized particles. Compared with micro particles the nanoparticles balanced for a longer time and possess a much higher surface area. The ratio surface/volume of nanoparticles is 1000 times larger than that of microparticles. The high surface area of nanoparticles effects the heat conduction of nanofluids since heat transfer occurs on the

surface of the particle. Other benefits of using nanoparticles include reduced pumping power, reduced inventory of heat transfer fluids and high significant energy savings.

In the nanofluids the size is the most important factor because it is used to raise the thermal properties as well as the suspension stability of the nanoparticles. The nanotechnology offers excellent forecast for producing a new type of heat transfer fluid that has an excellent thermal properties and cooling capacity. Table 1.1 contrasts postponement of microparticles and nanoparticles and shows the benefits of nanofluids containing nanoparticles. Other factors which influence the thermo physical properties of nanofluids are: shape, material, base fluid, surfactants, temperature, volumetric concentration, dispersants, pH value etc.

Table 1.1 Comparison of microparticles and nanoparticles.

	Microparticles	**Nanoparticles**
Stability	Settle	Stable (remain in suspension almost indefinitely)
Surface/volume ratio	1	1000 times larger than that of microparticles
Thermal conductivity	Low	High
Clog to microchannel	Yes	No
Erosion	Yes	No
Pumping power	Large	Small
Nanoscale phenomena	No	Yes

The above table shows that thermal conductivity, stability and surface/volume ratio of nanoparticles is more than the microparticles and there is least problem of clogging and wearing away in nanoparticles at the same volume fraction in base fluids.

1.3 Manufacturing of nanofluids

There are generally two methods which are used to fabricate nanoparticles 1) Physical process. 2) Chemical process. The physical process includes inert gas condensation process and mechanical grinding. Chemical processes include chemical vapour deposition, chemical precipitation, micro emulsions, and thermal spray and spray paralysis. Stable and highly conductive nanofluids are produced by one and two step production methods.

The two step method first made nanoparticles by using either physical or chemical process and then disperses them in the base fluid. The one step method simultaneously makes and disperses nanoparticles directly into the base fluid. In two step method, to create a stable suspension is one of the key issue, as in this method the particles, they have tendency into agglomerate.

1.4 Materials for nanoparticles and base fluid

Nanostructure or nanophase materials are made of nanometer sized matters engineered on the atomic or molecular scale to produce either new material or enhanced physical properties, which are not exhibited by conservative bulk solids. So the particles smaller than 100 nm exhibit different properties as compared with the conventional solids. The thermal, mechanical, optical, magnetic and electrical properties of nanophase materials are more superior than those materials have uncouth grain structure.

Materials for nanoparticles and base fluids are diverse:

1. Nanoparticle materials include:

- Oxide ceramics – Al_2O_3, CuO
- Metal carbides – SiC
- Nitrides – AlN, SiN
- Metals – Al, Cu
- Nonmetals – Graphite, carbon nanotubes
- Layered – Al + Al_2O_3, Cu + C
- PCM – S/S

2. Base fluids include:

- Water
- Ethylene- or tri-ethylene-glycols, refrigerant other coolants
- Oil and other lubricants
- Bio-fluids
- Polymer solutions
- Other common fluids

2 Nanorefrigerant vapor compression refrigeration system

2.1 Nanorefrigerant

Recently scientists are using nanoparticles in refrigeration systems because of its extraordinary improvement in thermo-physical, and heat transfer capabilities to enhance the efficiency and dependability of refrigeration and air conditioning system. In general, performance of any refrigerant undergoes from its poor heat transfer properties like other conventional thermo fluids. Maxwell initiated a work of fiction concept of dispersing solid particles in base fluids to break the fundamental limit of heat transfer fluids having low thermal conductivities. Most of these previous studies on this concept used millimeter or micrometer solid particles, which lead to major problems such as express settling of the solid spherical particles in the fluids, clogging in micro channels and surface scrape. In addition, the high pressure drop caused by these particles limited their practical applications. Nanorefrigerants are established to have good potential to overcome these problems. By using nanoparticles in refrigeration system, three main advantages can be obtained:

(i) Nanoparticle as additive can enhance the solubility between the lubricant and the refrigerant.

(ii) Thermal conductivity and heat transfer characteristics of the refrigerant can be increased.

(iii) Nanoparticles diffusion into lubricant may decrease the friction coefficient and wear rate.

Elcock et al., 2011 originate that TiO_2 nanoparticles can be used as additives to enhance the solubility of the mineral oil with the hydro-fluorocarbon (HFC) refrigerant. Authors also described that refrigeration systems using a mixture of R134a and mineral oil with TiO_2 nanoparticles appear to give better performance by returning more lubricant oil to the compressor with similar performance to systems using R134a and POE oil. Hindawi et al. (2010) carried out an experimental study on the boiling heat transfer characteristics of R22 refrigerant with Al_2O_3 nanoparticles and originate that the nanoparticles enhanced the refrigerant heat transfer characteristics with reduced bubble sizes. Eastman et al. (2012) mixed Al_2O_3 nanoparticles in PAG oil as nanorefrigerant R134a vapour compression refrigeration system. An experimental setup was designed and fabricated in the lab work. The system performance was considered using energy consumption test and freeze capacity test. The obtain results indicate that Al_2O_3 nanorefrigerant operates normally and safely in the refrigeration system. The refrigeration system performance was improved than pure lubricant with R134a working fluid with 10.32% less energy used with 0.2%Vol. of the concentration used. The results indicate that

heat transfer coefficient improves with the usage of nanoparticles Al_2O_3. Thus using Al_2O_3 nanorefrigerant in refrigeration system is found to be feasible. Eastman et al. (2007) investigated the pool boiling heat transfer characteristics of R11 refrigerant with TiO_2 nanoparticles and explained that the heat transfer enhancement reached 20% at a particle loading of 0.01 g/L. Liu et al. (2009) shows investigated the effects of carbon nanotubes (CNTs) on the nucleate boiling heat transfer of R123 and R134a refrigerants. Authors obtained that (CNTs) increase the nucleate boiling heat transfer coefficients for these refrigerants. Authors noticed large enhancements of up to 36.6% at low heat fluxes of less than (30 kW/m^2). Thus, the use of nanoparticles in refrigeration systems is a new, innovative way to enhance the efficiency and dependability in the refrigeration system.

From the number of reviews on thermal and rheological properties, different modes of heat transfer of nanofluids have been reported by many researchers. However, to the best of authors' knowledge, there is no complete literature on the nanoparticles as additives with conventional refrigerants directly and oils used in refrigeration system. It is authors' hope that this review will be useful to fill recognized research gaps and to overcome the challenges of nanorefrigerant. The nanofluid is a new type of heat transfer fluid by suspending nanoscale materials nanoparticles in a conventional host fluid and has higher thermal conductivity than the conventional host fluid is a refrigerant as R11, R22, R600 and R134a.

2.2 Thermal conductivity of nanorefrigerant

Different concentrations of nanoparticles of CuO, Al_2O_3, SiO_2, CNT, and TiO2 were used in base refrigerants such as R11, R113, R600, R123, R134a, and R141b as found in the available literatures. Thermal conductivity enhancement of some refrigerants with nanoparticles. A nanorefrigerant has higher heat transfer coefficient than the host refrigerant and it can be used to improve the performance of refrigeration systems. The nanofluid is a new type of heat transfer fluid by suspending nanoscale materials in a conventional host fluid and has higher thermal conductivity than the conventional host fluid. The nanorefrigerant is one kind of nanofluid and its host fluid is a refrigerant. The heat transfer coefficient of a fluid with higher thermal conductivity is bigger than that of a fluid with lesser thermal conductivity if the Nusselt numbers of them are the same. Therefore, researches on improving thermal conductivities of nanorefrigerants are important. There are two methods to improve the thermal conductivity of a nanorefrigerant. The first one is to enhance the volume fraction of nanoscale. Materials in the

nanorefrigerant and the second one are to use nanoscale materials with high thermal conductivity.

2.3 Vapour compression refrigeration system

Command for the refrigeration and air conditioning is needed day by day. In the energy consuming world there is use of artificial appliances in the world. Manufacturing as well as in the homes there is need for the control of the environment for human as well as for manufacturing products. This is met by the refrigeration and air conditioning. Vapour compression refrigeration is the systems in the middle of the most used for this purpose. In this there is use of refrigerant as the base fluid. Refrigerant properties and the available technology guide the layout and the system which is present today. Technology also improves time by time and made the alterations in the system all around the world. Recently there is use of nanoparticles in the thermal systems. There is scope of using nanoparticles in the vapour compression refrigeration cycle. Now in this time, in refrigeration equipment R134a is used as a refrigerant. Traditional mineral oil is avoided as a lubricant due to the strong chemical polarity of R134a in refrigeration equipment. POE oil as a lubricant also has the problems of flow choking and severe friction in the compressor. So nanoparticles can be used to enhance the working fluid properties and energy efficiency of the refrigerating system associated with reduction in CO_2 emission. Sheng et al. (2008) investigated the performance of the refrigerator using R134a and POE oil as the base data and then compared using R134a and mineral oil, and with different nanoparticles of TiO_2 and Al_2O_3 with the same and different mass fractions with R134a for the same tests. Routbort et al. (2010) employed nanofluids for industrial cooling and showed great energy savings and resulting emission reductions. They showed that replacement of cooling and heating water with nanofluids has the potential to conserve about 300 million kWh of energy for industries. For the electric power industry using nanofluids could save about 3000-9000 million kWh of energy per year which is equivalent to the annual energy consumption of about 50,000-150,000 households. The associated emission reductions would be approximately 5600 million kg of carbon dioxide, 8.6 million kg of nitrogen oxides and 21 million kg of sulfur dioxide.

CHAPTER-2

LITERATURE SURVEY

2.1Literature survey of nanofluids

2.1.1 Introduction

Nanofluid research could lead to a major breakthrough in developing next generation coolants for the number of engineering applications. Better aptitude to manage the thermal properties translates into greater energy efficiency, smaller and greater thermal systems and lowers the operating costs. Many studies on nanofluids were carried out by many researchers in the past.

This chapter reviews the previous published literatures, which positions foundation and basic for further work in these investigations.These dues to give a better understanding about the topic and also acts as a guideline for this thesis. The minor focus of the following study is on the nanofluids and to check the viscous behavior with various fluids and thermal conductivity. This section deals with literature review on nanofluids, its preparation and characterization, thermo physical properties of nanofluids.

2.1.2 Thermo physical properties of nanofluids

Nanofluids were found to exhibit thermo physical properties such as higher thermal conductivity, thermal diffusivity and viscosity than those of base fluids. Heat transfer enhancement in a solid fluid two phase flow has been investigated for many years ago. Research on gas particle flow seen that by adding particles, particularly small particles in gas, the convection heat transfer coefficient can be significantly increased. The enhancement of heat transfer, in case addition to the possible increase in the efficient thermal conductivity was mainly due to the reduced thickness of the thermal boundary layer. In the processes involving liquid vapor phase change, particles may also reduce the thickness of the gas layer near the wall. The particles used in the previous studies were on the scale of a micrometer or larger. It is very likely that the motion of nanoparticles in the fluid will also enhance heat transfer. Therefore, more studies are needed on heat transfer enhancement in nanoparticle-fluid mixtures. Thermal conductivities of nanoparticle-fluid mixtures have been reported by Masuda et al. (1993), Eastman et al. (2001) adding a small volume fraction of metal or metal oxide powders in fluids increased the thermal conductivities of the particle fluid mixtures over those of the base fluids.

The viscosity of nanofluids, which is one of the key influencing factors in heat transfer, has not received as much attention so far. The experimental and simulation results indicate that nanoparticle size is of crucially important to the viscosity of the nanofluid, as the nanoparticle size increases or changes. Although viscosity influences interfacial phenomena and flow characteristics, very few studies have been performed on the effective viscosity of nanofluids as a function of volumetric loading of nanoparticles. The primary results from these studies indicate that the viscosity of a nanofluid increases with increasing nanoparticle volume fraction. In addition to the very few experimental studies have been carried out, few theoretical models are available for the prediction of the effective viscosity of nanofluids as a function of temperature and particle volume fraction. But they lack in consistency. It is worthwhile to study temperature dependent viscosity and thermal conductivity of nanofluids for their potential applications especially in nanofluids systems.

2.1.3 Nanofluids preparation and characterization

2.1.3.1 Preparation of nanofluids

Preparation of nanofluids is the first step in experimental studies with nanofluids. Nanofluids are not simply liquid-solid mixtures only. Some important special requirements are essential e.g. even and fixed suspension, durable suspension, negligible agglomeration of particles, no any chemical change of the fluid, etc. Nanofluids are produced by dispersing nanometer scale solid particles into base liquids such as water, ethylene glycol, oils, refrigerant, etc. There are mainly two techniques used to produce nanofluids.

1. Single-step method
2. Two-step method

Single step method: The single step direct evaporation approach was urbanized by (Akoh et al. 2006) and it is called the VEROS (Vacuum Evaporation onto a Running Oil Substrate) technique. The original design of this method was to produce nanoparticles, but it is difficult to subsequently separate the particles from the fluids to produce dry nanoparticles. A modified VEROS process was developed by (Wagener et al. 2008). They in employment high pressure magnetron sputtering for the preparation of suspensions with metal nanoparticles such as Ag, Cu and Fe. Eastman et al. (2001) also developed a modified VEROS technique, that Cu vapour is

directly condensed into nanoparticles by contact with a flowing low vapor pressure liquid (Ethylene Glycol). A vacuum SANSS (submerged arc nanoparticle synthesis system) method has been employed by (Lo et al. 2010) to prepare Cu particles based nanofluids with different dielectric liquids such as de ionized water, with 30%, 50%, 60% volume solutions of ethylene glycol and pure ethylene glycol. Different morphologies, which are got, are mainly influenced and resolute by the thermal conductivity of the dielectric liquids. CuO, Cu_2O, and Cu based nanofluids also can be prepared by this technique. An advantage of the one-step technique is that nanoparticle agglomeration is minimized, while the disadvantage is that only low vapor pressure fluids are companionable with such a process. Recently, a Ni nanomagnetic fluid was also produced by (Lo et al., 2010) using the SANSS method.

Two step method: R.A. Buhrman set up the two- step process. In this firstly, nanoparticles are produced as a dry powder, characteristically by inert gas condensation. The second step involves dispersion of dry nanoparticle powder into a base fluid, like water, oil, ethylene glycol and refrigerant. Romano et al. (1998) reported an advantage of the two-step process is that the inert gas condensation technique has been scaled up to profitable nanopowder production. A deficiency of this method is the tendency of nanopowder to agglomerate through storage and dispersion in the base fluids, particularly with heavier metallic nanoparticles. Surfactants and other surface stabilization additives can be used to complete more homogeneous and more stable suspensions. In addition to mechanical homogeneous mixing, also ultra-sonic mixers can be used to break up agglomerates and give more uniform dispersions.

2.1.3.2 Characterizations of nanofluids

Illustration analysis of nanofluids is done using electron microscope (SEM/TEM, TEM being preferred over SEM for nanofluids) and most of the reported studies makes use of TEM for characterizing nanofluids. Cryogenic transmission electron microscopy might give a powerful characterization method, but little laboratories are prepared to apply this technique. Scanning probe microscopy (SPM) has not get much use for characterizing nanofluids. A basic approach makes use of particle size analyzer based on dynamic light scattering (DLS). Robert et al. (2006) used DLS systems for particle size distribution to supplement the results with TEM as main characterization tool. A important characterization tool for the structure of suspensions at

nanoscale is the small angle x-ray scattering (SAXS) and small angle neutron scattering (SANS). In these techniques a nanofluid is clarified by a collimated x-ray or neutron beam and the intensity of scattering is checked as a function of angle. Lurio et al. (2004) measured the equilibrium dynamics by using a relatively recent x-ray scattering technique is called x-ray photon correlation spectroscopy (XPCS), which is based on the traditional laser based on photon correlation spectroscopy (PCS). In the XPCS technique a sample is illuminated with a fully coherent x-ray beam; in preference to the more characteristic situation in which the incident x-rays consist of a more number of incoherent regions. The consequence of coherent illumination is to be obtaining a speckle pattern superimposed on the usual SAXS pattern.

2.2 Literature survey of nanorefrigerant

2.2.1 Introduction

Nanorefrigerant is one type of nanofluids. This is mixed of nanoparticles with refrigerants. It has higher heat transfer performance than traditional pure refrigerants. Also, some researchers have been done about nanorefrigerants. Most of them were related to thermal conductivity of these fluids. Viscosity also deserves as increase consideration as thermal conductivity. Pumping power consumption and pressure drop depends on viscosity. Convective heat transfer is important in the HVAC, refrigeration and microelectronics cooling applications. R134a is most extensively adopted alternate refrigerant in refrigeration systems, such as domestic refrigerators and air conditioners. While the global warming up potential of R134a is relatively high, it is acknowledged that it is a long term alternate refrigerants in lots of countries. The adding of nanoparticles to the refrigerant results in improvements in the thermo-physical properties and heat transfer characteristics of the refrigerant, thereby improving the performance of the refrigeration system.

Pawl et al. (2005) achieved studies on nanofluids and found that there was the significant increase in the thermal conductivity of nanofluid compared to the base fluid. They also found that addition of nanoparticles results in significant increased in the critical heat flux.

Bi et al. (2007) achieved studies on a domestic refrigerator using nanorefrigerants. In their studies R134a was used the refrigerant, and a mixture of mineral oil TiO_2 was used as the lubricant. They found that the refrigeration system with the nanorefrigerant worked normally and efficiently and the energy consumption reduces by 21.2%. When compared with R134a+POE oil

system. Also, Bi et al. (2008) found that there was remarkable reduction in the power consumption and significant improvement in freezing capacity. They pointed out the improvement in the system performance is due to better thermo physical properties of mineral oil and the presence of nanoparticles in the refrigerant.

Jwo et al. (2009) achieved studies on a refrigeration system replacing R134a refrigerant and polyester lubricant with a hydrocarbon refrigerant and mineral lubricant. The mineral lubricant included added Al_2O_3 nanoparticles to improve the lubrication and heat transfer performance. Their studies show that the 60% R134a and 0.1 vol.% Al_2O_3 nanoparticles were optimal. Under these conditions, the power consumption was reduced by about 2.4%, and the coefficient of performance was increased by 4.4%.

Peng et al. (2010) achieved experimental studies on the nucleate pool boiling heat transfer characteristics of refrigerant and adding to base oil mixture with diamond nanoparticles. The refrigerant used was R113 and the oil was VG68. They found out that the nucleate pool boiling heat transfer coefficient of R113 and oil mixture with diamond nanoparticles was larger than the R113 and oil mixture. They also proposed a general association for predicting the nucleate pool boiling heat transfer coefficient of refrigerant and oil mixture with nanoparticles, which good satisfies their experimental results.

Henderson et al. (2010) achieved an experimental analysis on the flow boiling heat transfer of R134a based nanofluids in a horizontal tube. They found excellent dispersion of CuO nanoparticle with R134a and POE oil and the heat transfer coefficient increases more than 100% over baseline R134a and POE oil results.

Bobbo et al. (2010) achieved a study on the influence of dispersion of single wall carbon nanohorns (SWCNH) and TiO_2 on the tribological properties of POE oil together with the effects on the solubility of R134a at different temperatures. They confirmed that the tribological performance of the base lubricant can be either improved or worsen by adding nanoparticles. On the other hand the nanoparticle dispersion did not affect significantly the solubility of R134a.

Bi et al. (2011) conducted an experimental study on the performance of a domestic refrigerator using TiO_2 and R600a nanorefrigerant as working fluid. They confirmed that the TiO_2 with R600a system worked normally and efficiently in the refrigerator and an energy saving of 9.6%. They too cited that the freezing capacity of nanorefrigerating system was more than that with

pure R600a system. The purpose of this article is to report the results obtained from the experimental performance of nanorefrigerant studies on a vapour compression system.

Wang and Xie (2011) instituted that TiO_2 nanoparticles could be used as additives to improve the solubility between mineral oil and hydro fluorocarbon (HFC) refrigerant. The refrigeration systems using the mixture of R134a and mineral oil appended with nanoparticles TiO_2, appeared to give better performance by rejected more lubricant oil back to the compressor, and had the similar performance compared to the systems using polyolester (POE) and R134a. In the present study the refrigerant selected was R600a and the nanoparticle was alumina (Al_2O_3). Isobutene (R600a) was more widely adopted in domestic refrigerator because of its better environmental and energy performances. A domestic R134a refrigerator was selected as CuO and R134a nanorefrigerant was prepared and used as working fluid. The energy consumption test and freeze capacity test were conducted to compare the performance of the refrigerator with nanorefrigerant and pure R134a refrigerant so as to provide the basic data for the application of the nanoparticles in the refrigeration system.

Table 2.1: Literature survey applications of nanorefrigerant

Reference	Refrigerant+ Nanoparticles	Size	%volume concentration	Parameters finding
Bi et al. 2006	R134a +TiO_2	–	–	Reduction in energy consumption by 7.43%
Park et al. 2007	R123,R134a+ CNT	20nm	1.00%	Heat transfer coefficient enhancement up to 36.6%
Trisaksri et al. 2009	R141b + TiO_2	21nm	0.01%, 0.03%, 0.05%	Nucleate pool boiling heat transfer deteriorated with increasing particle concentrations
Hao et al. 2009	R113 + CuO	40nm	0.15–1.5%	Maximum enhancement of heat transfer coefficient, 29.7%
Peng et al. 2009	R113 + CuO	40nm	0, 0.1%, 0.2%, 0.5%	Frictional pressure drop increased by 20.8%

Kedzierski et al. 2009	R134a + CuO	30nm	0.50%	Enhancement of heat transfer coefficient between 50 % and 275%
Hao et al. 2010	R113+Diamond	10nm	0–0.05%	Nucleate pool boiling heat transfer coefficient increased by 63.4%
Jin et al. 2010	NH_3/H_2O+ Al_2O_3/CNT	–	0.06%/0.08%	Heat transfer rate was 20% higher than those without nanoparticles
Loaiza et al. 2010	H_2O+Cu,Al_2O_3, CuO, TiO_2	10-50nm	1-5%	Reduction in evaporator area Cu ($0.238m^2$), followed by CuO ($0.250m^2$), TiO_2 ($0.251m^2$) and Al_2O_3 ($0.256m^2$) results increase in COP
Subramani et al. 2010	R134a + Al_2O_3	50nm	0.06%	28% time reduction to bring down temperature, 28% reduction in power consumption and 33% increase in COP by nanolubricant
Mahbubul et al. 2011	R123 + TiO_2	-	0.05-1%	Pressure gradient increases rapidly with the increment of volume concentrations compared to vapor quality
Hafez et al. 2011	R134a + CuO	15-70nm	0.1-1%	Heat Transfer Coefficient increases linearly with the increase of heat flux up to 0.55% CuO and increases with CuO nanoparticle size up to 25nm and then decreases with size.
Kumar et al. 2012	R134a + Al_2O_3	50nm	0.20%	10.32% reduction in power consumption and 12% increase in COP by nanolubricant
Kumar et al. 2013	R600a + TiO_2	50nm	0.1-0.5g/L	Energy reduction by 5.94% for 0.1 g/L and 9.6% for 0.5g/L

Lee et al. (2010) investigated the friction coefficient of the mineral oil mixed with 0.1 vol.% fullerene nanoparticles, and the results showed that the friction coefficient decreased by 90% in comparison with raw lubricant, which lead us to the conclusion that nanoparticles can improve the efficiency and reliability of the compressor. The appearance of some modern micro control means, such as atomic force microscope (AFM), friction force microscope (FFM), and scanning tunneling microscope (STM) together with the continuous improvement of the performance, making people could reveal the lubrication mechanism. Lubricating oil additive can improve the using performance of base oil; additives nanoparticles have high load capacity and special lower friction capacity in aspects of lubrication. Nanoparticles in oil have good lubrication properties and antifriction properties. Lubrication made with nanoparticles can observably improve its lubrication performance, load capacity and product quality.

For lubrication mechanism of refrigeration system generally:

(i) Add the so called "active element" to base oil, such as Cl, S, and P etc. the mechanism was forming the physical and chemical adsorption film on friction surface or production inorganic protective film with low melting and low shear strength in the chemical reaction such as FeC_{l3}, FeS, $FePO_4$, etc. but corrosive wear problems inevitably accompany this process at same time.
(ii) The mechanism of nanoparticles additive was effect such as small size effect and surface effect, it was different from above materials. So may have new tribological properties. Tribological aspects of metal are pits and crevice in the metal surface rugged by microscope. The size of pits and cracks are mostly micron level so mechanical processing techniques can not break through this limitation. The below figure of SEM photograph of crankshaft surface.

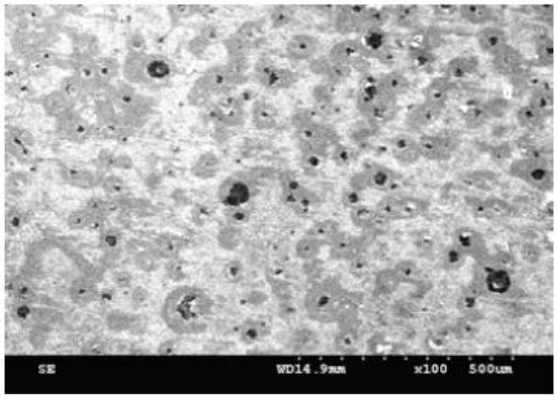

Figure 2.1: Surface microscope **(**Lee et al., 2010)

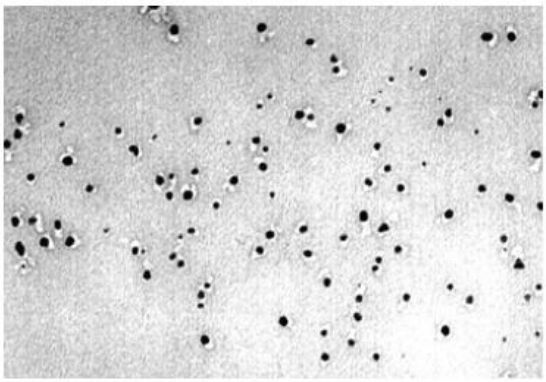

Figure 2.2: TEM Morphology of nanoparticle

The operational principle of nanofluids: metal based ion dispersant in refrigeration oils, which can run along with the oil flow to friction parts, fill the pores of metal surface automatically and gather to repair the metal surface, refer to figure (2.1). The friction reduces since the friction coefficient decreases then increase in output energy of compressor because less losses of friction.

Experiment before and after oil changed in rotary compressor: Firstly, these tests of three samples by inject the common NM 56EP refrigeration oils into the samples; add certain percentage nanoparticles into the refrigeration oil. Table and table are compared in same sample before and after adding nanoparticles to the oil refrigeration and checking the changes in performance.

Table 2.2: Test normal mass compressor

No.	Capacity /W	Power /W	COP/ W/W	Current /W
1	3607	1182	3.05	5.46
2	3633	1194	3.04	5.51
3	3644	1190	3.06	5.49
Average	3628	1189	3.05	5.49

Table 2.3: Test samples with nanofluids

No.	Capacity /W	Power /W	COP/ W/W	Current /W
1	3642	1162	3.13	5.38
2	3661	1173	3.11	5.43
3	3679	1160	3.16	5.37
Average	3661	1165	3.13	5.39

When compared between the samples before and after addition nanofluids, the cooling capacity increased by 33 W, power decreased by 24 W, COP increased by 0.08, the current decreased by 0.09 A as shown in figure 2.3 below.

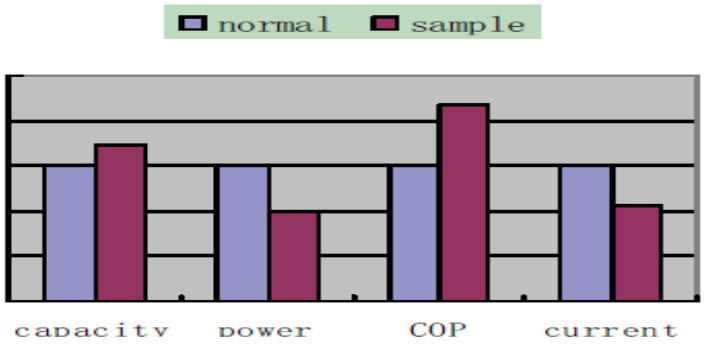

Figure 2.3: Chart of performance change before and after using nanofluids **(**Lee et al., 2010)

Performance before and after of long term life test: The life test of samples when compressor operation at time 1000 hours, R22 as refrigerant, refrigeration oil contained nanofluids in the sealed sample machines. After the life test, compressor performance test result shown table (2.4).

Table 2.4: Life test before and after using nanofluids in rotary compressor (Lee et al., 2010)

Items	sample 2			sample 3		
	Before life test	After life test	Data Contrast	Before life test	After life test	Data Contrast
Capacity/W	3661	3701	+39.8(+1.09%)	3679	3694	+15 (0.41%)
Power/W	1173	1162	-10.9 (-0.93%)	1160	1156	-4.7 (-0.41%)
COP /W/W	3.11	3.18	+0.08 (2.54%)	3.16	3.19	+0.03 (0.85%)
Current/A	5.43	5.30	-0.13 (-2.36%)	5.37	5.33	-0.04 (-0.74%)

From table, it is found that two samples mixed nanofluids refrigeration oil have the same change trend before accelerated life test in performance. Sample 2 have more significantly improved in performance compared with simple 3. After 1000 hours life test, the cooling capacity increased by 1.09%, the power decreased 1%, therefore the efficiency (COP) rose by 2.54%. Accordingly, COP of sample 3 increased by 0.85%.

Experiment on large volume compressor in refrigeration system: The nanofluids have the universal effect on sealed compressors; large volume compressors are also considered which have a worse operating condition, a large load for friction pairs. Similar to the previous experiment method, three mass produced large volume compressors are performance test as shown in tables 2.5, 2.6.

Table 2.5: Performance of normal large volume compressor Table 2.6: Performance after using nanofluids in refrigeration system **(**Lee et al., 2010)

No.	Capacity /W	Power /W	COP /W/W	Current /A
1	5208	1676	3.11	7.72
2	5189	1663	3.12	7.66
3	5211	1661	3.14	7.66
Average	5203	1667	3.12	7.68

No.	Capacity /W	Power /W	COP /W/W	Current /A
1	5238	1616	3.24	7.48
2	5248	1623	3.23	7.51
3	5239	1614	3.25	7.47
Average	5242	1618	3.24	7.49

Also the compared between normal sample with using nanofluids change by chart below

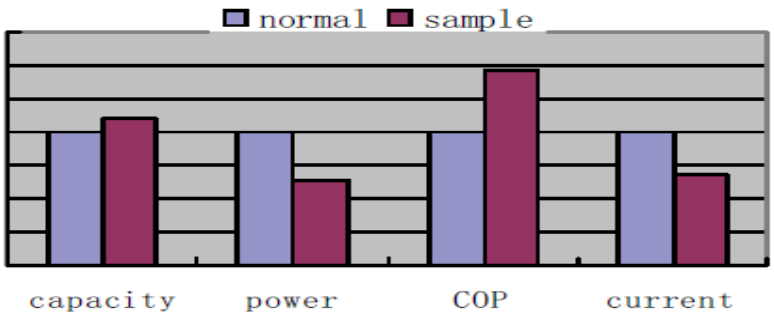

Figure 2.4: Chart of performance change on large compressor using nanofluids **(**Lee et al., 2010)

from tables and compared between the samples before and after added nanofluids in refrigeration oils we have results, cooling capacity increased by 39W, power lower by 49W, COP increased by 0.12, current decreased by 0.19A,as shown in figure 2.4.

N. Subramani et al. (2007) investigated heat transfer performance which was very important in the HVAC, refrigeration and microelectronics cooling applications. R134a was most widely adopted alternate refrigerant in refrigeration equipment, such as domestic refrigerators and air conditioners. Though the global warming up potential of R134a is relatively high, it was affirmed that it was a long term alternate refrigerants in lots of countries. The addition of nanoparticles to the refrigerant results in improvements in the thermo physical properties and heat transfer characteristics of the refrigerant, thereby improving the performance of the refrigeration system. Stable nanolubricant had been prepared for the study. The experimental studies indicate that the refrigeration system with nanorefrigerant works normally. It was found that the freezing capacity was higher and the power consumption reduces by 25% when POE oil was replaced by a mixture of mineral oil and alumina nanoparticles. Calculations show that the enhancement factor in the evaporator was 1.53 when nanorefrigerants were used instead of pure refrigerant.

An experiment of domestic vapor compression system using Al_2O_3 nanoparticles and R134a. In this paper experimental study, three cases had been considered. The hermetic compressor filled

(i) Pure POE oil

(ii) SUNISO 3GS oil (mineral oil) and

(iii) SUNISO 3GS+ alumina nanoparticles as lubricant (0.06%).

The evaporator cooling load temperature – time chart:

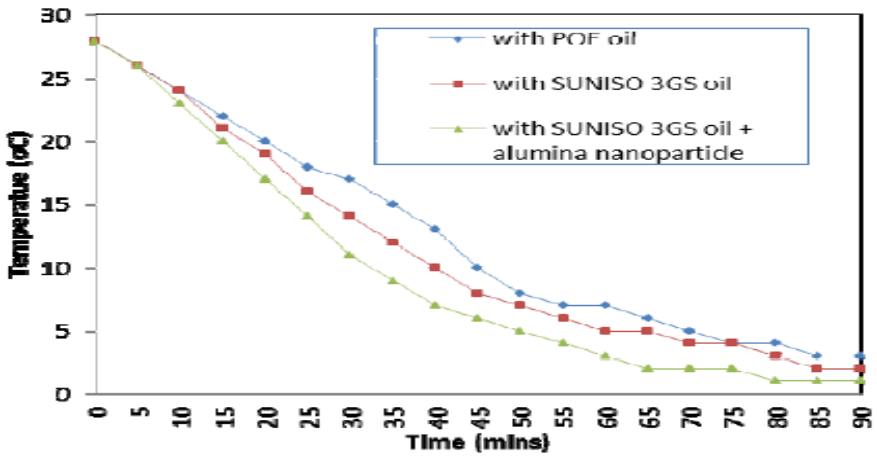

Figure 2.5: Evaporator temperature – time history (Peng et al., 2009)

The theoretical analysis showed that the enhancement factor in the evaporator with nanorefrigerant was (1.53) or in other words the heat transfer coefficient increases by (53%) when nanorefrigerant was used instead of R134a. The value of heat transfer coefficient without nanoparticles was calculated using the boiling correlations for conventional refrigerants and its value was found to be (1612 W/m^2K). Peng et al. (2009) have reported that the value of energy enhance factor is in the range (1.17 – 1.63). The cooling load temperature – time history is shown in figure 2.5 and the freezing capacity for the three cases was shown in Figure 2.5. In all the cases the condenser pressure has been observed 1.2 MPa (180 Psi) and the evaporator pressure was 0.2 MPa (30 Psi). No appreciable pressures dropped due to friction were observed in the condenser and evaporator. From the figure it was clear that, the time required for reducing cooling load temperature was less for the SUNISO 3GS oil + alumina nanoparticle mixture. For example, with SUNISO 3GS oil + alumina nanoparticle, the time required to bring the cooling load temperature from (28^oC) to (5^oC) was 50 minutes where as that with SUNISO 3GS and POE oil was 60 and 70 minutes respectively. It was clear that, the freezing capacity of the SUNISO 3GS + Alumina nanoparticle mixture was higher when compared with the other two cases The time taken to reduce the temperature of the cooling load from (28^oC) to (1^oC) with POE oil was 110 minutes and it reduced by (27%) if SUNINSO 3GS oil + alumina nanoparticle had been used.

Effect of alumina nanoparticle on the freezing capacity:

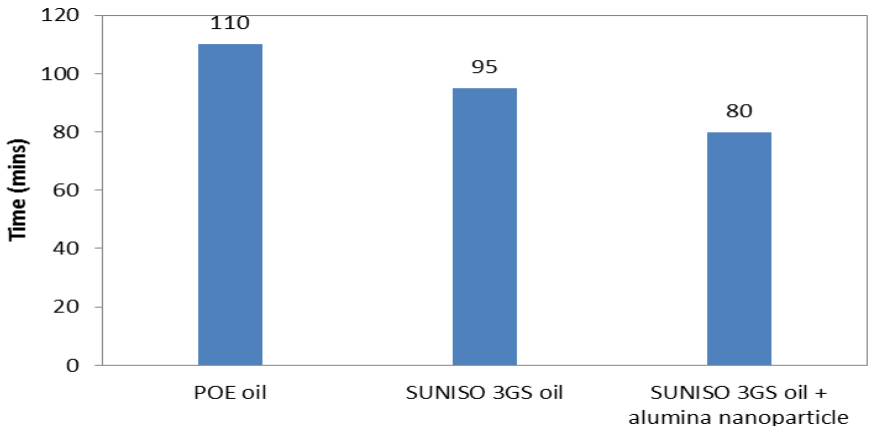

Figure 2.6: Effect alumni of nanoparticle on freezing capacity (Peng et al., 2009)

Figure 2.6 shows dropping in the refrigerant temperature in the condenser of the refrigeration system. Temperature drop of their refrigerant was high with nanorefrigerant when compared with the other cases. The temperature of the refrigerant at the inlet of the condenser was in the range (85 – 80^{o}C). The saturation temperature of R134a corresponding to the condenser pressure of 1.2 MPa was (46.3^{o}C). In the case of SUNISO 3GS nanoparticle mixture the temperature at the exit of the condenser was (38^{o}C) and the sub cooling obtained was (8.3^{o}C). In fact there was no sub cooling when POE oil was used as the lubricant. The enhanced heat transfer rate in the condenser was due to the presence of nanoparticles in the refrigerant. Figure 2.7 shown below.

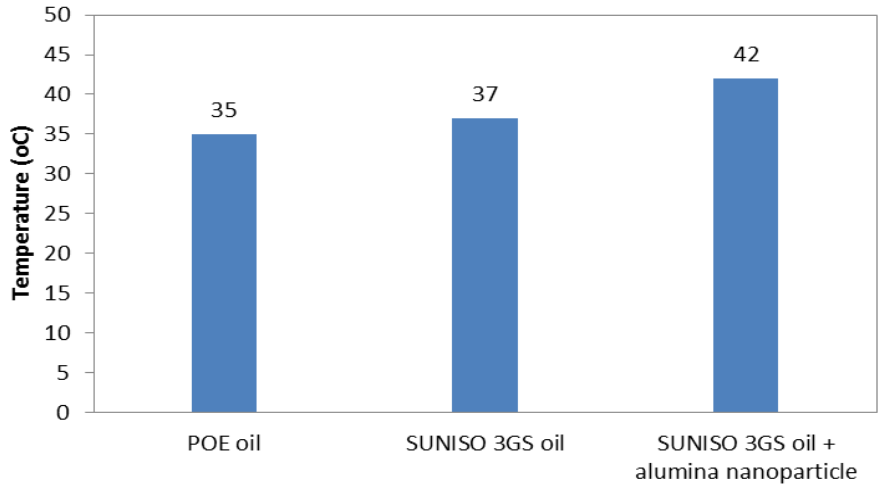

Figure 2.7: Reduction in refrigerant temperature in the condenser (Peng et al., 2009)

Energy consumption by the compressor: Figure 2.7 shows the comparison of power consumption of the compressor. The reduction in power consumption was (18%) if the SUSISO 3GS had been used instead of POE Oil and a reduction of (25%) was observed when SUNISO 3GS was mixed nanoparticles. Bi et al. (2007) conducted that found a refrigeration system using R134a as refrigerant the power consumption can be reduced by (26.1%) if mineral oil with TiO_2 nanoparticle was used instead of POE oil. Figure 2.8 shows the coefficient of performance (COP) calculated using the experimental data. The actual COP was calculated using the cooling load and the power input. The theoretical values are also shown for comparison. In all cases the actual COP has been less than the theoretical COP. It has been observed that the condenser pressure was 1.2 MPa (180 Psi) and the evaporator pressure was 0.2 MPa (30 Psi). The temperatures at the salient points of the refrigeration system are shown in Table 2.7. It has been shown below that the SUNISO 3GS + alumina nanoparticle mixture had the highest COP when compared with the other cases. The advantages of adding nanoparticle to the lubricant was manifold. It reduces the power consumption of the compressor and there was sub cooling of the nanorefrigerant in the condenser which in turn increases the COP. The Actual COP was calculated using the energy meter reading and the cooling load. For the calculation of theoretical COP the enthalpy values at the salient points were taken from P-h chart for R134a.

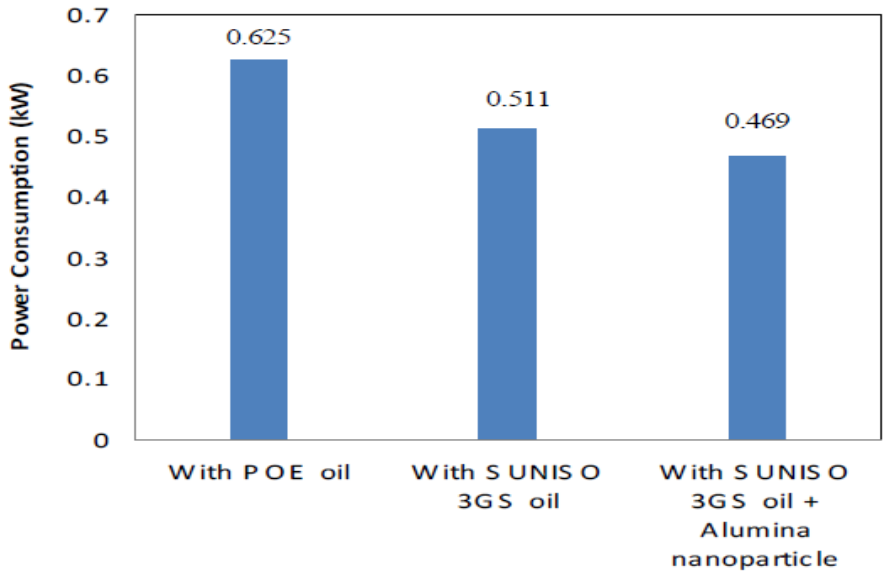

Figure 2.8: Comparison of power consumption (Peng et al., 2009)

Temperature of salient points: Table 2.7: Temperature at salient points (Peng et al., 2009)

Quantity	POE oil °C	SUNISO 3GS oil °C	SUNISO 3GS oil with Al_2O_3 nanoparticle °C
Temperature at the inlet to the compressor	19	19	4
Temperature at the inlet to the condenser	85	82	80
Temperature at the outlet of the condenser	50	45	38
Temperature at the outlet of the expansion device	-7	-8	-7
Temperature at the inlet to the evaporator	-6	-7	-6

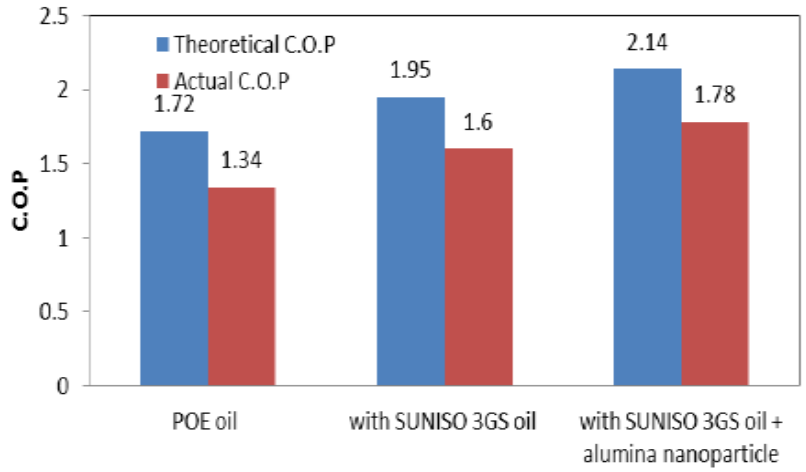

Figure 2.9: Comparison of coefficients performance (COP) for three cases (Peng et al., 2009)

Figure 2.9 shows the coefficient of performance (COP) calculated using the experimental data. The actual COP was calculated using the cooling load and the power input. The theoretical values were also shown for comparison. In all cases the actual COP was less than the theoretical COP. The temperatures at the salient points of the refrigeration system were shown in Table 2.7. It was very much clear from the histogram shown below that the SUNISO 3GS + alumina nanoparticle mixture had the highest COP when compared with the other cases. The advantages of adding nanoparticle to the lubricant had been manifold. It reduces the power consumption of the compressor and there was sub cooling of the nanorefrigerant in the condenser which in turn increases the COP. The Actual COP was calculated using the energy meter reading and the cooling load. For the calculation of theoretical COP the enthalpy values at the salient points were taken from P-h chart for R134a.

CHAPTER-3

GAPS STUDY AND OBJECTIVES

3.1 Gaps study:

Work is done by many researchers on the thermo-physical properties of nanofluid and factor affecting it like; viscosity, thermal conductivity, properties of nanofluids, particle volume fraction, particle material, base fluid, particle size and particle shape. Researchers have been trying different concentrations of nanoparticles in the base fluids in order to investigate their performance. A limited work has been reported on the nanorefrigerants and its effect on the performance of vapour compression cycle. There is a range of conventional refrigerants which are used in vapour compression cycle. As a fact of matter, properties of the refrigerant affect the performance of the refrigeration system. As the literature suggests that addition of nanoparticles in base fluid improves its characteristics & performance. It is believed that nanoparticles based refrigerant so called nanorefrigerant will also improve the performance of refrigeration system.

3.2 Study objectives

Followings are the key issues which are required to address in order to carry out the investigations on any nanorefrigerant based refrigeration system:

(i) COP, Power consumption, pressure drop at different nanoparticles size & volume fraction

(ii) Stability of nanoparticle in refrigerant in refrigeration system

(iii) Preparation of nanolubricant and charging nanorefrigerant

(iv) Study of mass flow rate by varying nanoparticles volume concentration

(v) Time required for achieving desired temperature

(vi) Temperature at all points, such as across Condenser, Evaporator, Compressor inlet and outlet

(vii) Effect of shape and size of nanoparticles on thermo-physical properties of nanorefrigerant

(viii) Change in pressure ratio with varying load and concentration of nanorefrigerant R134a

(ix) Parameters effecting sub cooling conditions in domestic refrigeration system

(x) Compare the experimental results before and after using nanoparticles in the system

3.2.1Parameters to be varied

(i) Evaporator temperature (40-25^{0}C)

(i) Heat flux and cooling load in evaporator at 35-36^{0}C

(ii) Effect of sub cooling and superheating

(iii)Concentration of CuO nanoparticles (0.25-2%)

(iv) Copper oxide particle size 20 nm scale and spherical shape

(v) Varying nanorefrigerant mass flow rate (10 & 15 LPH)

3.2.2 Parameters to be studied

(i) COP in cases 10, 15 LPH of nanorefrigerant mass flow rate

(ii) Power consumption at varying heat flux

(iii) Pressure drop in condenser and evaporator at constant heat flux

(iv) Time required achieving a desired drop in temperature (40-25 ^{o}C) with vol. fraction

(v) Study the parameters with varying mass flow rate and concentration

(vi) Time required to achieve a desired temperature across condenser and evaporator

(vii) Change pressure ratio of nanorefrigerant (R134a+CuO) of compressor of system

(viii)Temperature at all points such as; condenser, evaporator, compressor inlet and outlet

(ix) Temperature drop across condenser

(x) Evaporator temperature gain and condenser temperature drop with concentration

(xi) Comparison the performance for nanorefrigerant based refrigeration system and pure refrigerant R134a.

CHAPTER-4

NANOREFRIGERANT SELECTION AND CHARACTERIZATION

Thermo physical properties of nanorefrigerant (CuO+R134a)

4.1 Thermo physical properties of nanoparticles (CuO powder)

Table 4.1: Physical properties of CuO nanoparticles

Physical properties of CuO Particles	
• Appearance	Black powder
• Content of CuO	98%
• Grain size (nm)	<60nm
• Thermal conductivity	78 w/m.k
• Specific heat	880 J/kg.k
• Flash Point	non-flammable
• Surface area	0.5-50 m^2/g
• Average Primary Particle size	50 nm
• Specific surface area (m^2/g)	>80m^2/g
• P H	7-9

Properties

- It is insoluble in water.
- Stable under normal, temperature and pressures.
- It is odorless.

Cupric oxide (CuO) nanoparticles with an average size of 6 nm have been successfully prepared by an alcothermal method. The prepared CuO nanoparticles were characterized by X-ray

diffraction (XRD), transmission electron microscopy (TEM), Fourier-transform infrared (FT-IR) and UV visible absorption spectroscopy. A strong sharp emission under UV excitation is reported from the prepared CuO nanoparticles. The results show that the CuO nanoparticles have high dispersion and narrow size distribution. The fluorescence emission spectra display an intense sharp emission at 365 nm and weak broad intensity emission at 470 nm. In neutral and alkaline solutions, Zeta potential values of CuO nanoparticles are negative, due to the adsorption of CO_2 group via the coordination of bidentate. At low pH the zeta potential value is positive due to the increased potential of H+ ions in solution. Comparative UV–visible absorption experiments with the model amino acid compounds of positive and negative charges as argentine and aspartic acid, respectively confirmed the negative surface of CuO nanoparticles.

Table 4.2: Thermo-physical properties of CuO nanofluids at different concentrations

(Choi et al., 1998)

S. No.	Volume fraction, φ in %	Thermal conductivity W/m K		Density Kg/m³		Viscosity Pa-s		Specific heat J/Kg K	
		Present Data	Wasp [1977]	Present data	Pak and Cho [1998]	Present data $\nu\times10^6$	Einstein $\nu\times10^6$	Present data	Pak and Cho [1998]
1	0.025	0.3142	0.3120	1025.2	1024.9	0.00761	0.00761	3672.4	3861.1
2	0.1	0.3206	0.3161	1029.9	1028.9	0.00765	0.00762	3669.1	3858.3
5	0.4	0.3361	0.3276	1048.9	1044.7	0.0077	0.00768	3659.1	3847.1
8	0.8	0.3579	0.3434	1074.5	1065.9	0.00775	0.00775	3645.0	3832.1
8	1.2	0.3806	0.3597	1074.5	1065.9	0.0078	0.00783	3645.0	3832.1

The CuO nanoparticles having an average size of 50 nm and density of 6.3 gm/cm^3 is procured from a USA based company (Sigma-Aldrich Chemicals Private Ltd) and is used for investigation in the present experimental work. The photographic view of the nanoparticles as seen by the naked eyes is shown in the plate.

Figure 4.1: Picture of CuO nanoparticles

4.1.1 TEM Characterization of copper oxide nanoparticles

The one-step nanofluids production method resulted in very small copper oxide particles (10 nm diameter order of magnitude).

Very little agglomeration and sedimentation occurs with this new and patented method.

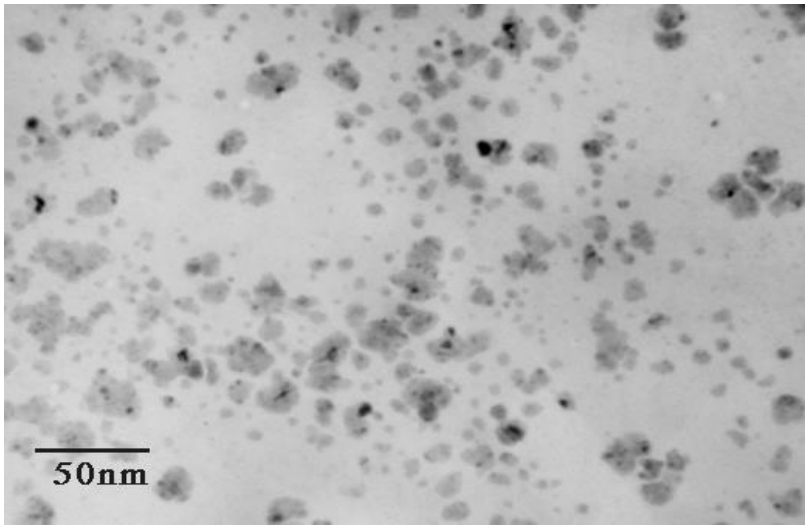

Figure 4.2: Bright-field TEM micrograph of CuO nanoparticles produced by direct evaporation into ethylene glycol (Choi et al., 1998)

4.1.2 SEM Characterization of copper oxide nanoparticles

The distribution of CuO nanoparticles at nanoscale can be observed under a Scanning electron microscope (SEM). The SEM images of CuO nanoparticles at 1 m magnifications is shown in Plate.3.2(a) and SEM image of CuO nanoparticle on a 500 nm scale is shown in Plate.3.2(b). Preparation of nanofluids is an important stage. And nanofluids are prepared in a systematic and careful manner. A stable Nanofluid with uniform particle dispersion is required and the same is used for measuring the thermo physical properties of nanofluids.

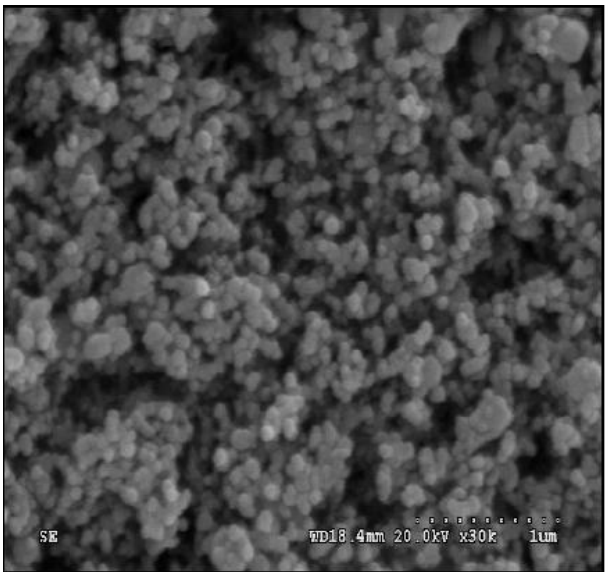

Plate (a)

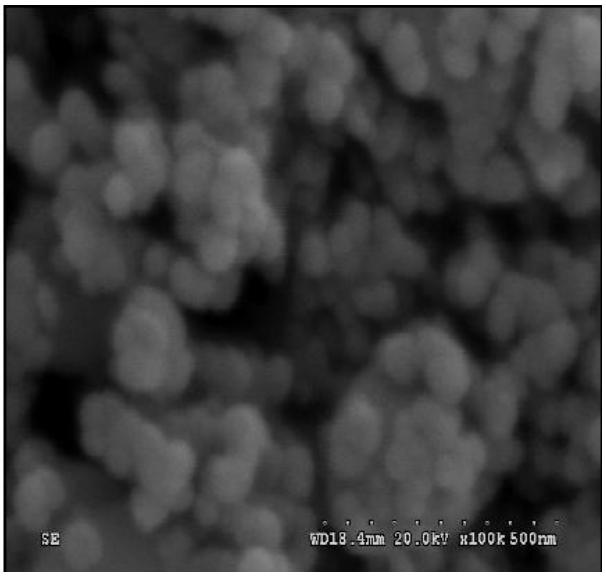

plate (b)

Figure 4.3: SEM images of CuO nanoparticles on 1 µ m and 500 nm scales (Choi et al., 1998)

4.2 Thermo physical properties of base refrigerant.

Its numerical designation is R134a or Isobutene. Its chemical formula (CH2FCF3).

Gas Properties

- Molecular weight : 102.03 g/mol

Solid phase

- Melting point (1.013 bar) : -101 °C

Liquid phase

- Liquid density (1.013 bar and 25 °C (77 °F)) : 1206 kg/m^3
- Boiling point (1.013 bar) : -26.55 °C
- Latent heat of vaporization (1.013 bar at boiling point) : 215.9 kJ/kg
- Vapor pressure (at 20 °C or 68 °F) : 5.7 bar
- Vapor pressure (at 5 °C or 41 °F) : 3.5 bar
- Vapor pressure (at 15 °C or 59 °F) : 4.9 bar
- Vapor pressure (at 50 °C or 122 °F) : 13.2 bar

Critical point

- Critical temperature : 100.95 °C
- Critical pressure : 40.6 bar
- Critical density : 512 kg/m^3

Triple point

- Triple point temperature : -103.3 °C

Gaseous phase

- Gas density (1.013 bar at boiling point) : 5.28 kg/m^3
- Gas density (1.013 bar and 15 °C (59 °F)) : 4.25 kg/m^3
- Compressibility factor (Z) (1.013 bar and 15 °C (59 °F)) : 1
- Specific gravity : 3.25
- Specific volume (1.013 bar and 15 °C (59 °F)) : 0.235 m^3/kg
- Heat capacity at constant pressure (Cp) (1.013 bar and 25 °C (77 °F)): 0.08754 kJ/(mol.K).

Miscellaneous

- Solubility in water (1.013 bar and 25 °C (77 °F)) : 0.21 vol./vol.

CHAPTER-5

EXPERIMENTAL SET-UP AND METHODOLOGY

In this experimental work a domestic vapor compression system has been used. In any compression refrigeration system there are two different pressure conditions. One is called the low side pressure (evaporator), heat is absorbed in low side and suction line entrance to the compressor suction valve is also on the low side. The condenser is in high side pressure where the heat is released from the refrigerant. The compressor exhaust valve, liquid receiver by filter-drier and the refrigerant control are also on the high side. Expansion unit joins both pressure side and it is designed so that no liquid refrigerant will flow through it unless the pressure in the evaporator is reduced by running of the compressor. Refrigerant is sprayed into the evaporator due to low pressure; it boils rapidly and absorbs heat. The vaporized refrigerant moves back to compressor through the suction line and it are compressed to high side pressure as vapor. While through the condenser it is cooled, gives up heat that absorbed in the evaporator and returns to liquid then flows into liquid receiver ready to repeat the cycle of system.

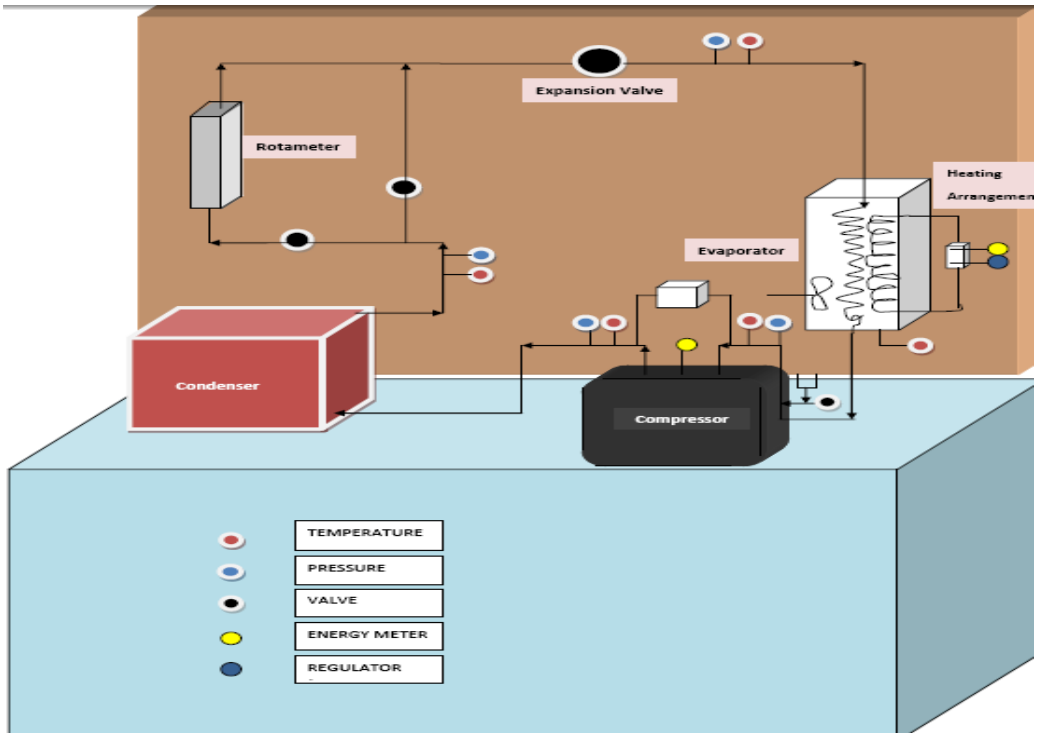

Figure 5.1: 3 Dimensions layout of vapour compression system [RAC Lab, Thapar Uni.]

5.1 Layout of vapour compression refrigeration system

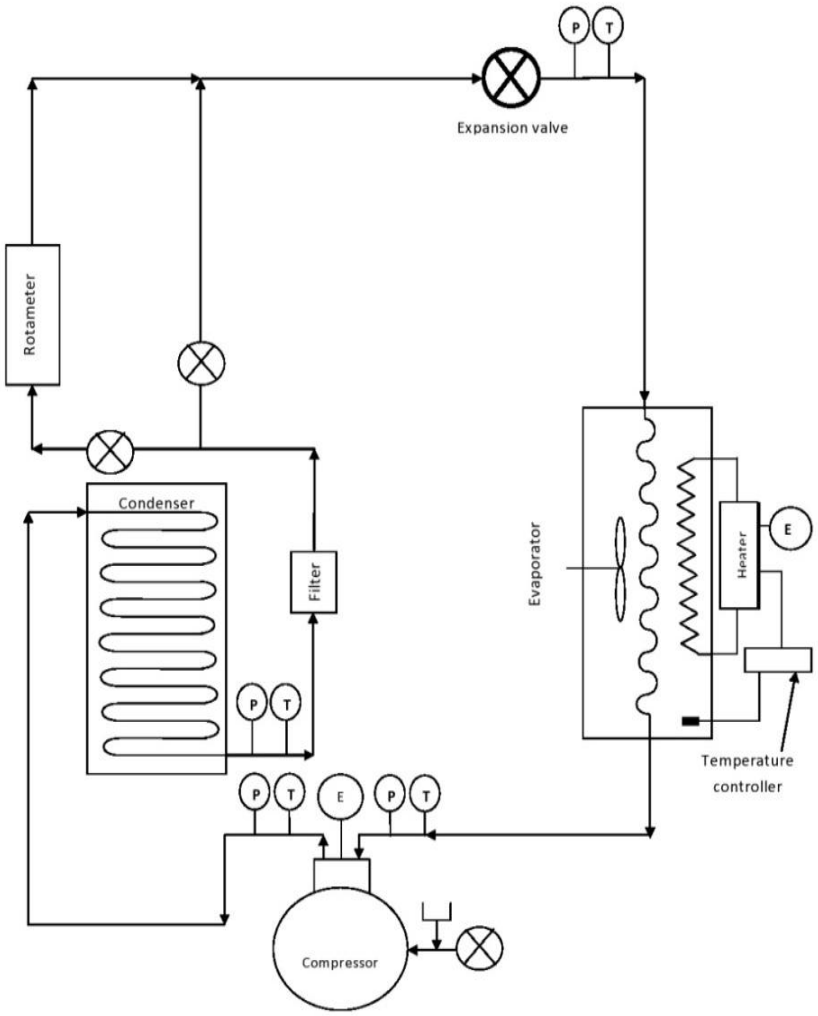

No.	Component
1	Compressor (R134a)
2	Condenser
3	Evaporator
4	Expansion Device (Manual)
5	Drier
6	Heating Element
7	Agitator
8	Temperature Gauge (Thermometer)
9	Pressure Gauge
10	Rota meter
11	Energy Meter
12	Ampere Meter
13	Volt Meter
14	Low pressure high pressure cut off
15	Regulator

Figure 5.2: Layout of vapour compression system [RAC Lab, Thapar Uni.]

The operation characteristics of the system are quite satisfactory , the compressor motor control by mechanical external load to the handing expansion valve not as refrigenertor the thermal element at the end of evaporator is used to control the motor and compressor is stopped but in this system the compressor stop when shut down the current mechanically. The refrigerant oil is circulated without trouble. This type refrigeration cycle is used widely because the pressure does not balance on the off cycle, the motor compressor must start under load.

5.2 Vapour compression refrigeration components

Table 5.1: Experimental set-up components and specifications [RAC Lab, Thapar Uni.]

S. No.	Component	Qty.	Specification
1	Compressor (R134a)	1	165 LPH
2	Condenser	1	as per compressor
3	Evaporator	1	as per compressor
4	Expansion Device (Manual)	1	as per compressor
5	Drier	1	Without Silica Gel
6	Heating Element	1	
7	Agitator	1	
8	Temperature Gauge (Thermometer)	5	Mercury Thermometer
9	Pressure Gauge	5	
10	Rota meter	1	
11	Energy Meter	2	
12	Ampere Meter	1	
13	Volt Meter	1	
14	Low pressure high pressure cut off	1	

Figure 5.3: Experimental set-up components refrigeration system [RAC Lab, Thapar Uni.]

Refrigeration Compressor: In this setup we used reciprocating hermetic compressor, single cylinder with 165 LPH capacities to raise the pressure and temperature of the refrigerant. And also to overcome the frictional loss, the original energy source is usually an electric motor. Its rotary motion must be changed to reciprocating motion. This change is made by crank and a rod connecting crank to the piston. The complete mechanism is housed in a leak proof container called a crankcase. It is very efficient, its construction resembles in many ways that of automobile compressor. A typical external drive reciprocating compressor show below in Figure. The compressor is at top and motor at bottom. Assembly is mounted on springs inside dome of motor rotor and stator and glass sealed electrical connections through compressor dome. Basically, this compressor is a single cylinder and piston; figure shows the principle of operation of a reciprocating compressor. In illustration no.1, the piston has moved downward in cylinder and has moved refrigerant vapor from suction line through intake valve and into the cylinder space. In illustration no.2, the piston has moved upward in cylinder and compressed the vaporized refrigerant into a much smaller space (clearance space) marked and has pushed the compressed vapor through valve into the condenser to remove absorbing heat of evaporator into sky as shown in figure below.

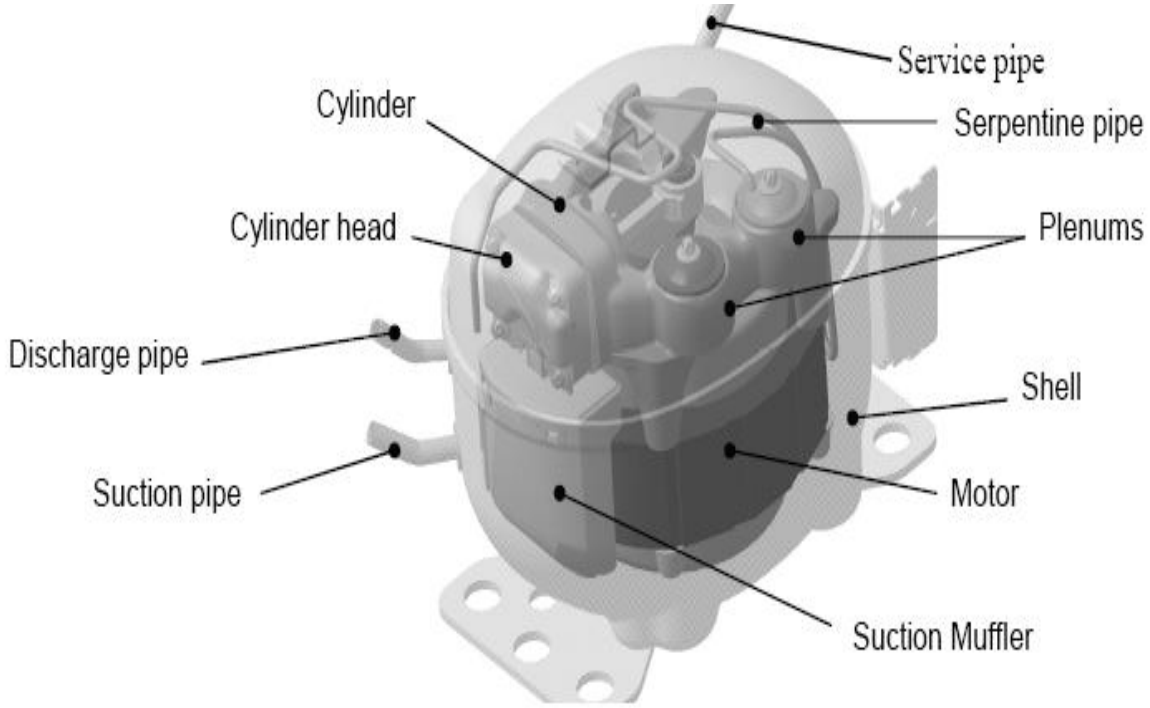

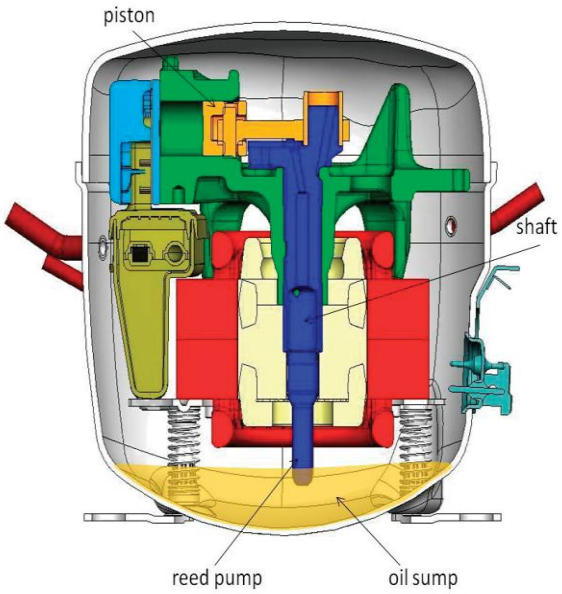

Figure 5.4: Compressor, dimensions and circuit diagrams [RAC Lab, Thapar Uni.]

Table 5.2: Compressor specifications

Compressor Specifications		
Manufacturer	Godrej & Boyce Mfg. Co. Ltd.	
Model	POWER COOL COMP R134a G1-1+CAPCT	
Dimensions	m*m*m	0.201*0.164*0.175
Capacity	Btu/hr.	410
Motor input	Watts	107
EER	Btu/Whr.	3.83
Displacement	CC	4.6
Voltage range	V	150-260
L.V. Pickup	V	160V
Oil Charge	CC	300
Net Weight	KG	7.8
Overload protector		OLPA

Refrigerant flow control device: Handing Expansion Valve (HEV) has been used in the set-up. Refrigerant must be at low pressure (liquid refrigerant) to enter the evaporator so it will evaporate at a low temperature and the liquid refrigerant in condenser unit at high pressure at the same time maintains the required pressure in the evaporator is lowered. The handing expansion valve have has been developed for controlling refrigerant flow into the evaporator and also for controlling the electric motor which drives the mechanism. The principle of setup expansion valve using is control based on volume or quantity changes. Handing expansion valve with double spring on needle balances the forces and gives smoother control of the refrigerant flow such the flowing past the expansion valve is the same weight as the vapor pumped by the compressor. It is made of phosphor bronze soldered, the valve body and a soldered connection a standard flange, a flared connection or pipe thread with screen designed for easy removal. The screen is made of brass wire 60 mesh. The expansion of valve must be adjusted for atmospheric pressure which effects their operation.

Figure 5.5: Handing operated expansion valve [RAC Lab, Thapar Uni.]

Air-cooled condenser: The condenser unit in refrigeration cycle removes heat from the refrigerant vapor by it condense vapor into liquid. In my thesis domestic refrigerator has been used air cooled finned type static condenser (natural convection). Static means that air circulation through the condenser tubing and fins is by natural convection; that, warm air tends to rise. As

the air contact with the fins and tubes becomes heated, it rise and cooler air takes its place. The tubes and fins are made of steel.

Condenser Specifications	
Type	Natural Convection
Diameter of Pipe	0.00635 m
Length of Pipe	13.7 m
Area of Condenser	0.2732 m^2
Material	Copper

Figure 5.6: Finned-static air cooled condenser and specifications [RAC Lab, Thapar Uni.]

Emersion coil evaporator: The liquid refrigerant entering the evaporator from the refrigerant flow control is suddenly under low pressure. This makes it vaporize and absorb heat. The emersion coil evaporator type is used as a dry system evaporator. Refrigerant is fed into the dry system evaporator only as fast as is needed to maintain the required temperature. The evaporator coil inside the cylinder is in tank full of water and the outside of the cylinder is insulated.

Evaporator specifications	
Type	Emersion coil type
Diameter of Pipe	0.00635 m
Length of Pipe	7.62 m
Area of Evaporator	0.152 m^2
Material	Copper

Figure 5.7: Coil type cylindrical evaporator and specifications [RAC Lab, Thapar Uni.]

Filter dryer: It is common practice to install a filter dryer in the liquid line to obstruct any impurity present in the system. This accessory keeps moisture dirt, metal and chips from entering the refrigerant flow control (expansion valve); the drying element in the filter removes the moisture which might otherwise freeze in the refrigerant flow control or expansion valve. Moisture is also harmful when mixed with oil in system. It is especially harmful to hermetic compressor. Filter dryer shown figure below

Figure 5.8: Filter dryer to remove moisture [RAC Lab, Thapar Uni.]

Rota-meter gauge: Rota-meter is used to measure the refrigeration mass flow rate in liquid phase through system. It consists of a tube, normally made of glass with a float, actually a shaped weight inside that is pushed up by the drag force of the flow and pulled down by gravity. To see the flow rate of refrigerant glass tube Rota-meter has been used.

Rota meter gauge	Mass flow rate
High rate Side	4 LPH
Low rate Side	40 LPH

Figure 5.8: Rota meter gauge and specification model [RAC Lab, Thapar Uni.]

Heating element: A heating element convert electricity into heat the procedure of resistive or joule heating. Refrigerant takes the heat from the water present in evaporator and heating add heat to the evaporator at constant rate as heating load flux and maintain the required flux as temperature of evaporator. It is used to give heating load to the evaporator by electrical power input. It is made from steel and metal heating type.

Heater specifications	
Specification	230V,50Hz A/C
Power	2000W

Figure 5.9: Heating heater and specification model [RAC Lab, Thapar Uni.]

Pressure Gauges: Pressure gauges are used by technician to measure pressure of the R-134a refrigerant in system. Gauges use a Bourdon tube as the operating element. The Bourdon tube is a flattened metal tube (copper alloy) sealed at one end, curved and soldered to the gauge fitting at the other end. A pressure rise in a Bourdon tubes makes it tend to straighten. This movement will pull on the link, which turn the gear sector counterclockwise. The pointer shaft will then turn clockwise to move the needle. In this system, the high pressure gauges have been used in both sides of refrigeration system and this type is calibrated in both English and metric units (AMETEK U.S. Gauge). This high pressure gauges has single continuous scale, usually calibrated (marked off) to read from 0 to 500 psi and refrigerants R22,R407,R404a,R134a .figure below shows typical gauge is used.

Pressure Gauge	Unit
High Pressure Side	0-300 psi
Low Pressure Side	(-30) - 150 psi

Figure 5.10: Pressure gauge for R-134a refrigerant [RAC Lab, Thapar Uni.]

Refrigerant (R134a): In the experimental setup we used R134a as a refrigerant. R134a is stable and is nontoxic, noncorrosive, nonirritating and nonflammable. Water mixes batter with R134a ratio 19.5 ppm by weight, that drier should be used to remove most of the moisture. R134a has good solubility in oil down (-9^{o}C). This refrigerant relatively low condenser pressure and temperature increases the life of compressor valves and other parts. Better lubrication is possible because of increased viscosity of the oil at the low condensing temperature. Because of the lower condensing pressure, it is possible to eliminate liquid injection to cool the compressor that helps in injection of nanoparticles with refrigerant to compressor.

Refrigerant Properties	
Manufacturer	Seattle Gas, Italy
Purity	0.999
Moisture	5ppm(max)
Acidity	0.1ppm(max)
Vapor residue	100ppm (max)
Product	1.1.1.2-Tetraflouroethane

Figure 5.11: Refrigerant cylinder and data properties of R134a [RAC Lab, Thapar Uni.]

Voltmeter: It is a device used to measured supply voltage of the electrical power. It is designed such that it disturbs the circuit as little as possible so the instrument should draw a smallest amount of current to operate and using a sensitive galvanometer in series with high resistance.

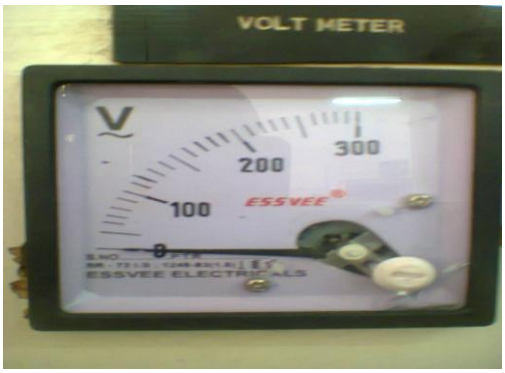

Voltmeter specifications	
Manufacturer	ESS VEE Electricals
Type	72 sq mm
Range	0-300 V

Figure 5.12: Voltmeter system and model specifications [RAC Lab, Thapar Uni.]

Ampere meter: An ammeter is measuring device used to reading electric current an electrical circuit. The bulk of ammeters are connected in series with the circuit carrying the electrical current to be measured with unit ampere (A). Digital ammeter type has been used in this set-up.

Ampere meter specifications	
Manufacturer	Pyrotron
Type	Digital
Range	0-15 amp

Figure 5.13: Ampere meter measurement and specifications [RAC Lab, Thapar Uni.]

Energy meter: To measure power input to the system. There are two energy meter used in the system. One for the compressor and other for the heater. The unit of energy meter is kilowatt hour (kWh). The energy input for both the devices is used to calculate the performance of system

Energy meter specifications	
Manufacturer	Jaipur Metals and Electricals
Type	AC, 1 Phase, 2 wire, 50Hz
Range	0-20 amp
Rev/kWh	600

Figure 5.14: Energy meter power measurement and specifications [RAC Lab, Thapar Uni.]

Digital temperature controller: To measuring the water evaporator temperature and controlling it by cut off the heater supply when the temperature exceeds a particular value in the evaporator. It is connected to relay device which is connected to heating element. This device sends signal to relay switch which cuts off the supply as well as on the supply of heating element. There is a sending element which always dipped in the evaporator water. With the help of digital temperature controller constant heat flux condition in the evaporator can be maintained.

Digital Temperature Controller	
Manufacturer	ACR Inst & Valve Pvt. Ltd.
Type	Digital
Range	-40^{o}C - 50^{o}C

Figure 5.15: Digital temperature controller and specifications [RAC Lab, Thapar Uni.]

Relay control system: To cut off power supply of heater by digital control thermostat while it is connected with the thermostat.

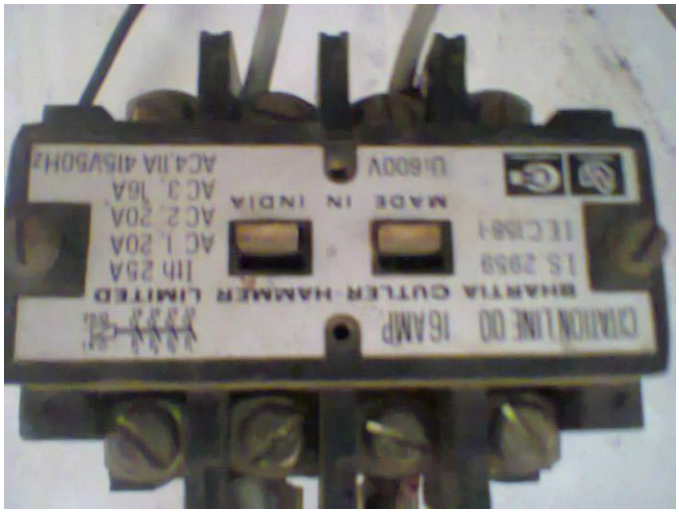

Figure 5.16: Relay control thermostat system [RAC Lab, Thapar Uni.]

Celsius glass stems thermometers: Temperature measures the heat intensity or heat level and it measured with thermometer usually through uniform expansion of mercury in sealed glass tube. There is bulb at the bottom of the tube and a quantity of mercury inside. The mercury will rise and fall in the tube as the temperature changes. The tube is calibrated or marked off in degree using the desired temperature scale. In this refrigeration system we used 4 glass stem thermometers before and after of condenser and evaporator to reading temperature.

Figure 5.17: Celsius glass stems thermometers [RAC Lab, Thapar Uni.]

Vapour compression refrigeration tools and materials

Soft copper tubing: Most tubing used in refrigeration and air conditioning is made of copper and soft copper tubing is used in domestic work commercial refrigeration work. It is heated and allowed to cool. This makes it flexible; therefore, easy to bend and flare. Being easily bent, this tubing must be supported clamps or suitable brackets. Soft copper tubing is most often used in connection with flared fittings. The size has been used is1/4 in. out site diameter (OD). Wall thickness tubing is 0.03 and L type has been used in our setup project to connect all parts of refrigeration system. These tubes are sold in rolls 25+, 50+, 100 feet long. The soft copper tubing length has been used is 20 meter including the part used emersion coil of evaporator in system.

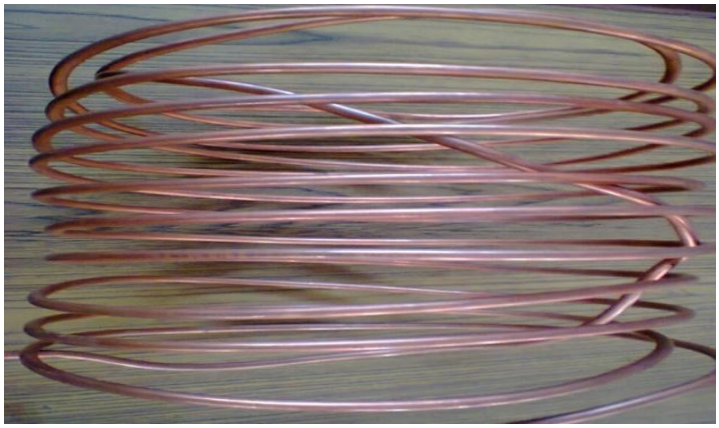

Figure5.18: Soft copper tubing has been used [RAC Lab, Thapar Uni.]

Connecting soft copper tubing:

Flared tubing fittings connections: A flared type connection is generally used. The fittings are made of drop-forged brass and machined to form the National Fine (NF) threads, the National Pipe (NP) threads, the hexagonal shapes for wrench attachment, and the 45 degree. Fitting against the tubing flare. Flare nut attaches using ¼ in with tubing size as ¼ in, tubing to a flared fitting even through it has 7/16 in, NF internal threads and uses a wrench with a ¾ in.

Figure 5.19: Flared connections tubes and nuts in system [RAC Lab, Thapar Uni.]

Silver Brazing connections: Best method of making leak proof connections joints. The procedure is firstly clean the joints after silver soldering process and fit the joints closely and supports all parts; apply the clean flux recommended for silver brazing alloy. An oxyacetylene

torch is an excellent heat source for silver brazing evenly to recommended temperature. Apply silver brazing alloy to heated parts and keep the joint covered with flame, cool the joint and clean it using warm water and brush.

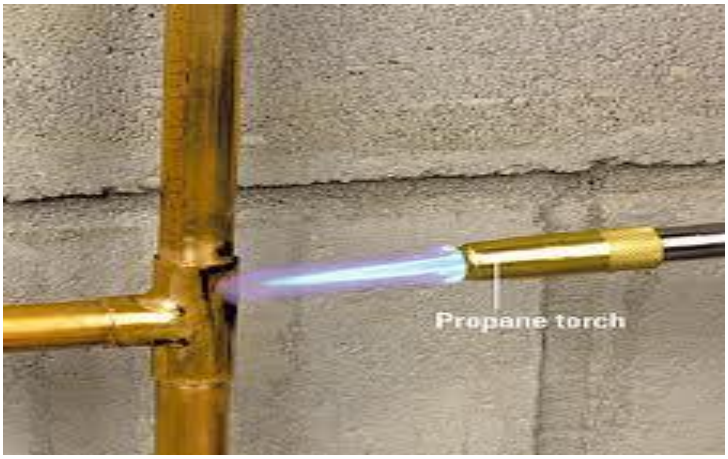

Figure 5.20: Silver brazed Tubing process [RAC Lab, Thapar Uni.]

Hand Tools Used:

Table 5.4: Handing tools and materials have been used [RAC Lab, Thapar Uni.]

1-Wrenches	2- Hammers & Stamps	3- Mallets
4-VisesTwist	5- Drills	6-Taps
7-DiesInstruments	8- Measuring rules	9- tapes
10-Micrometer	11- Abrasives	12- Brushes
13-Cleaning solvents	14- Cold chisels	15- Punches Files
16-Hacksaws	17-Fastening devices	18-Machine screws
19-Bolts	20-Cap screws	21-Gaskets
22- Pliers	23- Screwdrivers	24-Service Valves

5.4 Experimental methodology

The main aim of this thesis is to prepare nanofluids with CuO nanoparticles and refrigerant as fluid for improving the performance of the system. These analyses are performed by measuring different temperatures and pressures for the different volume concentrations of nanorefrigerant.

The temperature of the refrigerant inlet/outlet of each component of the refrigerator is measured with copper constantan thermocouples (T type). The thermocouple sensors are fitted at inlet and outlet of the compressor, condenser. It is important to take temperature measurement is necessary at entry and exit of each component of the system in order to investigate the performance. Similarly measurements at the inlet and outlet of each component are also necessary to find out their pressure drop at corresponding states. The pressure gauges are fitted at the inlet and outlet of the compressor and expansion valve as shown in Fig 5.21. The pressure gauges are fitted with the T-joint and then brazed with the tube to measure the pressure at desired position. The range of the pressure transducer is 0 to + 7 bars. A rotameter gauge is installed at the before of expansion valve and filter dryer to measuring the mass flow rate of the refrigerant. The location of the rotameter is shown in Fig 5.15. The digital thermostat has been used to measuring and controlling heater temperature. A power meter is connected with compressor and heater to measure the power and energy consumptions.

Figure 5.21: The domestic vapor compression refrigeration system setup in RAC Lab in Mechanical Engineering Department in Thapar University

5.4.1 Preparation of CuO particles

Copper oxide (CuO) nanoparticles were purchased from Reinste Nano Ventures Pvt. Ltd. New Delhi. The size of nanoparticles is 20 nm as it was mentioned by the company.

Structural Characterization

Structural Characterization of nanoparticles can be done by using techniques such as BET, XRD, SEM, TEM, and HRTEM. As this research work is more concerned about the application of nanofluids so XRD analysis is done for the authentication of nanoparticles.

XRD for sample (Purchased) is shown.

Purchased Sample XRD:

Company Name: Reinste Nano Venture Pvt. Ltd.

Cooper Oxide

CuO Nanoparticle Powder, purity: >99%

Particle Shape: Spherical

Average particle size: 20nm

Specific surface area: >8 m^2/g

Bulk Density: 0.8 g/cm^3

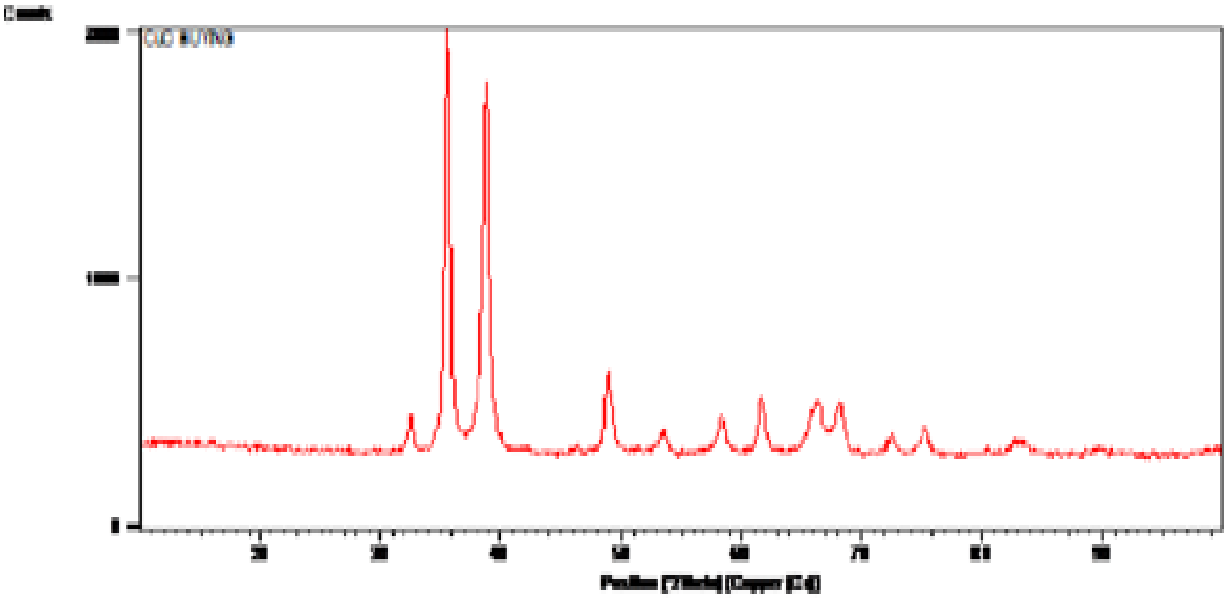

Figure 5.22: XRD result for CuO nanoparticle diameter 20 nm

5.4.2 Preparation of nanorefrigerant

To prepare the CuO nanorefrigerant, there is a need to determine the weight of CuO for different concentration and the volume of the refrigerant R134a. The weight of CuO can be evaluated by using the standard expression.

V particles = M sample / M total Φ= V particles/V R134a

division the total amount on basic volume fraction by distribution on the percentage concentration as such as 0.25 gram step so first weight become 0.25 gm then 0.5 gm, 0.75 gm,1 gm,1.25gm,1.5gm,1.75 gm, 2gm with 100 ml of R134a refrigerant.

Figure 5.23: Electronic weight machine [RAC Lab, Thapar Uni.]

5.4.3 Evacuation of refrigeration system

Moisture combines in varying degree with most of the commonly used refrigerants and reacts with the lubricating oil and with other materials in the system, producing highly corrosive compound. The resulting chemical reaction often produces pitting and other damage on the valves seals, cylinder wall and other polished surface of the system. It may cause the deterioration of the lubricating oil and the formation of sludge that can gum up valves, clog oil passages, score bearing surface and produce other effect that reduce the life of the system. Moisture in the system may exist in solution or as free water. Free water can freeze into the ice crystals inside the metering device and in the evaporator tubes of system that operate below the freezing point of the water. This reaction is called freeze up. When freeze up occurs, the formation of ice within the orifice of the metering device temporarily stops the flow of the liquid refrigerant .To get rid of the detrimental effect of moisture. Vacuum compressor was used to evacuate the system. This system evacuates fast and better which is deep enough to get rid of contaminant that could cause system failure. The evacuation system consists of a vacuum compressor, a pressure gauge and hoses. The hoses were connected with the service port to remove the moisture from the system.

Figure 5.24: Vacuum compressor [RAC Lab, Thapar Uni.]

5.4.5 Charging of nanorefrigerant (R134a+CuO):

Preparation of nanorefrigerant is the first step in the experimental studies on nanorefrigerants. These are not simply liquid solid mixtures. Special requirements are even, stable and durable suspension, negligible agglomeration of particles, and no chemical change of the nanorefrigerant. It can be prepared using single step or two step methods. In the present study two step procedures is used. Commercially available nanoparticles of copper oxide with average size 20 nm and having density 0.26 g/cc are used for the preparation of nanorefrigerant. Mass fraction of CuO nanoparticles in the nanoparticle and R134a refrigerant mixtures is 0.25 gm then 0.5 gm, 0.75 gm, 1 gm, 1.25 gm, 1.5 gm, 1.75 gm, 2 gm per 1 litter of R134a. An experimental observation shows that the stable dispersion of copper oxide nanoparticles can be injected with refrigerant when charged to system by the main valve before compressor from refrigerant cylinder by pressure different and it is injected first time pure refrigerant R134a. When taken the results reading by varied the system parameters like heat flux and mass flow rate of pure R134a. And then escape little R134a from control valve, injection 0.25 gm of CuO nanoparticles with concentration (0.25%) nanorefrigerant.

Figure 5.35: System charging nanorefrigerant (R134a+CuO) [RAC Lab, Thapar Uni.]

Important specifications

- Concentration of particle (0.25 gm then 0.5 gm, 0.75 gm, 1 gm, 1.25gm, 1.5gm, 1.75 gm and 2gm) with Litter of R134a, become eight concentrations (0.25% - 2%).
- Size of particles: CuO - 20nm (10gm) with spherical shape of powder nanoparticles.
- Nanorefrigerant charged mass flow rate (10 and 15 LPH).
- Constant heat flux (35-36 ^{o}C) then varying it on ranges (40-25 ^{o}C).

5.4.6 CuO nanoparticles injection to refrigeration system

A compressor unit has been also used to clean the system from the moisture and traps of copper. Charging of system is done mechanically with pure refrigerant R134a so that it can charge the desired amount in the system accurately. The charging system consists of a platform, an LCD, plastic pipe, mechanical controlled valve and charging hose. The refrigerant cylinder was placed on the platform which measures the weight of the cylinder. The LCD displays the weight and also acts as a control panel. One charging hose was connected with the outlet of the cylinder and inlet of the valve and another one was connected with the outlet of valve and inlet of the service port. Using this charging system refrigerants were charged into the system according to desired amount and handing control. After opening the charging hose, the R134a refrigerant pass through compressor and we is checked the pressures before condenser till become 2.3 bar and before evaporator 0.016 bar then stopping by close the valve. After taking the readings and data for pure refrigerant system is varied with parameters such as; heat flux and mass flow rate. Then in second step injection of nanoparticles is done to the system directly by first reduce the amount R134a refrigerant of system pressure by open the valve port slowly when become pressure less than 2 bar. A 0.25 gm from CuO nanoparticles are again injected with pure refrigerant R134a after connect the refrigerant cylinder by the main valve port. This concentration of copper oxide 0.25 gm to system, become R134a+0.25% CuO after pure R134a.

CHAPTER-6

RESULTS AND DISSCUTION

6.1 Performance of domestic nanorefrigeration system / nanorefrigerant (R134a+ CuO)

In the present experimental study, three cases have been considered. The hermetically sealed compressor is made to function under following conditions:

i) Volumetric concentration of CuO in R134a (0.25% -2%) with an increase in concentration by 0.25% in each step.

ii) Mass flow rate 10 LPH and 15 LPH.

iii) Constant heat flux at 35°C -36°C evaporator temperature and variation in heat flux at 40°C -25°C evaporator temperature

6.1.1 Constant heat flux /constant temperature of evaporator (35-36°C) (constant cooling load)

6.1.1.1 The performance at mass flow rate 10 LHP

Evaporator is maintained at 35-36°C, constant cooling load, under above condition it is decided to study the pressure and temperature variation across the condenser and evaporator of system.

Condenser pressure drop = P_{inlet}-P_{outlet} Condenser temperature drop = T_{inlet}-T_{outlet}

Evaporator pressure drop = P_{outlet}-P_{inlet} Evaporator temperature gain= T_{outlet}-T_{inlet}

Pressure drop in condenser

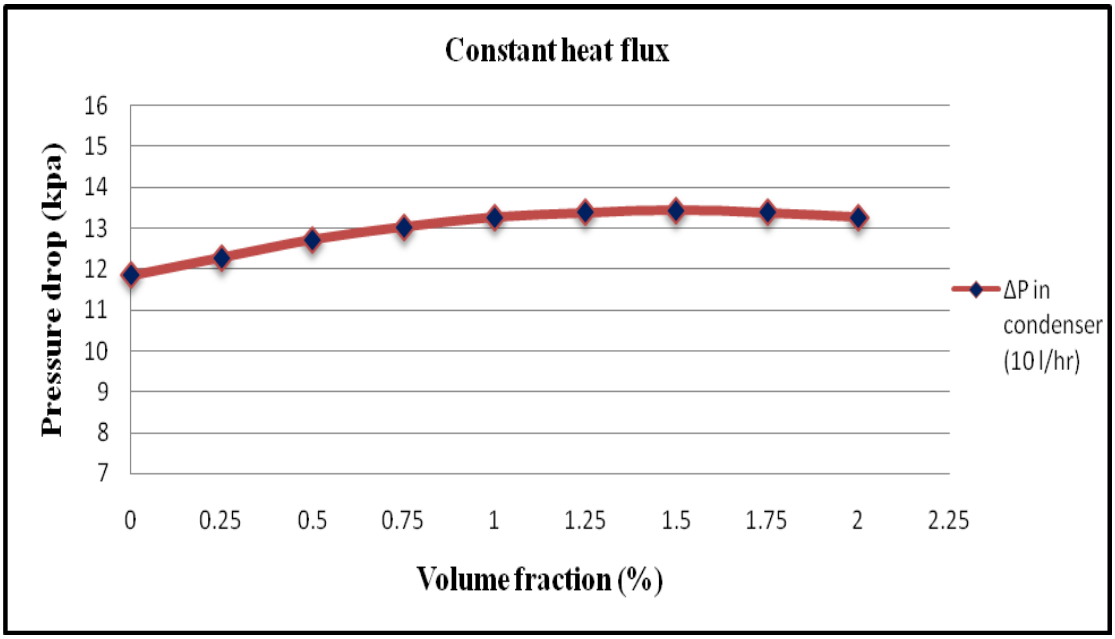

Figure 6.1: Pressure drops in condenser at constant cooling load (35-36°C) and 10 LPH

Figure 6.1 shows the pressure drop in condenser at constant cooling load (35-36°C) and at mass flow rate 10 LPH with different volumetric concentration of CuO in refrigerant R134a, it has been found that pressure drop enhancements across the condenser is minimum when pure refrigerant R134a is used which is equal 11.84 kpa. It has been increased nonlinearly with concentration and becomes maximum at volume fraction 1.5% which is equal 13.43 kpa. Then again reduces to 13.26 kpa at 2% concentration of CuO and the difference is only 1.42 kpa (11.8%) compared to pure refrigerant R134a. This will be increase the load on the compressor and hence will affect the system performance.

Pressure drop in evaporator

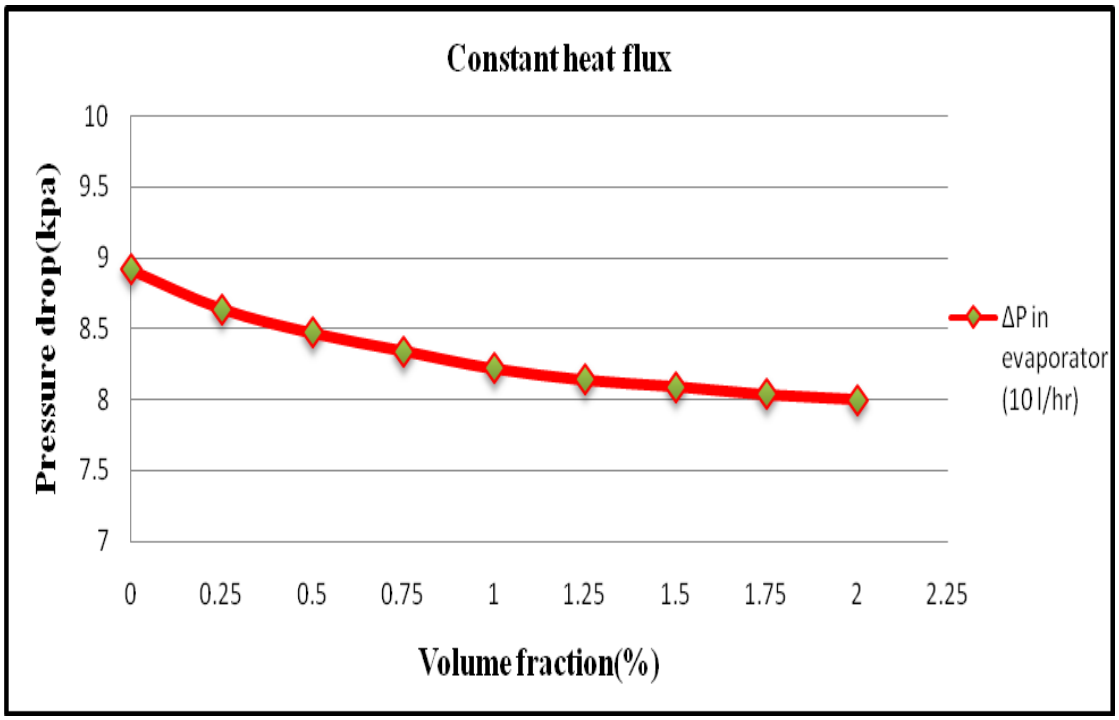

Figure 6.2: Pressure drop in evaporator at constant cooling load (35-36°C) and 10 LPH

Figure 6.2 shows the pressure drop in evaporator at constant cooling load (35-36°C) and at a mass flow rate of 10 LPH with different volumetric concentration of CuO in refrigerant R134a, the pressure drop is the maximum when pure refrigeration R134a (8.92 kpa) then it has been decreased with concentration and becomes minimum at volume fraction of 2% which is equal 8 kpa and the maximum difference is only 0.92 kpa compared to pure refrigerant R134a. A 10.3% reduction in pressure across evaporator will increase the load on the compressor; hence will affect the performance of the system.

Temperature drop in Condenser

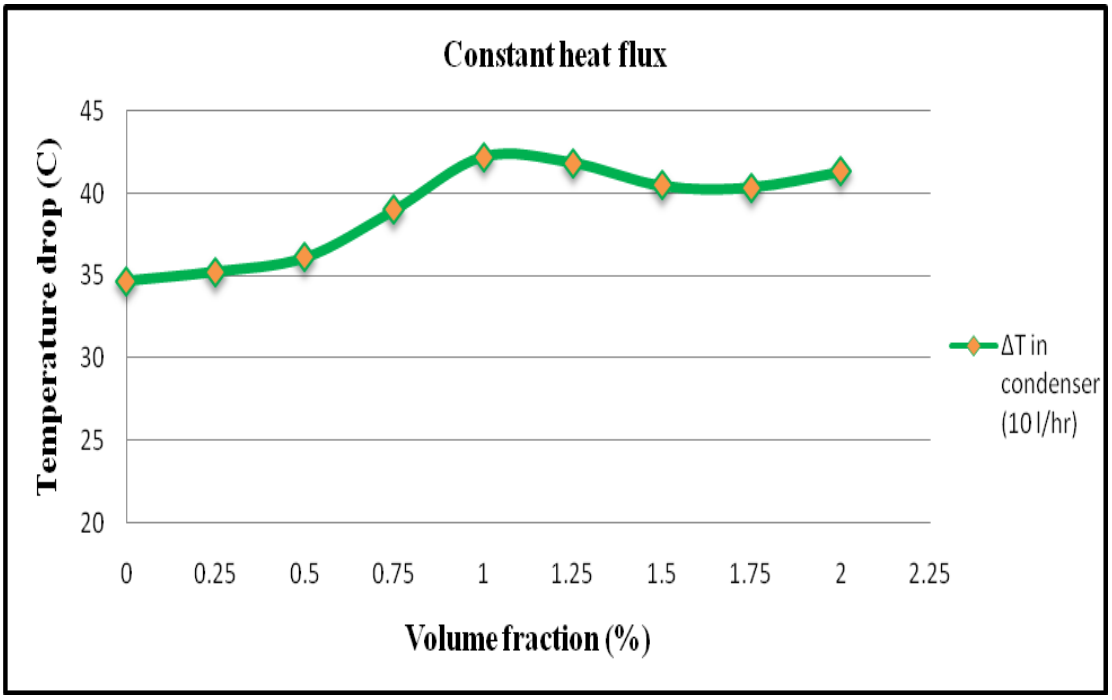

Figure 6.3: Temperature drop in condenser at constant cooling load (35-36°C) and 10 LPH

Temperature drop in evaporator

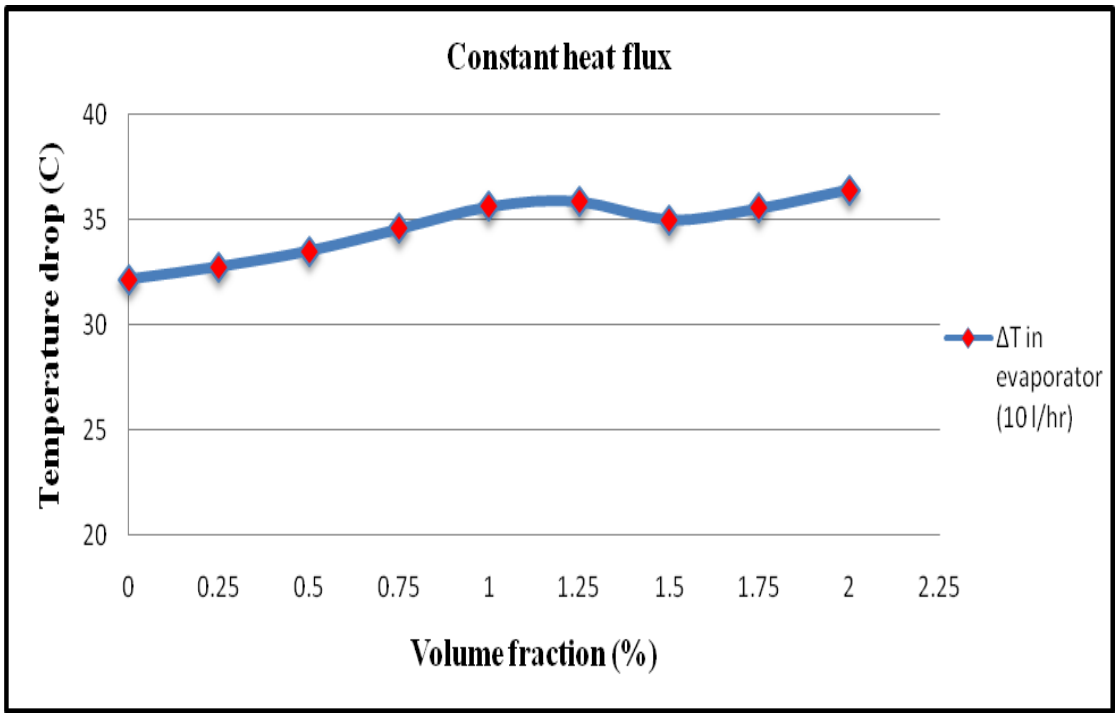

Figure 6.4 Temperature drops in evaporator at constant cooling load (35-36°C) and 10 LPH

Figure 6.3 shows the temperature drop in condenser at constant cooling load (35-36°C) and at mass flow rate of 10 LPH with different volumetric concentration of CuO in refrigerant R134a, the temperature drop is minimum when pure refrigerant R134a is used which is equal 34.7°C then it has been increased with concentration and becomes maximum at volume fraction 1% which is equal 42.24°C.Then it reduces to 40.38°C at volume fraction of 1.75% and again increases to 41.36°C at volume fraction of 2%. Maximum difference is of 7.54°C (17.85%) compared with pure refrigerant R134a at 1% volume concentration of CuO nanoparticles. High heat transfer to surrounding is observed because of increase in heat transfer coefficient of nanorefrigerant. Figure 6.4 shows the temperature drop in evaporator at constant cooling load (35-36°C) and at mass flow rate of 10 LPH with different volumetric concentration of CuO in refrigerant R134a. Temperature drop is minimum when pure refrigeration R134a is used which is equal 32.17°C then it has been increased with concentration to become maximum at volume fraction of 1.25% which is equal 35.88°C. The maximum observed difference is of 4.27°C (10.34%) compared with pure refrigerant R134a at 1.25% concentration of CuO nanoparticles. High heat transfer from water in the evaporator because of nanorefrigerant is believed to be the prime reason behind the enhanced temperature drop across the evaporator.

Compressor power consumption at 10 LPH

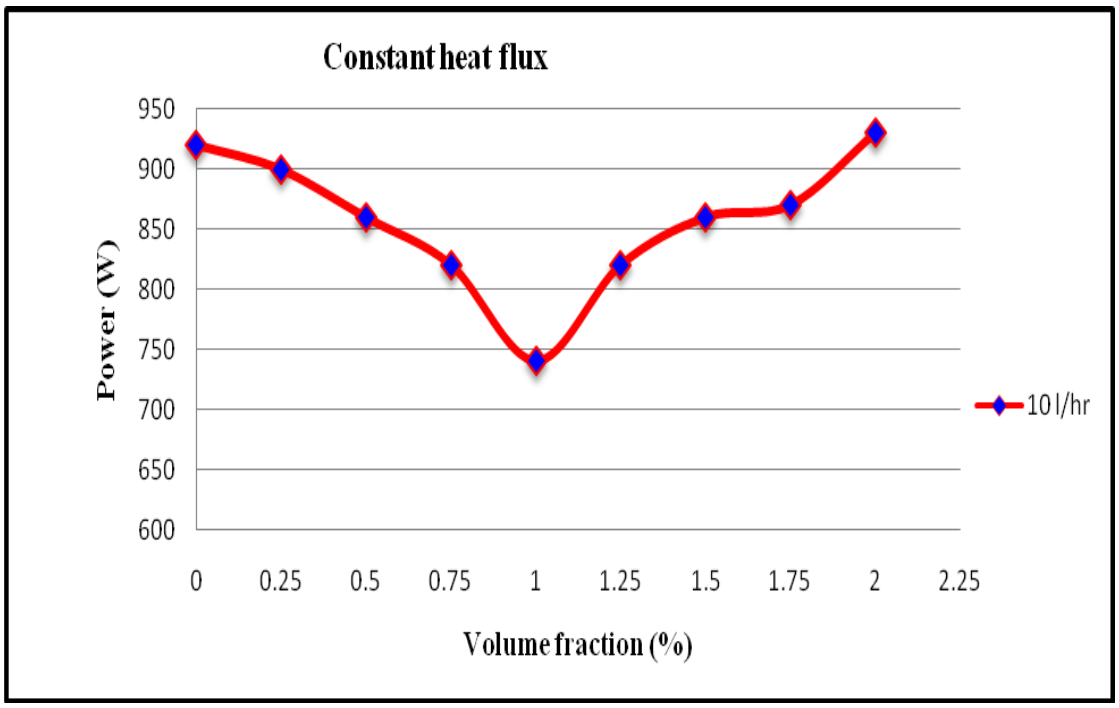

Figure 6.5: Compressor power consumption at constant cooling load (35-36°C) and 10 LPH

Figures 6.5 shows compressor power consumption at constant cooling load (35-36°C) and at mass flow rate of 10 LPH. The compressor power consumption to run the refrigeration system at a particular concentration is calculated after running the system for six hours. This value is 920W for pure refrigerant R134a. It is observed that power consumption decreases with volume fraction of CuO in refrigerant R134a. It becomes minimum at volumetric concentration of 1% which is equal 800W with maximum deference 120W (13%).Then again it is increases with concentration of CuO and becomes maximum 930W at 2% concentration. This is because the nanorefrigerant has been viscous nanofluid at higher concentration which needed more power to compress. Also because of more friction losses of viscous nanorefrigerant in evaporator, condenser and system tubes more work input is required in compressor.

COP of refrigeration system at 10 LPH

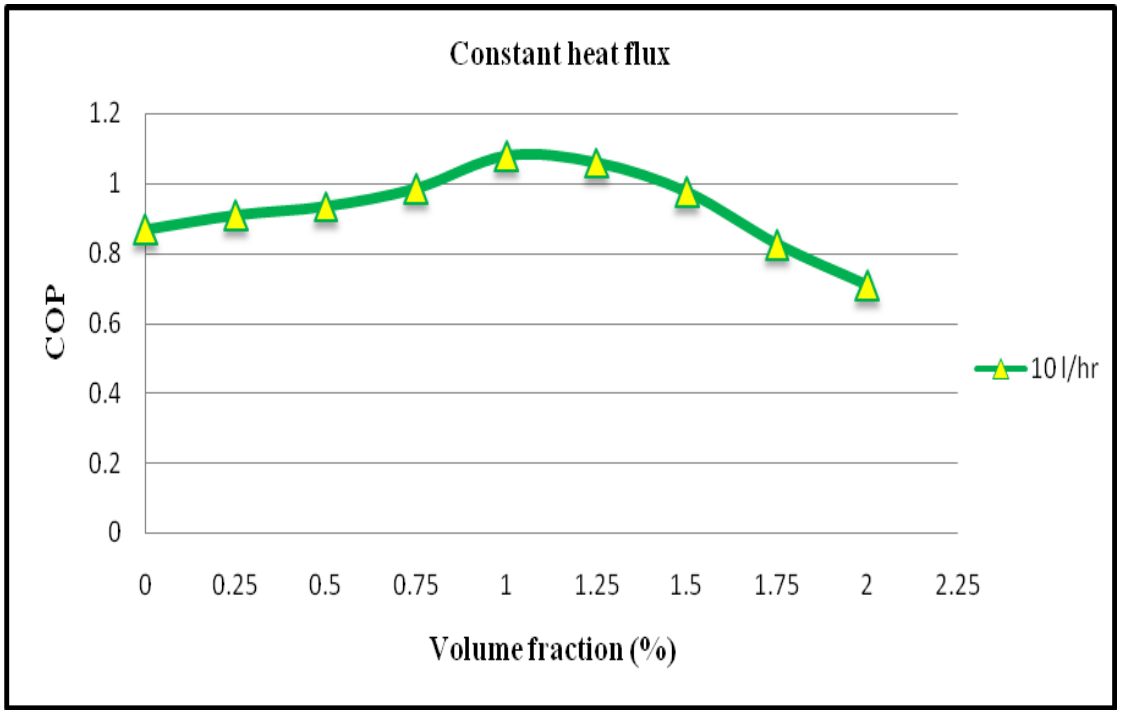

Figure 6.6: COP of system at constant cooling load (35-36°C) and of 10 LPH

Figure 6.6 shows COP of system at constant cooling load (35-36°C) and at mass flow rate of 10 LPH. COP of system increases with increases in concentration and becomes maximum (1.081) at the concentration equal 1%, where as for pure refrigerant R134a it is equal 0.869.This increasing

is 20%. Beyond 1% of concentration COP start decreasing and becomes minimum (0.709) for this system at 2% of concentration. This is because the fluid flow becomes viscous flow at higher concentration of CuO nanoparticles. This raises the power requirements of the compressor at constant heat flux.

6.1 The performance with mass flow rate at 15 LPH

Pressure drop in condenser

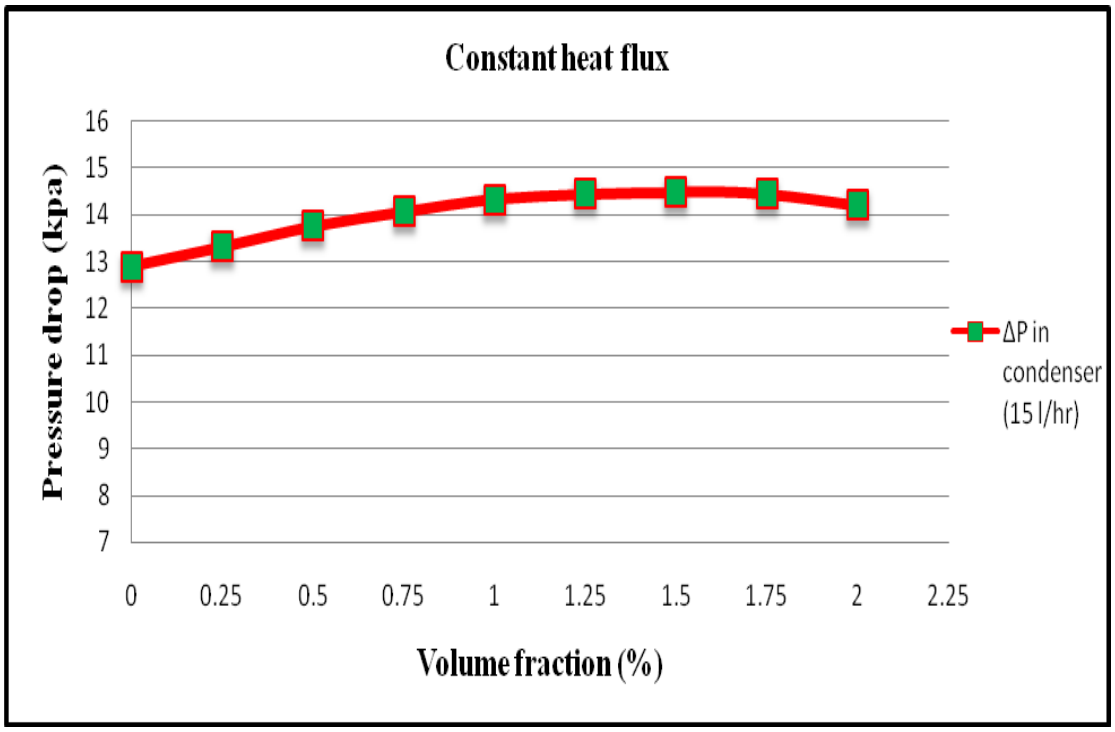

Figure 6.7: Pressure drops in condenser at constant cooling load (35-36°C) and 15 LPH

Figure 6.7 shows the pressure drop in condenser at constant cooling load (35-36°C) and at mass flow rate 15 LPH with different volumetric concentration of CuO in refrigerant R134a. it has been found that pressure drop enhancements across the condenser is minimum when pure refrigeration R134a is used which is equal 12.89 kpa. It has been increased nonlinearly with concentration and becomes maximum at volume fraction 1.5% which is equal 14.48 kpa. Then again reduces to 14.2 kpa at 2% concentration of CuO and the difference is only 1.59 kpa (10.9%) compared to pure refrigerant R134a. This will be increase the load on the compressor and hence will affect the system performance.

Pressure drop in evaporator

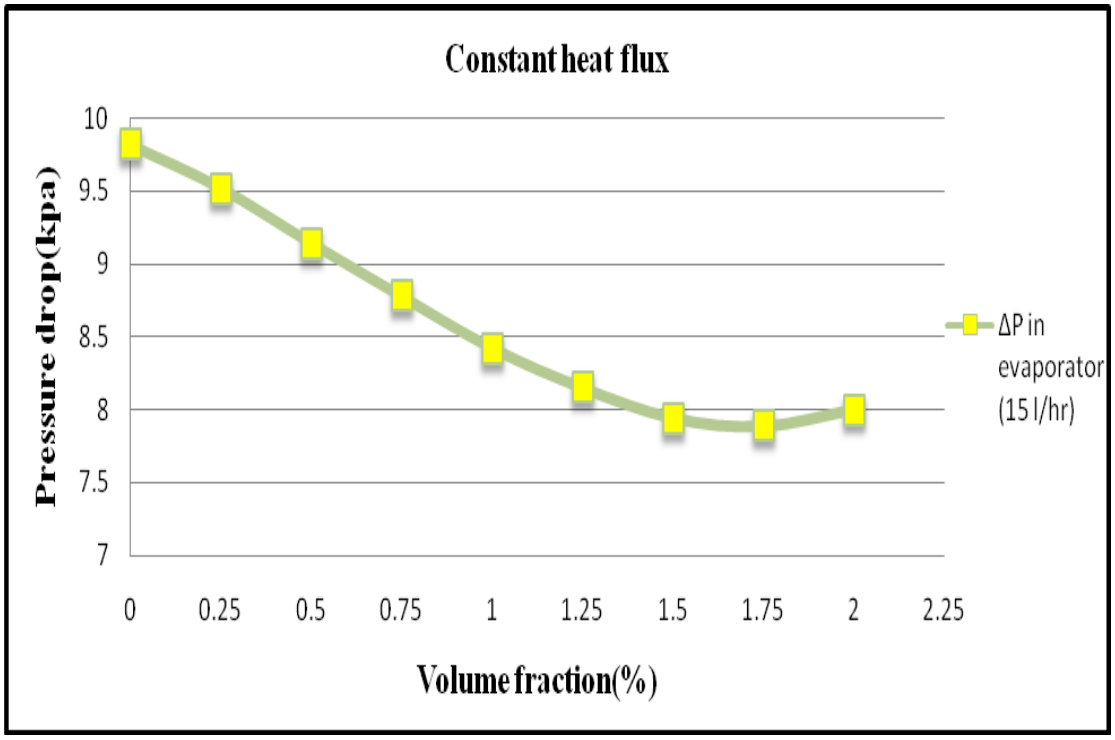

Figure 6.8: Pressure drop in evaporator at constant cooling load (35-36°C) and 15 LPH

Figure 6.8 shows the pressure drop in evaporator at constant cooling load (35-36°C) and at mass flow rate of 15 LPH with different volumetric concentration of CuO in refrigerant R134a. The pressure drop is the maximum (9.82kpa) when pure refrigeration R134a is used. Then it decreases with increase in concentration of CuO and becomes minimum (8kpa) at volume fraction of 2%. The maximum difference is only 1.82 kpa compared to pure R134a refrigerant. A 18.5% reduction in pressure across evaporator will increase the load on the compressor, hence will affect the performance of the system.

Temperature drop in condenser and evaporator

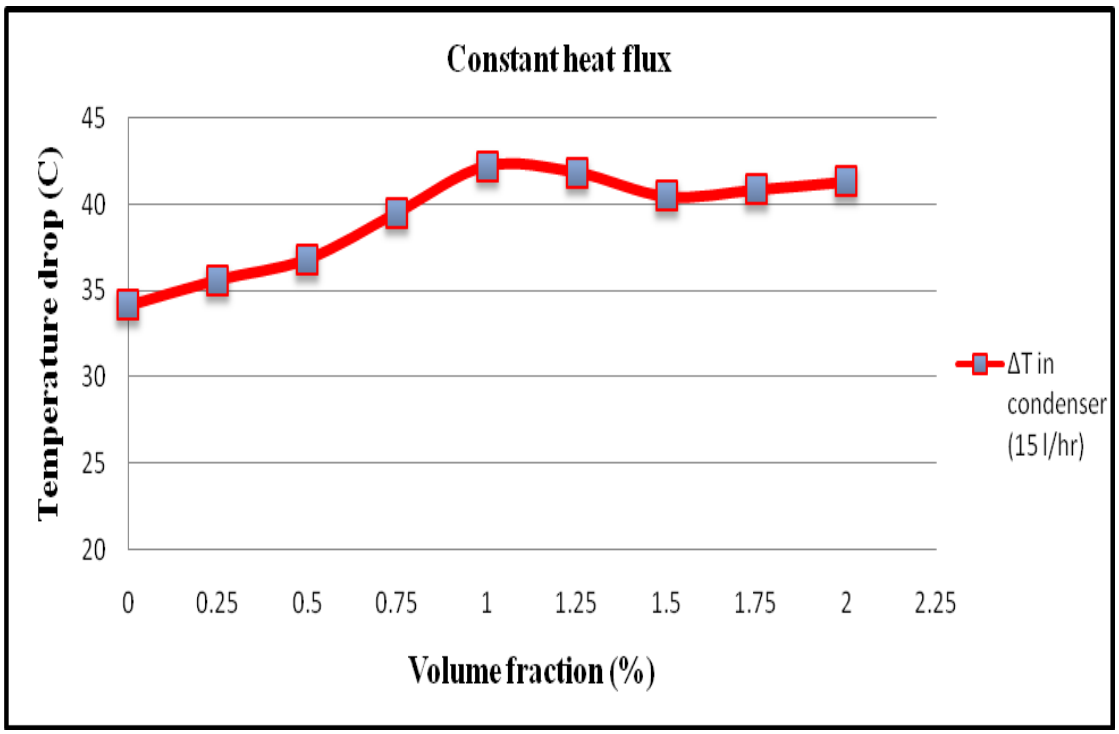

Figure 6.9: Temperature drop in condenser at constant cooling load (35-36°C) and 15 LPH

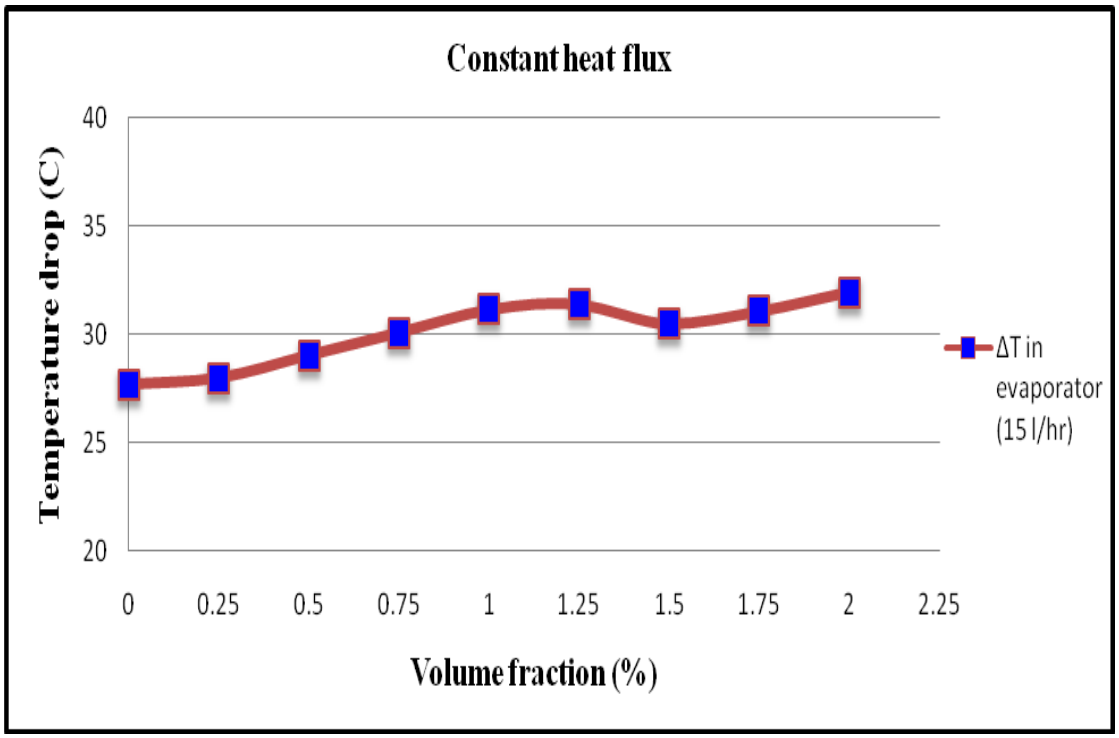

Figure 6.10: Temperature drop in evaporator at constant cooling (35-36°C) load and 15 LPH

Figure 6.9 shows the temperature drop in condenser at constant cooling load (35-36°C) and at mass flow rate of 15 LPH with different volumetric concentration of CuO in refrigerant R134a. The temperature drop is minimum when pure refrigeration R134a is used which is equal 34.18°C. Then it has been found increasing with concentration and becomes maximum at volume fraction 1% which is equal 42.24°C. Then it reduces to 40.38°C at volume fraction of 1.75% and again increases to 40.88°C at volume fraction of 2%. Maximum difference is of 8.06°C (19%) compared with pure refrigerant R134a at 1% volume concentration of CuO nanoparticles. High heat transfer to surrounding is observed because of increase in heat transfer coefficient of nanorefrigerant. Figure 6.10 shows the temperature drop in evaporator at same conditions with of concentrations of CuO in refrigerant R134a. Temperature drop is minimum when pure refrigerant R134a is used which is equal 27.67°C. It increases with concentration and becomes maximum at volume fraction of 1.25% which is equal 31.38°C. The maximum observed difference is of 4.27°C (13.6%) compared with pure refrigerant R134a at 1.25% concentration of CuO nanoparticles. High heat transfer from water in the evaporator because of nanorefrigerant is believed to be the prime reason behind the enhanced temperature drop across the evaporator.

Compressor power consumption at 15 LPH

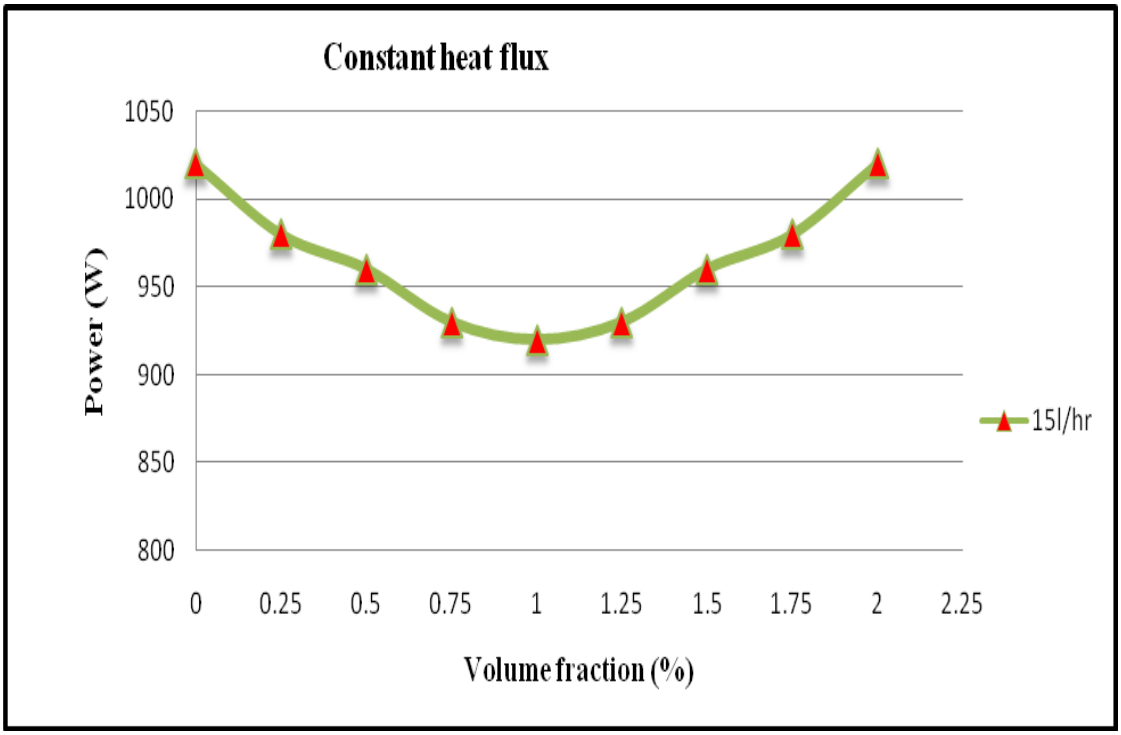

Figure 6.11: Compressor power consumption at constant cooling load (35-36°C) and 15 LPH

COP of refrigeration system at 15 LPH

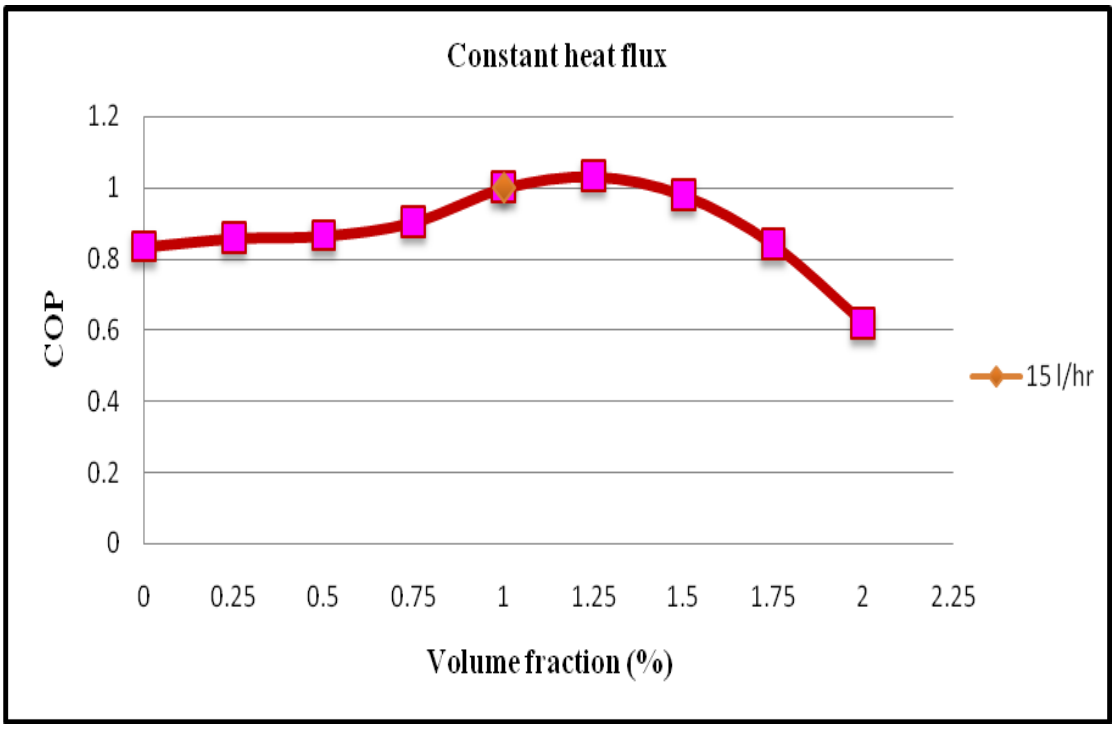

Figure 6.12: COP of system at constant cooling load (35-36°C) and 15 LPH

Figures 6.11 show the compressor power consumption at constant cooling load and at mass flow rate of 15 LPH. The compressor power consumption needed to run the refrigeration system is 1020W for pure R134a refrigeration. It has been found decreasing with volume fraction of CuO in refrigerant R134a and it becomes minimum (920W) at volumetric concentration of 1%. Then it again increases with increase in concentration of CuO nanoparticles and becomes maximum (1020W) at 2% concentration. As the nanorefrigerant has been viscous nanofluid, required more power to compress. Also friction flow losses of viscous nanorefrigerant in evaporator, condenser and system tubes are increased and need more work from compressor.

Figure 6.12 shows COP of system at constant cooling load and at mass flow rate of 15 LPH. COP of system increases with increases in concentration and becomes maximum (1.032) at the concentration equal 1.25%, where as for pure refrigerant R134a it is equal 0.833.This increase is by 19.3%. Beyond 1% of concentration, COP start decreasing and becomes minimum (0.617) for this system at 2% of concentration. This is because the fluid flow becomes viscous flow at higher concentration of CuO nanoparticles. This raises the power requirements of the compressor at constant heat flux.

6.1.3 Comparison the pressure drop and temperature drop, power consumption and COP at mass flow rates of 10 & 15 LPH

Pressure drop in condenser and evaporator

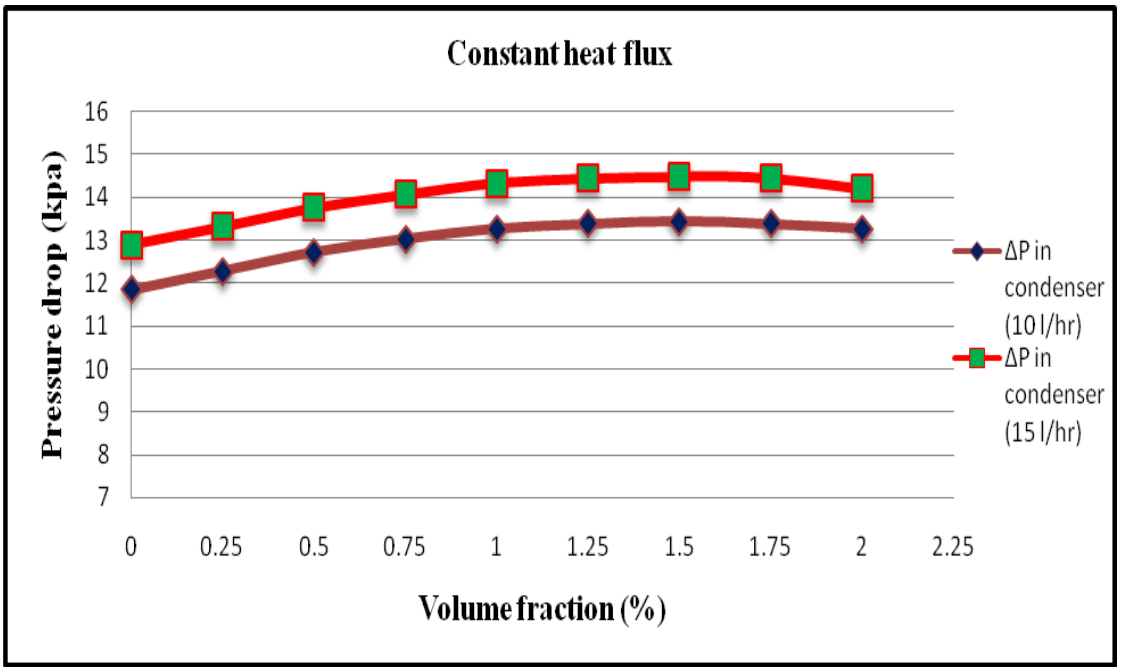

Figure 6.13: Pressure drop in the condenser at constant cooling load (35-36°C) and10 & 15 LPH

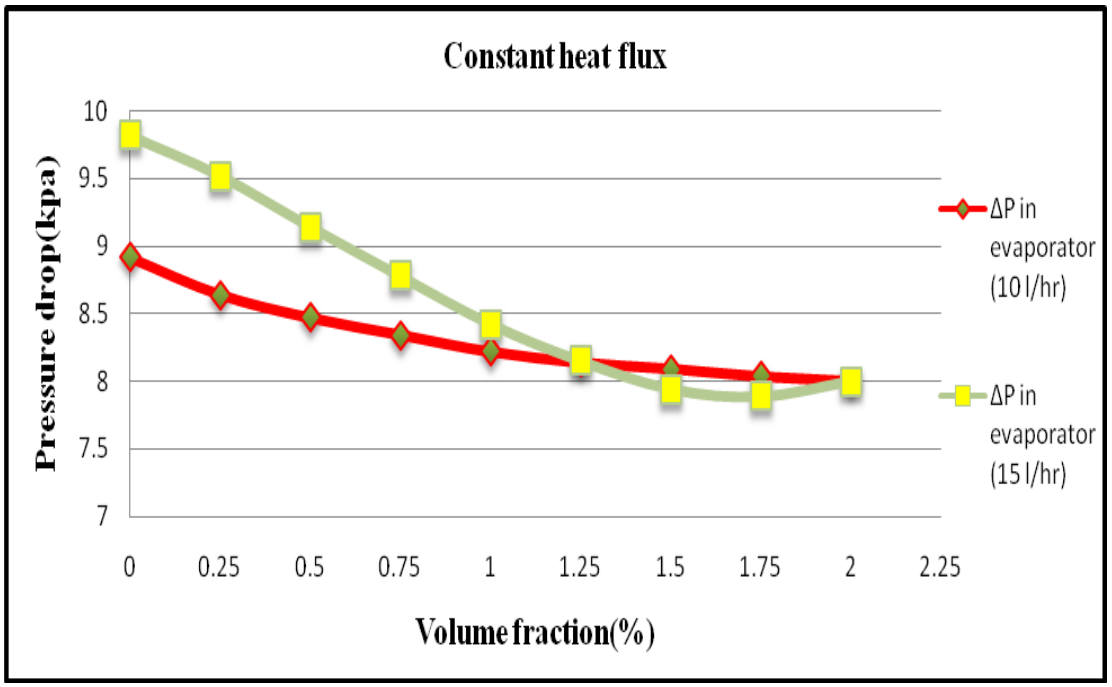

Figure 6.14: Pressure drops in evaporator at constant cooling load (35-36°C) and 10 &15 LPH

Figure 6.13 shows the pressure drop in condenser at constant cooling load (35-36°C) and at mass flow rate of 10 &15 LPH with different volumetric concentration of CuO in refrigerant R134a. It has been found that pressure drop across the condenser is minimum when pure refrigerant R134a is used which is equal to 11.84 kpa at 10 l/hr and 12.89 kpa at 5 LPH. This increases nonlinearly with increase in concentration and becomes maximum (13.43 kpa and 14.48 kpa) for both mass flow rates (10 &15 LPH) at volume fraction of 1.5%. Then again it reduces to 13.26 kpa and 14.2 kpa at 2% concentration of CuO nanoparticles.

Figure 6.14 shows the pressure drop in evaporator at constant cooling load (35-36 ^{0}C) and at mass flow rate of 10 and 15 LPH with different volumetric concentration of CuO in R134a refrigerant. Pressure drop is maximum (8.92 kpa & 9.82 kpa) compared to pressure drop for pure refrigerant R134a. Then it decreases to 8 kpa for both mass flow rates at concentration of 2 %.

Temperature drop in condenser

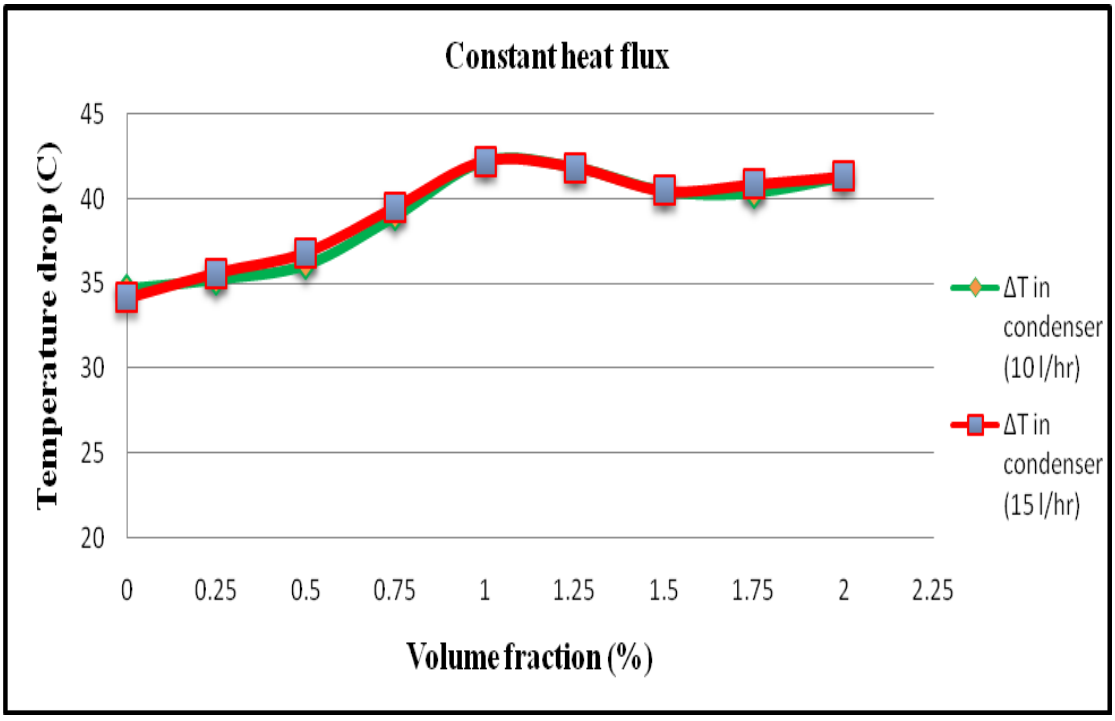

Figure 6.15: Temperature drop in condenser at constant cooling load (35-36°C) and 10 &15 LPH

Temperature drop in evaporator

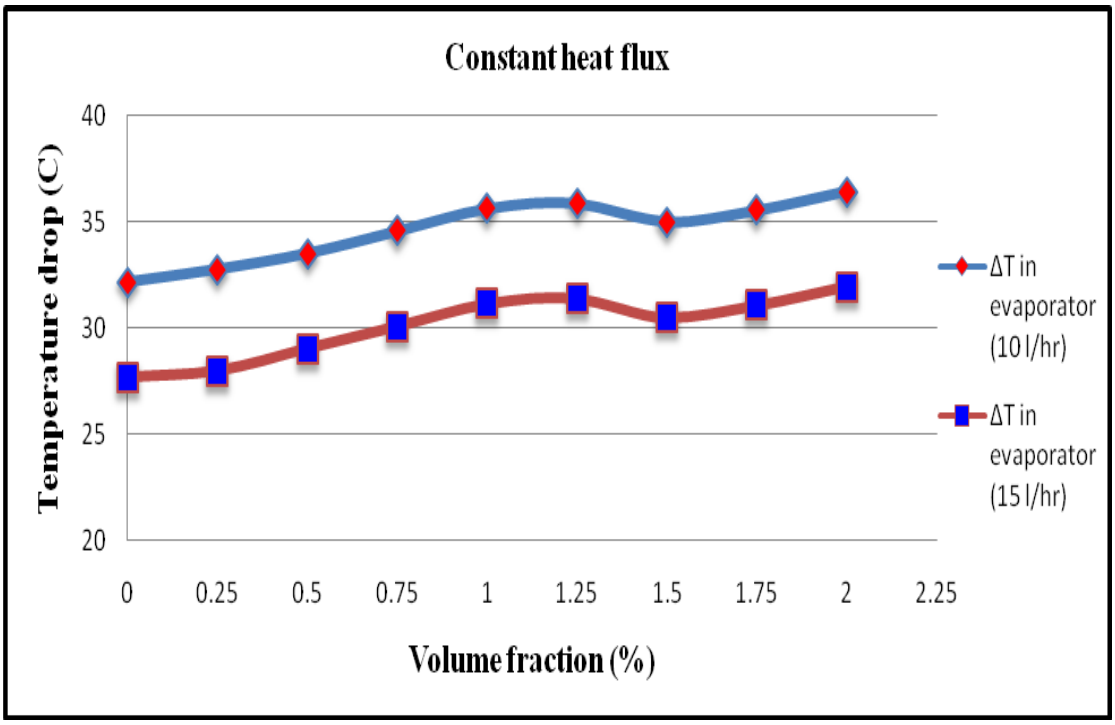

Figure 6.16: Temperature drop in evaporator at constant cooling load (35-36°C) and 10 &15 LPH

Figure 6.15 shows the temperature drop in condenser at constant cooling load (35-36°C) and at mass flow rates of 10 & 15 LPH with different volumetric concentration of CuO in refrigerant R134a. For both mass flow rates temperature drop is minimum (34.7°C and 34.18°C) when pure refrigerant R134a is used. It has been found increasing with increases in concentration and becomes maximum (42.24°C) at volume fraction of 1% for both mass flow rates. Then again it increases to become finally 41.36°C and 40.88°C at volume fraction 2 % and the maximum difference is 7.54°C (17.85%) and 8.06°C (19%) compared with pure refrigerantR134a at 1% of CuO concentration.

Figure 6.4 shows the temperature drop in evaporator at constant cooling load (35-36°C) and at mass flow rates of 10 & 15 LPH with different volumetric concentration of CuO in refrigerant R134a. The temperature drop enhancements is the minimum when pure refrigerant R134a is used which is equal 32.17°C and 27.67°C. Then it has been found increasing with increases in concentration and becomes maximum at volume fraction 1.25% for both mass flow rates which

is equal 35.88°C and 31.38°C. Then finally it increases to 36.44°C and 30.94°C at volume fraction 2% and the maximum difference is 4.27°C (10.34%) and 4.27°C (13.6%) compared with pure refrigerant R134a at 1.25% of CuO.

Compressor power consumption and COP of refrigeration system at 10 & 15 LPH

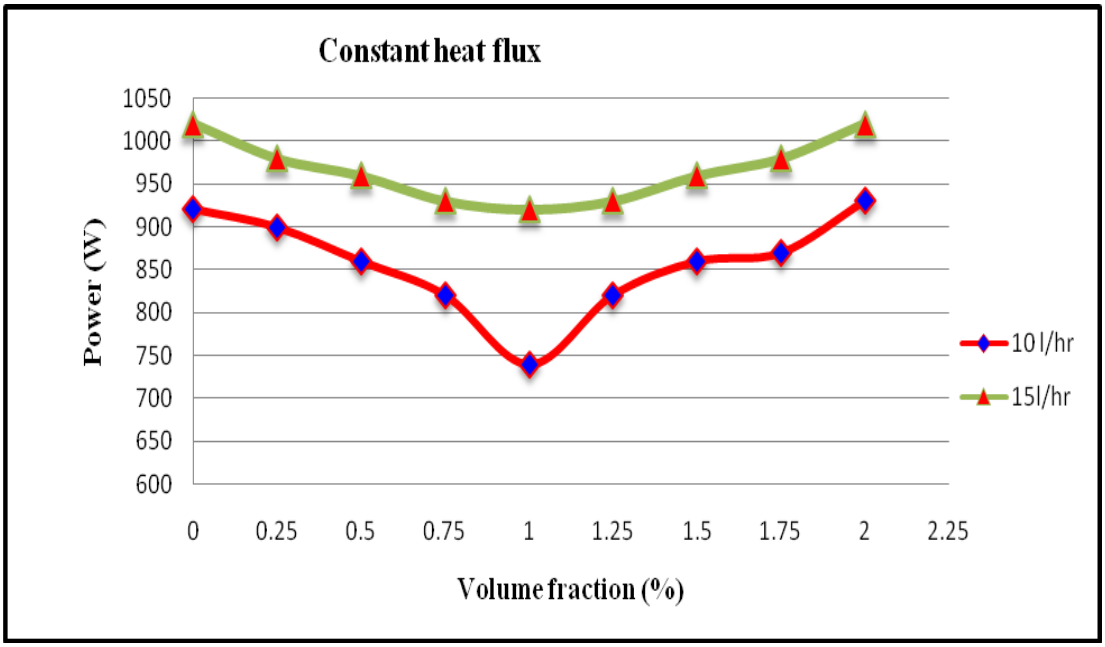

Figure 6.17: Power consumption at constant cooling load (35-36°C) and 10 & 15 LPH

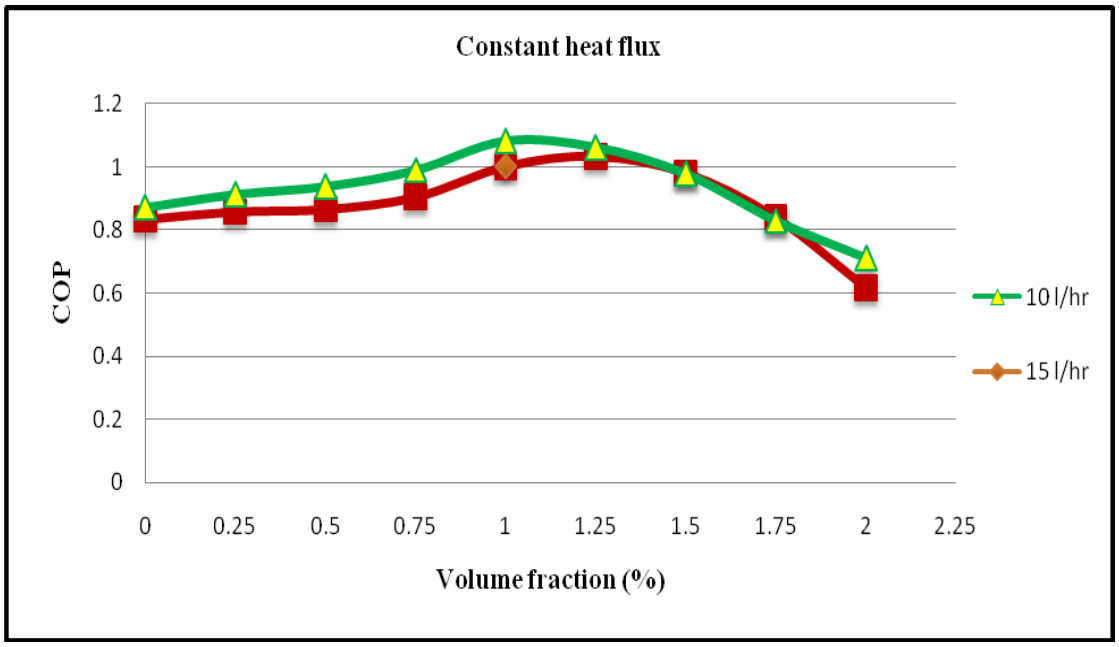

Figure 6.18: COP of system at constant cooling load (35-36°C) and 10 and 15 LPH

A figure 6.17 shows the compressor power consumption at constant cooling load and at mass flow rates of 10 and 15 LPH. For pure refrigerant R134a in both the cases the compressor power consumption needed to run the refrigeration system is 920W and 1020W. It decreases with increases in concentration of CuO in R134a refrigerant. It becomes minimum at volumetric concentration of 1% which is equal to 800W and 920W with maximum deference of 120W (13%) and 100W (10%) compared to pure refrigerant R134a. Then again it is increases with increases in concentration of CuO, finally becomes maximum (930W and 1020W) at 2% concentration.

Figure 6.18 shows COP of system at constant cooling load and at mass flow rates of 10 &15 LPH. COP of system becomes maximum (1.081 and 1.032) at concentration of 1% and 1.25%. This is compared to pure refrigerant R134a for both mass flow rates i.e. 0.869 (20%) and 0.833 (19.3%). COP becomes minimum (0.709 & 0.617) for both mass flow rates at 2% of concentration.

6.1.4 Comparison the results at (constant cooling load) condition

Figures 6.12 & 6.13 show the comparison the pressure drop through the Condenser and Evaporator in both mass flow rate 10 and 15 LPH at constant heat flux less than 2 kpa. Figures 6.14& 6.15 show at same conditions the comparison the temperature drop in condenser (19%) and evaporator (14%) are increases with concentration (maximum at range 1-1.25%). Figures 6.17 and 6.18 show the coefficient of performance (COP) calculated using the experimental data. The actual COP is calculated using the cooling load and the power input. Highest COP (19.3%) and minimum power consumption (13%) at range 1-1.25% when compare with pure R134a. that means the perfect range in case constant heat flux.

6.2 The temperature – time chart/ freezing capacity of the system

Evaporator temperature is varied from 40°C to 25 °C and for the different concentrations of CuO in refrigerant R134a time taken to reach a desired temperature has been studied

6.2.1 The performance at mass flow rate of 10 LPH

Temperature-time chart of evaporator

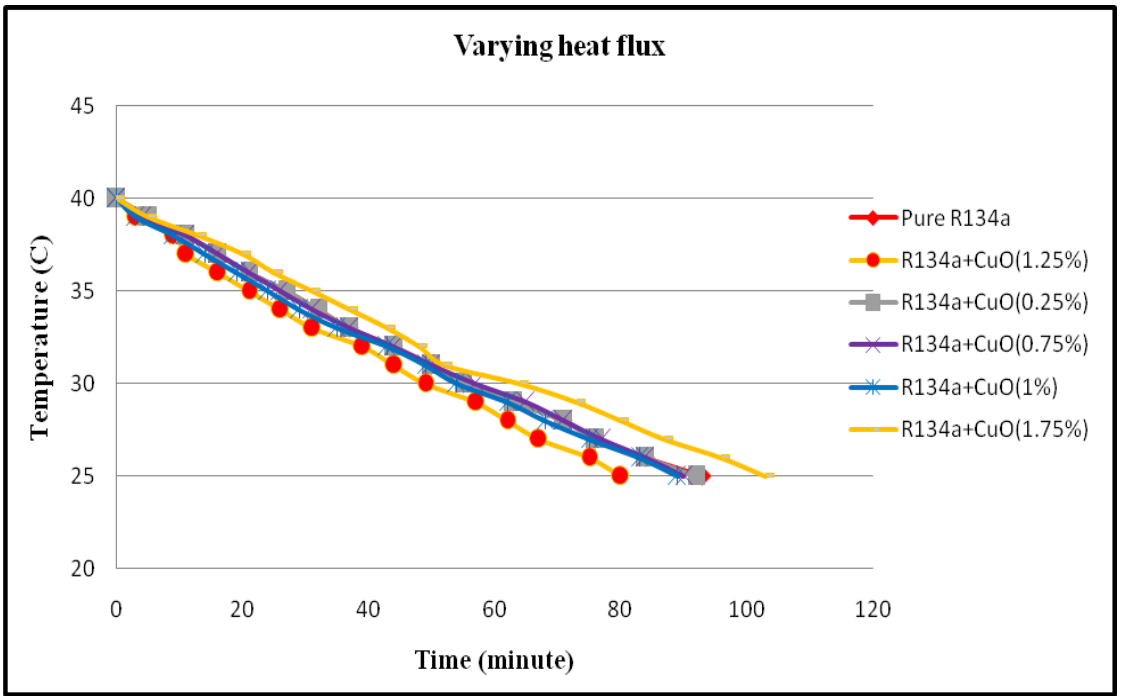

Figure 6.19: Evaporator temperature - time chart for temperature drop (40-25°C) and 10 LPH

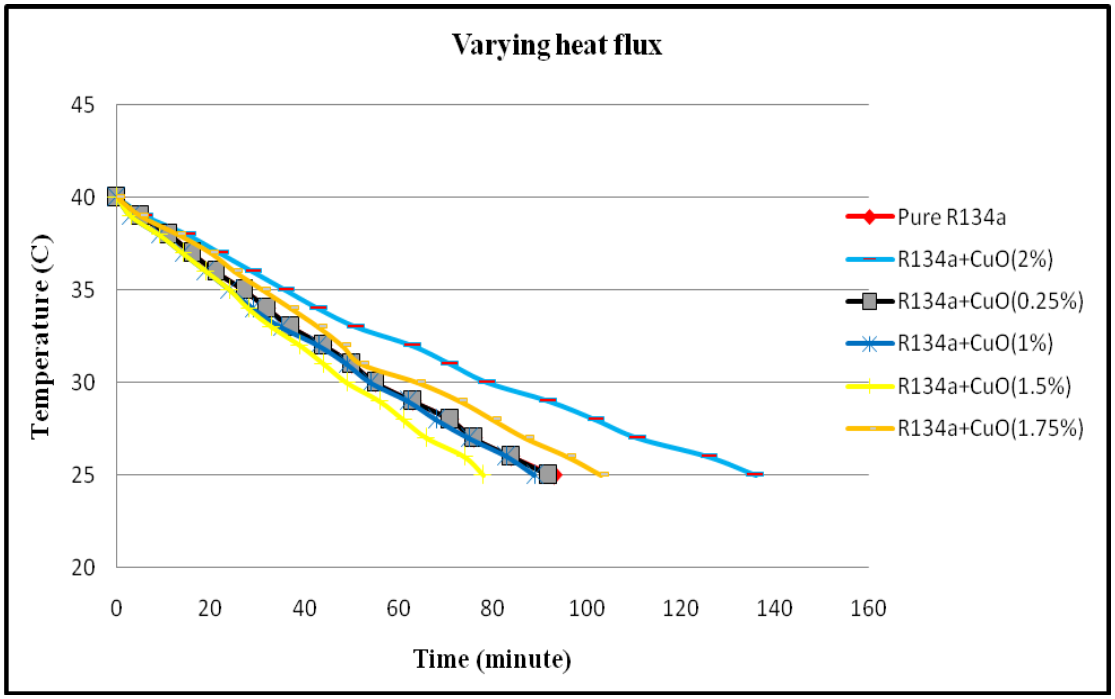

Figure 6.20: Evaporator temperature - time chart for temperature drop (40-25°C) and 10 LPH

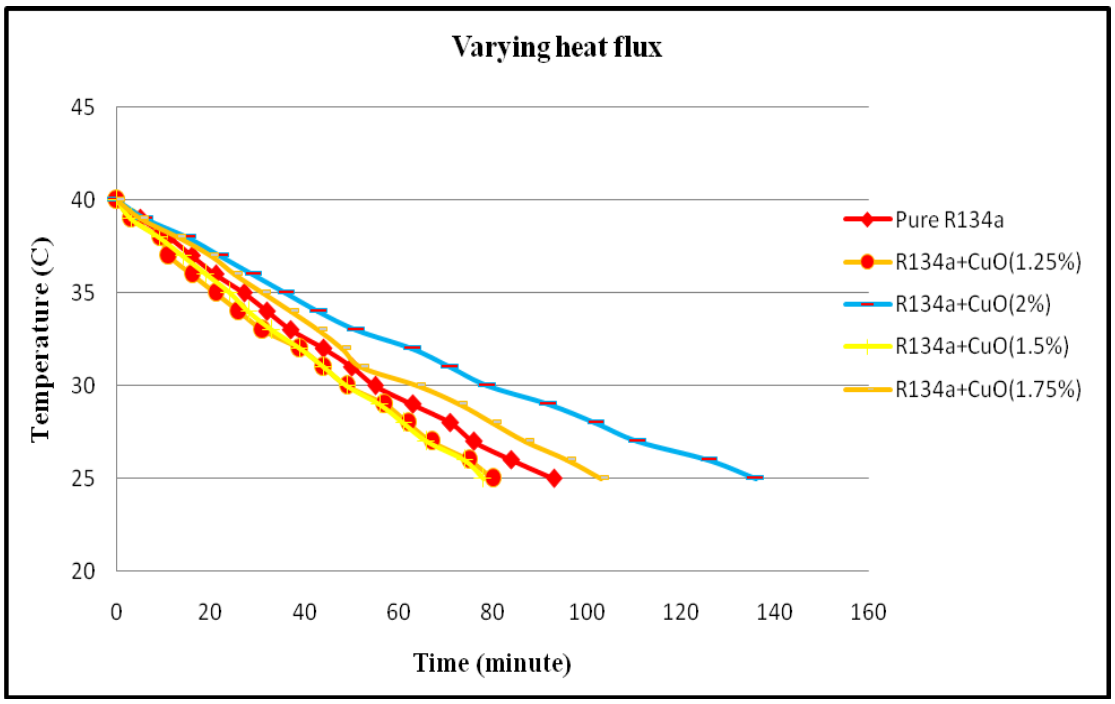

Figure 6.21: Evaporator temperature - time chart for temperature drop (40-25°C) and 10 LPH

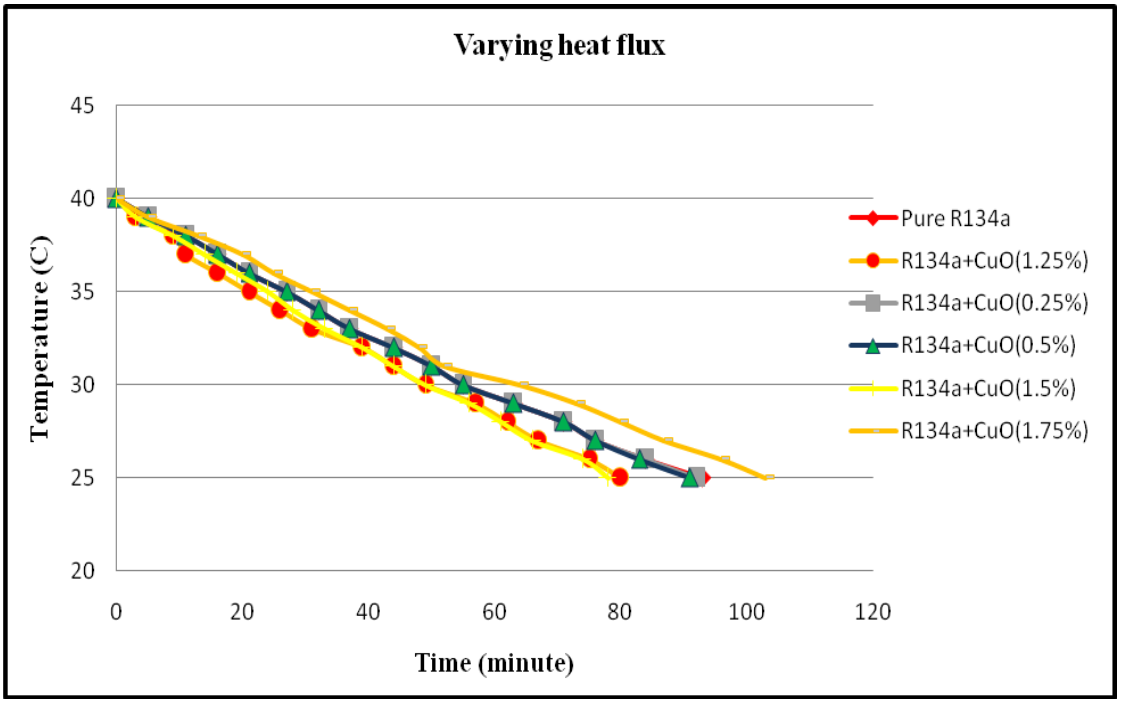

Figure 6.22: Evaporator temperature - time chart for temperature drop (40-25°C) and 10 LPH

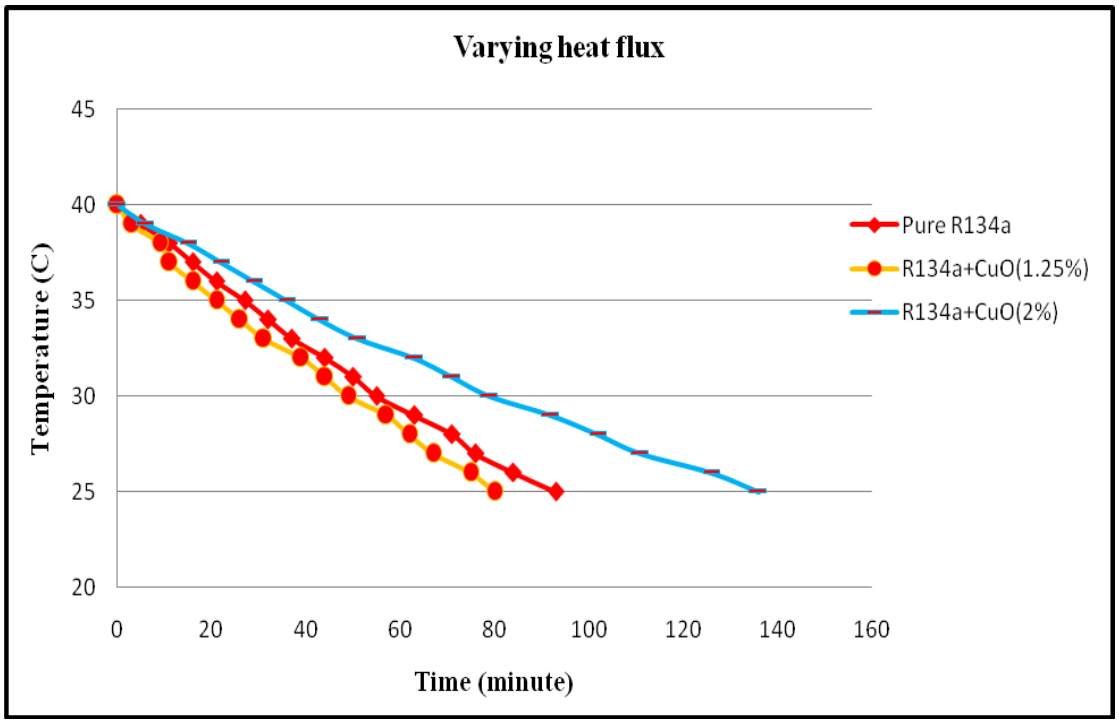

Figure 6.23: Max and Min Evaporator temperature - time chart for temperature drop (40-25°C) and 10 LPH

The cooling load temperature – time history is shown in figures 6.19, 20, 21, 22 and 23 and the freezing capacity for the different concentration of CuO in refrigerant R134a. In all the cases the condenser pressure is 2.3 bar and the evaporator pressure is 0.16 bar. No appreciable pressure drops due to friction is observed in the condenser and evaporator. From all the figures it is clear that, the time required to bring down the temperature from 40°C to 25°C is less for nanorefrigerant R134a +CuO nanoparticle mixture till 1.5% concentration than the time taken in case of pure refrigerant R134a. For example, with R134a + CuO (0.25%) nanoparticle, the time required to bring the temperature from 40- 25°C is 92 minute where as that with pure R134a is 93 minute and 83 minute with 1% concentration. It is clear that, the freezing capacity of the R134a +CuO nanoparticle mixture is higher when compared with the pure refrigerant. The time taken to reduce the temperature of the cooling load from 40- 25°C with increase in volume fraction of CuO% in mixture is minimum (76 minute) for concentration of 1.25%. Also maximum time taken is 136 minutes with concentration of 2%. This is due to the fact the nanoparticles present in the refrigerant enhances the heat transfer rate in the refrigerant side of the evaporator.

Effect of CuO nanoparticle on the freezing capacity and power consumption at 10 LPH

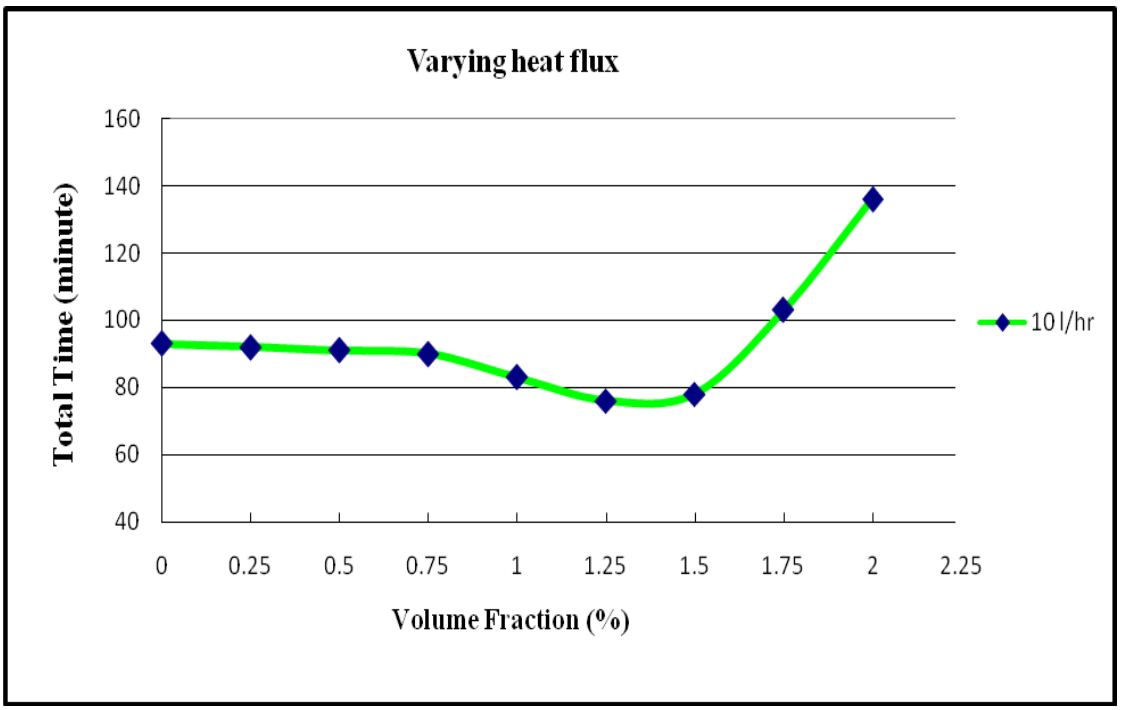

Figure 6.24: Evaporator freezing capacity for temperature drop (40-25°C) at 10 LPH

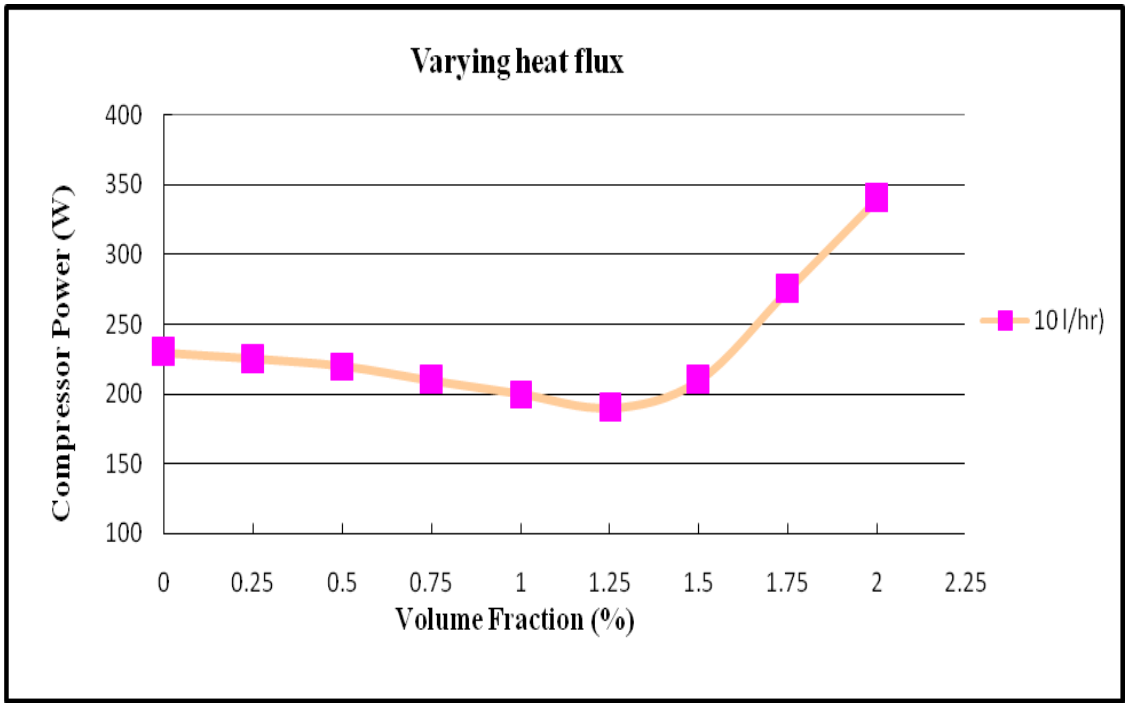

Figure 6.25: Compressor power consumption for temperature drop (40-25°C) at 10 LPH

Figure 6.24 shows evaporator freezing capacity for temperature drop from 40-25°C at mass flow rate 10 LPH. Figure shows a total time taken to bring down the temperature from 40°C to 25°C for different concentration of CuO in refrigerant R134a. Minimum time (76 minutes) is for 1.25% concentration where as time taken by pure R134a is 93 minute.

Figure 6.25 shows a compressor power requirement at varying cooling load and at mass flow rate of 10 LPH. The compressor power consumption needed to run the refrigeration system is 230W in case of pure refrigerant R134a. Then it has been found decreasing with volume fraction of CuO in refrigerant R134a, becomes minimum at volumetric concentration 1.25% which is equal 190W with maximum deference of 40W (21%). It again increases with increases in concentration of CuO, becomes maximum (340W) at 2% concentration. Because the nanorefrigerant has been viscous nanofluid which is needed more power during compression.

Comparison the results and optimization of system at mass flow rate 10 LPH

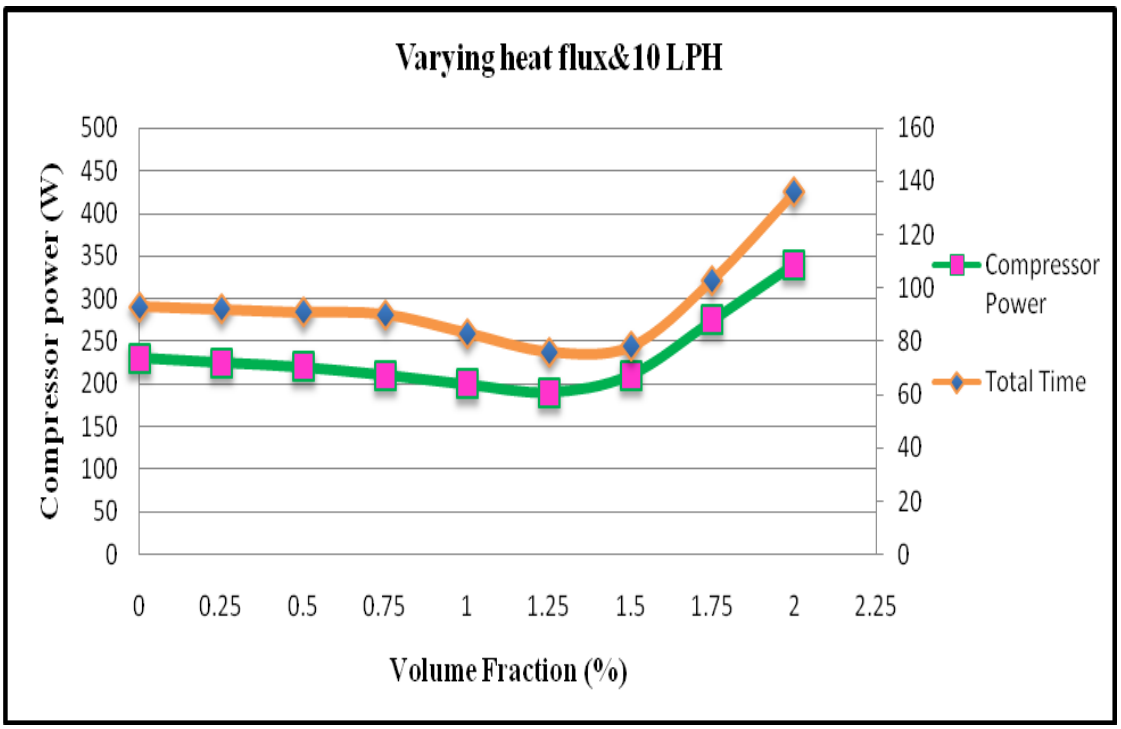

Figure 6.26: Comparison freezing capacity and power consumption at mass flow rate of 10 LPH

Figure 6.26 shows the power consumption of compressor which decreases with increase in volume fraction and becomes minimum (190W) at 1.25% concentration of CuO in refrigerant

R134a (17.4% less than what is needed for pure refrigerant R134a). This value for pure refrigerant R134a is found to be 230W.

Time taken (in minutes) to bring down the temperature from 40°C to 25°C at mass flow rate of 10 LPH is 76 minute at 1.25% concentration of CuO in refrigerantR134a. This time taken is found to be 18.27% less than the time taken (92 minutes) for pure refrigerant R134a under same conditions.

6.2.2 The performance at mass flow rate 15 LPH

Temperature-time chart in evaporator

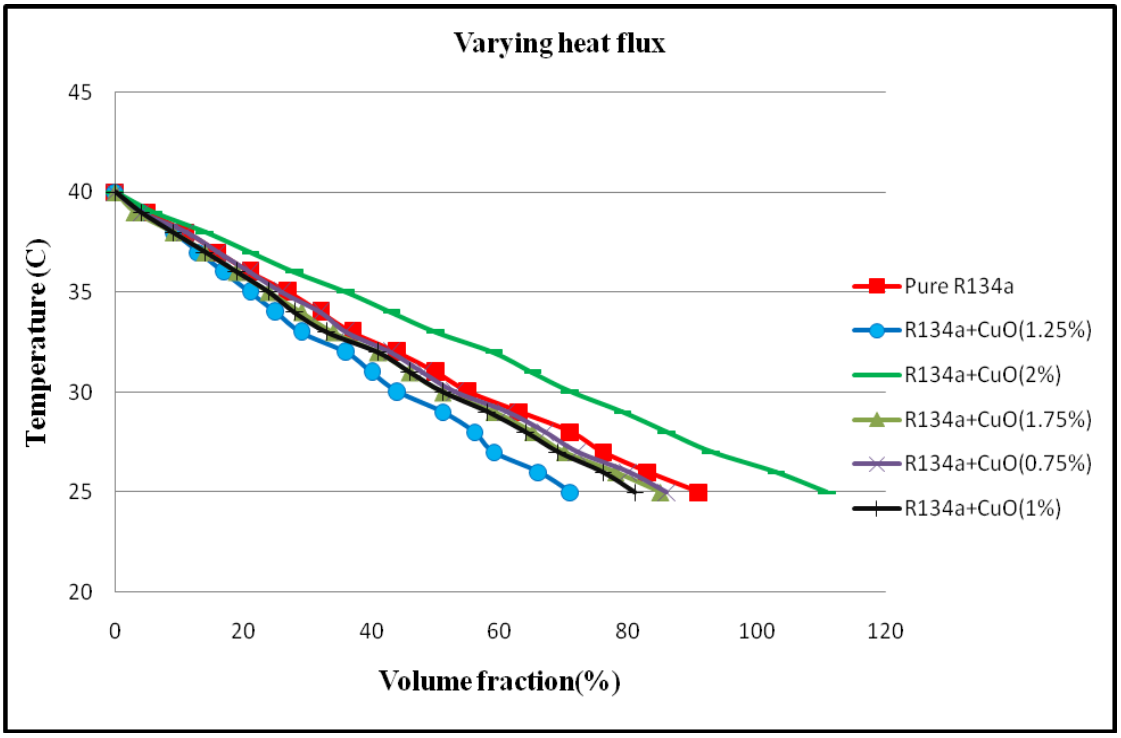

Figure 6.27: Temperature - Time chart for temperature drop (40-25°C) at 15 LPH

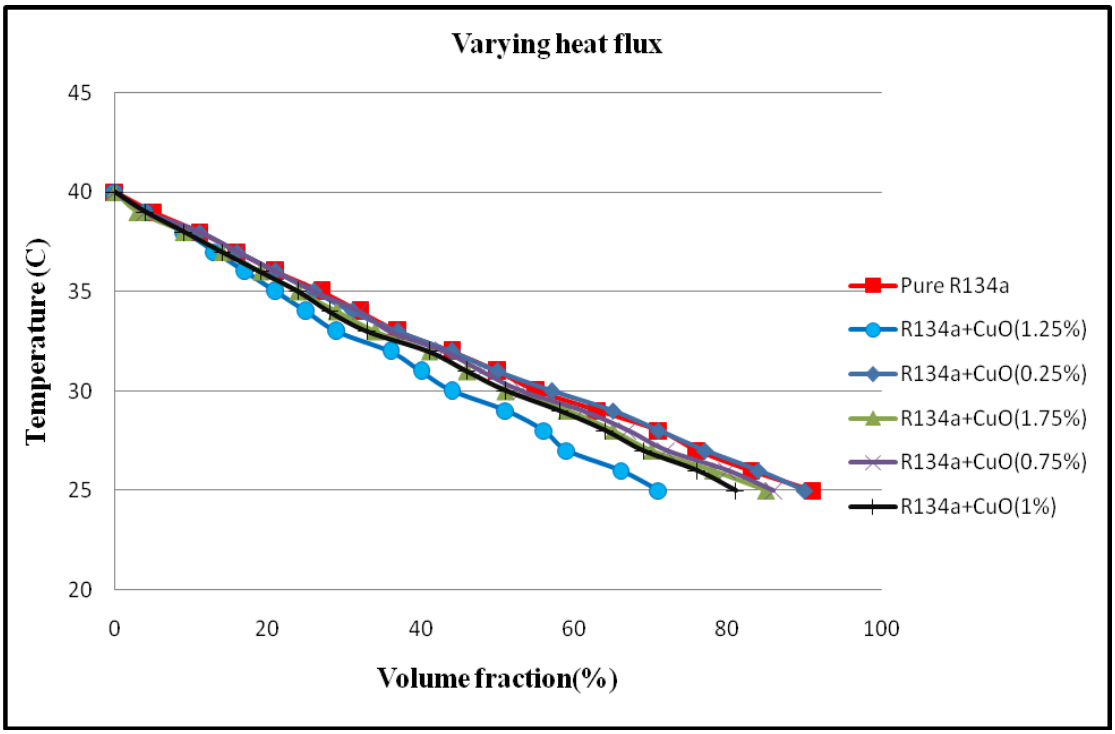

Figure 6.28: Temperature - Time chart for temperature drop (40-25°C) at mass flow rate 15 LPH

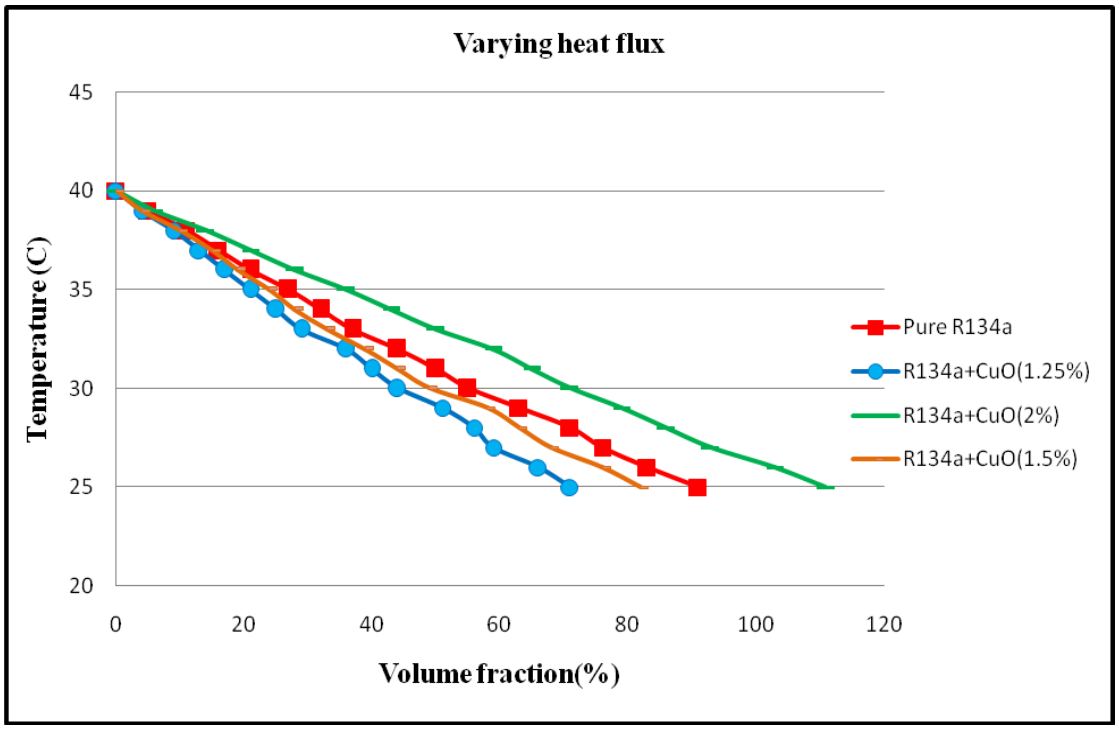

Figure 6.29: Temperature - Time chart for temperature drop (40-25°C) at 15 LPH

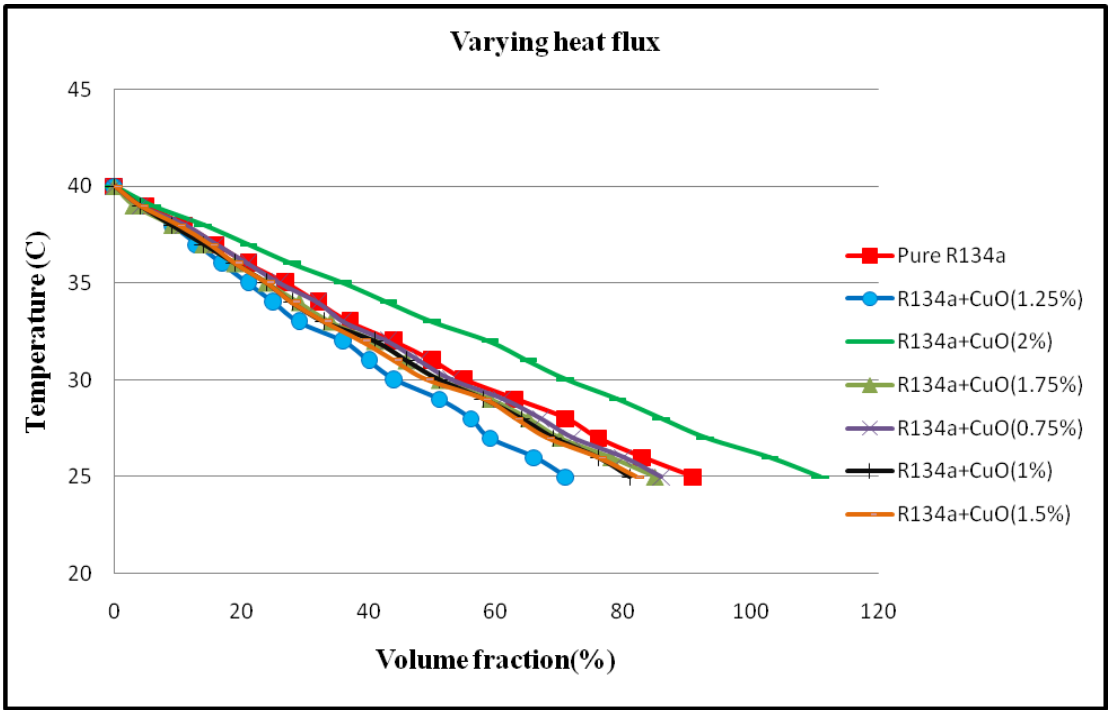

Figure 6.30: Temperature - Time chart for temperature drop (40-25°C) at mass flow rate 15 LPH

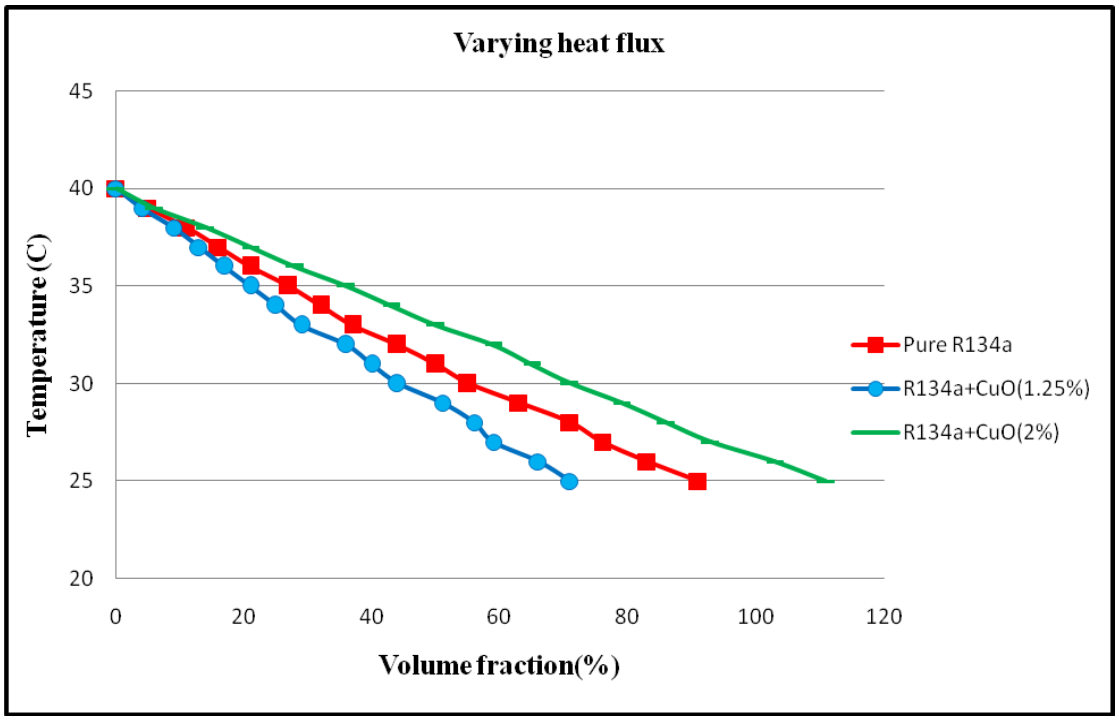

Figure 6.31: Max and Min Temperature - Time chart for mass flow rate of 15 LPH

The cooling load temperature – time history and the freezing capacity of nanorefrigerant (R134a+CuO) at mass flow rate 15 LPH is shown in Figures 6.27, 28, 29, 30 and 31. In all the

cases the condenser pressure is 2.5 bar and the evaporator pressure is 0.026 bar. No appreciable pressure drops is observed in the condenser and evaporator. From the figures it is clear that, the time required for reducing the cooling load temperature is less for nanorefrigerant (R134a+CuO) till 1.5% concentration of CuO in R134a. For example, for nanorefrigerant (R134a+CuO) with 0.25% concentration of nanoparticle, the time required to bring the cooling load temperature from 40-25°C is 90 minute where as for pure R134a it is 91 minute. It is clear that, the freezing capacity of the nanorefrigerant (R134a+CuO) is higher compared with pure refrigerant R134a. The time taken to reduce the temperature of the cooling load from 40- 25°C with increase volume fraction of CuO% in mixture is minimum (71 minute) at concentration of 1.25%. Also large time (111 minute) is taken at concentration of 2%. This is due to the fact the CuO nanoparticles present in the refrigerant enhances the heat transfer rate in the refrigerant side of the evaporator.

Effect of CuO nanoparticle on the freezing capacity (total time required) **of 15 LPH**

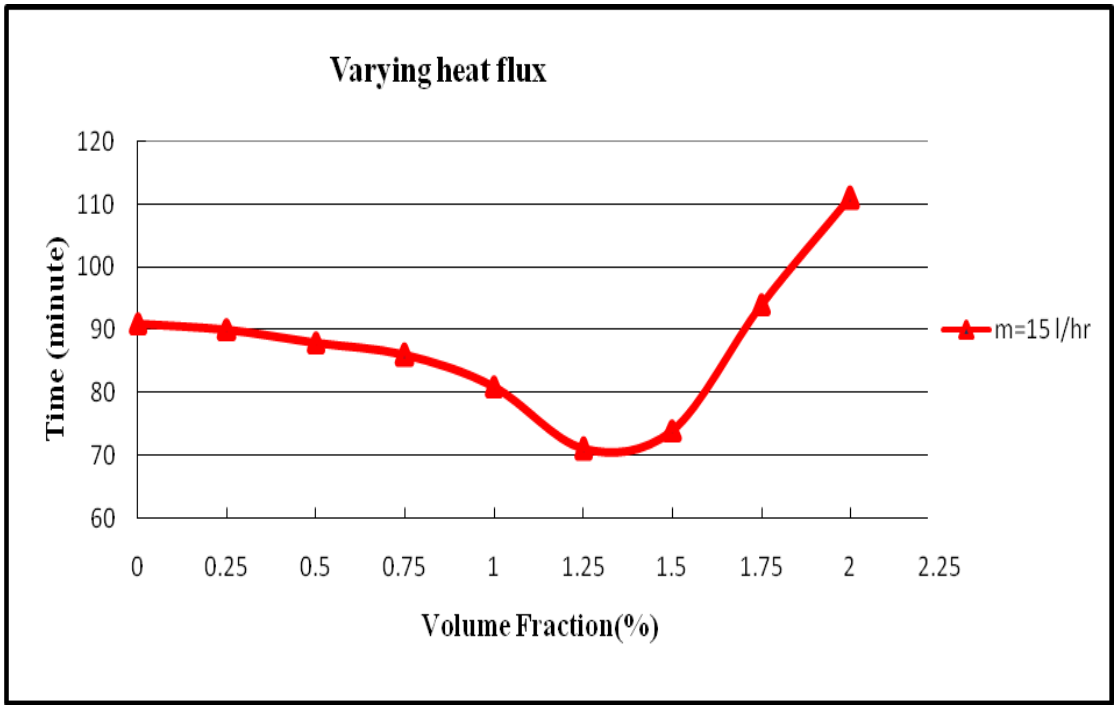

Figure 6.32: Evaporator freezing capacity, temperature drop (40-25°C) at mass flow rate 15 LPH

Figure 6.32 shows evaporator time taken for temperature drop (40-25°C) at mass flow rate 15 LPH. The time taken in minutes the effect concentration of CuO in refrigerant R134 on reduction time of pure refrigeration at mass flow rate 15 LPH to reduce the evaporator temperature from

(40-25°C), the time taken should be reduce with increase volume fraction till become maximum in concentration 1.25% is (71 minute) where time pure R134a is (91 minute) with reduction time percentage 21.97 % because of higher heat transfer for evaporator in refrigeration system.

Compressor power consumption for all concentration of CuO at 15 LPH

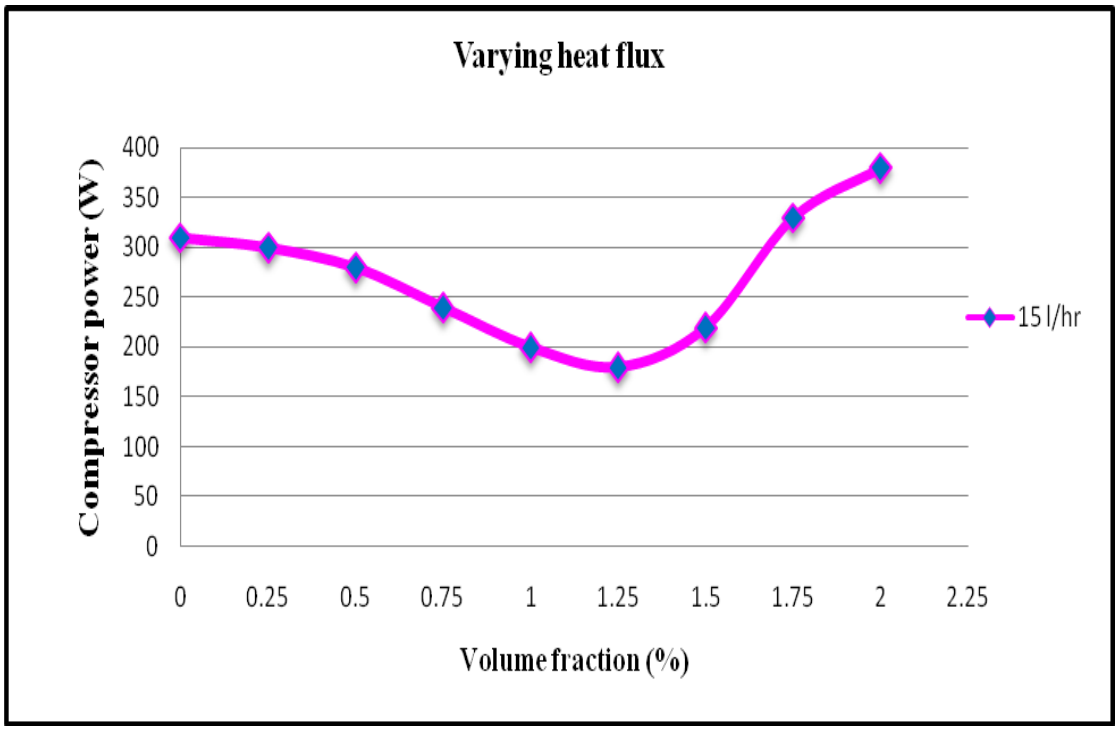

Figure 6.33: Compressor power consumption for temperature drop (40-25°C) at mass flow rate 15 LPH

Figure 6.33 shows compressor power consumption at varying cooling load and at mass flow rate of 15 LPH. It has been found decreasing with volume fraction of CuO in R134a refrigerant, and becomes minimum (180W) at volumetric concentration 1.25%. After this, power consumption of compressor increases and becomes maximum (380W) at 2% concentration.

Comparison the results and optimization of system at 15 LPH

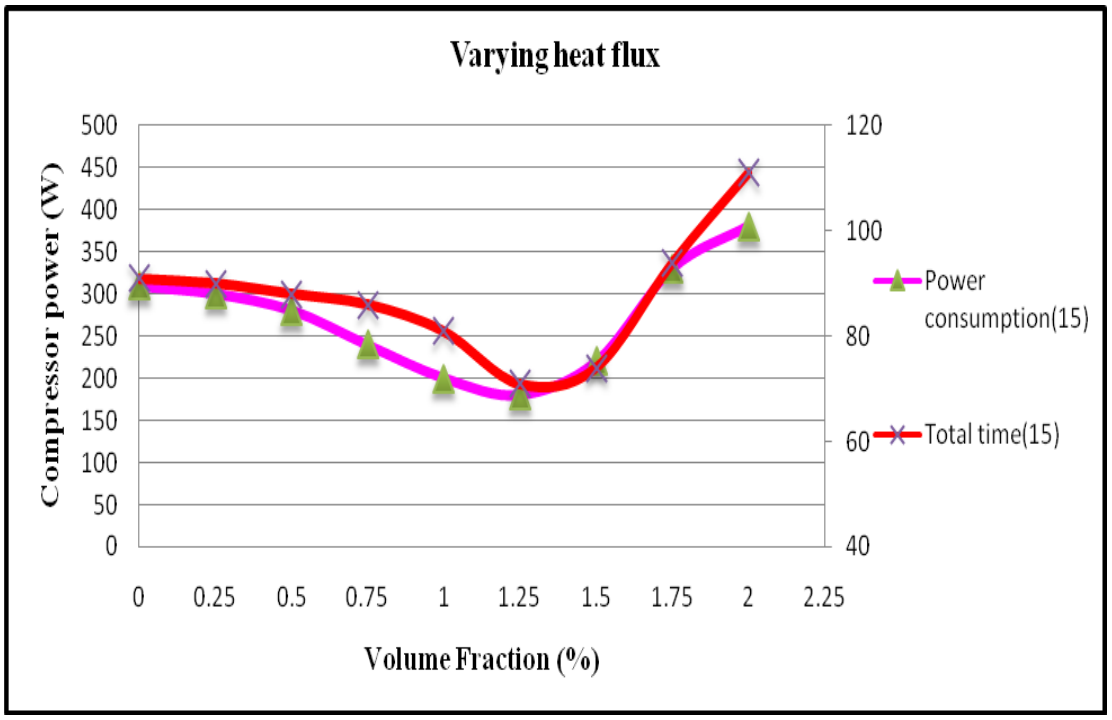

Figure 6.34: Comparison freezing capacity and power consumption at mass flow rate 15 LPH

Figure 6.34 shows the power consumption and freezing capacity of the nanorefrigerant (R134a +CuO) for the volume fraction form 0 to 2% at 15 LPH. This behavior is similar as what has been observed in case of mass flow rate of 10 LPH.

The power consumption of compressor which decreases with increase in volume fraction and becomes minimum (180W) at 1.25% concentration of CuO in refrigerant R134a (41% less than what is needed for pure refrigerant R134a). This value for pure refrigerant R134a is found to be 310W.

Time taken (in minutes) to bring down the temperature from 40°C to 25°C at mass flow rate of 15 LPH is 71 minute at 1.25% concentration of CuO in refrigerant R134a. This time taken is found to be 22% less than the time taken (91 minutes) for pure refrigerant R134a under same conditions.

6.2.3 Comparison the results (at varying evaporator temperature from 40-25°C)

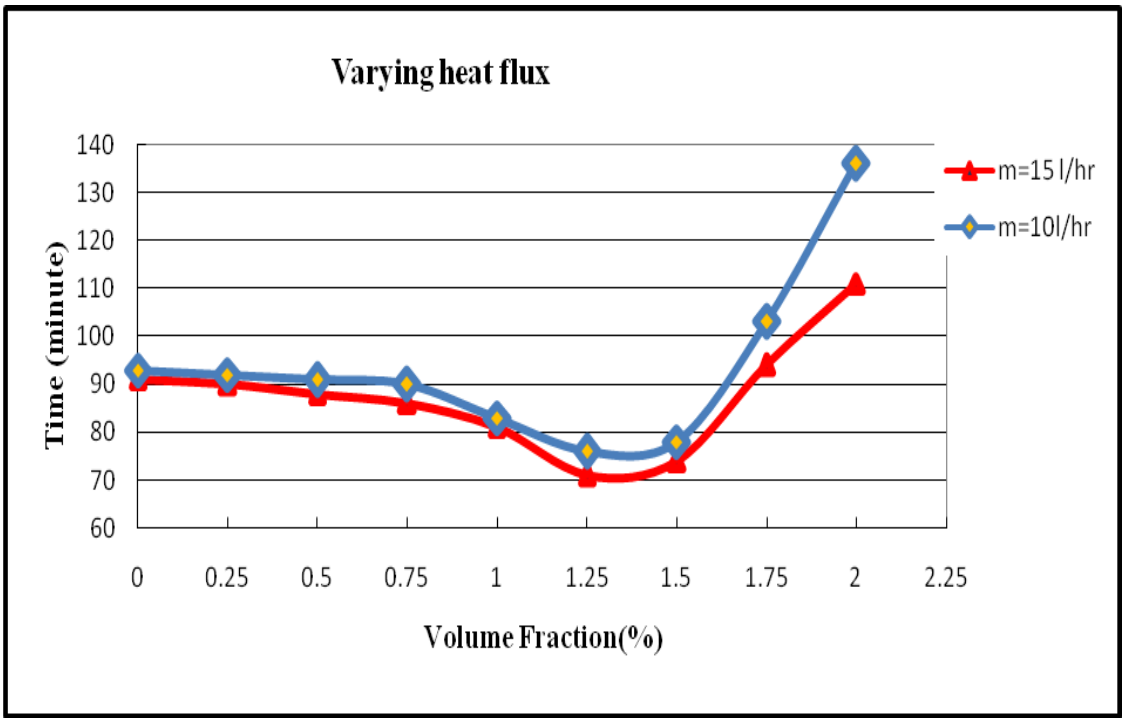

Figure 6.35: Comparison evaporator freezing capacity for temperature drop (40-25°C) at 15 LPH

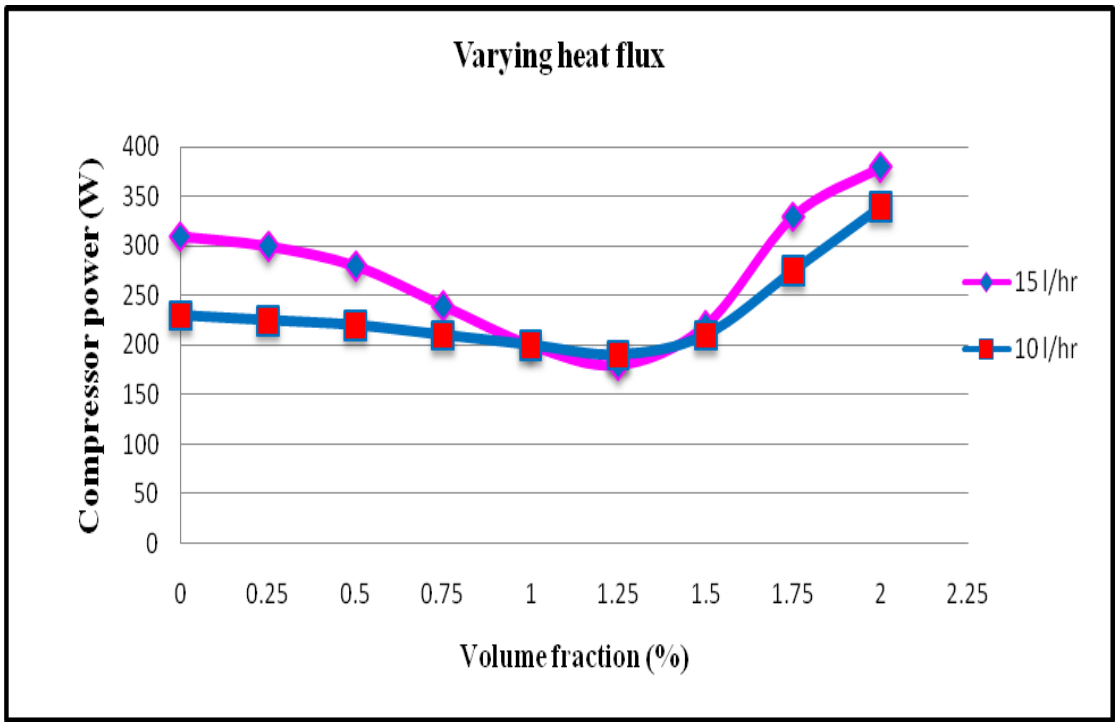

Figure 6.36: Comparison compressor power consumption at mass flow rates of 10&15 LPH

Figures 6.35 and 6.36 show the comparison of time of evaporator cooling load and power consumption of the compressor in both mass flow rates 10 and 15 LPH.

The percentage reduction in freezing capacity and power consumption are 18.27, 17.4% respectively for 10 LPH. While these are equal 22, 21% respectively for 15 LPH if the is concentration copper oxide mixed nanoparticles with refrigerant R134a. When compared with the other pure refrigerant R134a in both cases of mass flow rates and varying heat flux. The advantages of mixing nanoparticle with refrigerant are manifold. It reduces the power consumption of the compressor and there is sub cooling of the nanorefrigerant in the condenser which in turn increases and super heating in evaporator by absorbing heat gain.

6.3 Optimization of nanorefrigeration system and perfect concentration

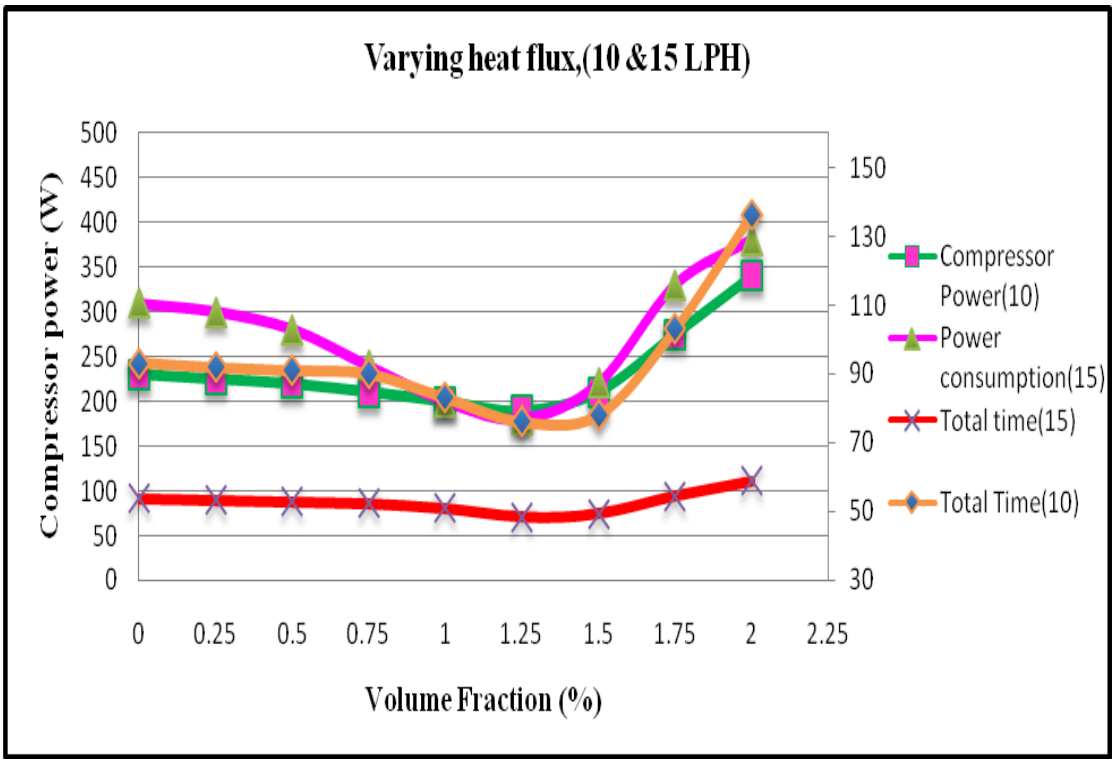

Figure 6.37: Comparison power consumption and freezing capacity at (10&15 LPH)

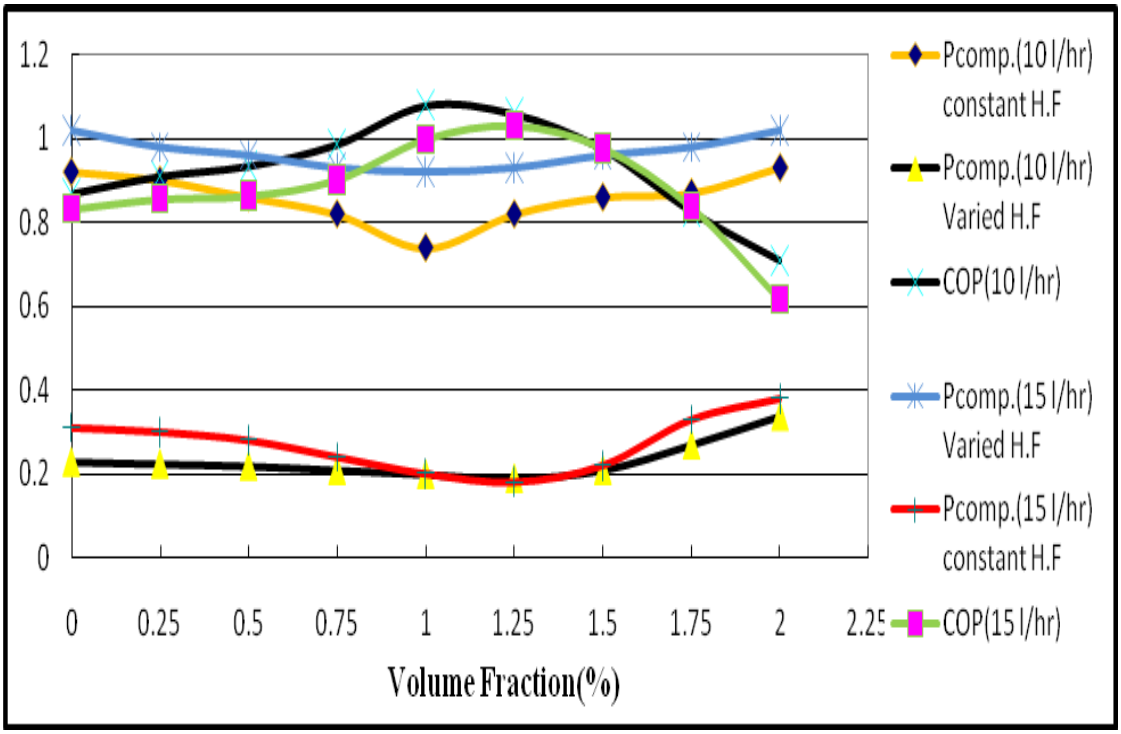

Figure 6.38: Comparison of power consumption and COP at heat flux and at different mass flow rates (10, 15 LPH)

Figure 6.37 and 6.38 show comparison the freezing capacity and power consumption at mass flow rate 10, 15 LPH, in cases of constant and varying heat flux in evaporator. Figures show that power consumption and freezing capacity at 1.25% volume fraction is minimum and recommended range of volume concentration for minimum power consumption is 1.25-1.5% at varying heat flux. It has been also found that the results of power consumption and COP of system minimum power consumption at constant heat flux condition lies in the range of 1 to 1.25% of volume fraction. Similarly, volume fraction range is from 1 to 1.25% for COP to be maximum at constant heat flux and 1.25 to 1.5% at varying heat flux. The freezing capacity at mass flow rates 10, 15 LPH that minimum time in same range of power consumption at (1.25%) volume fraction and recommended range of volume concentration for minimum freezing capacity is 1.25-1.5% at varying heat flux condition.

From the above discussion it has been cleared that for maximum COP and minimum power consumption the concentration of CuO in refrigerant R134a should be around 1.25%.

CHAPTER-7

CONCLUSION AND FUTURE SCOPE

7.1 Conclusions

1. In the refrigeration system, it is found that mixing of CuO nanoparticles with pure refrigerant R134a works normally.

2. Cooling capacity and COP of the system is found to be increasing with increase in concentration of CuO in refrigerant R134a till 1.5% concentration then decrease.

3. Extensive experimental studies have been conducted to evaluate the pressure and temperature drop in condenser and evaporator.

4. All investigated parameters found to be favorable with 0-1.5% of volume concentration of CuO in refrigerant R134a. Parameters show negative results when volume concentration of CuO is increased beyond 1.5%.

5. Maximum condenser pressure drop is 11.8% (1.42 kpa) at mass flow rate of 10 LPH and 10.9% (1.95 kpa) at 15 LPH at 1.5% concentration of CuO in refrigerant R134a compared to pure refrigerant R134a under constant heat flux condition (35-36^{o}C).

6. Minimum evaporator pressure drop is 10.3% (0.92 kpa) for 10 LPH and 18.5% (1.82 kpa) for 15 LPH at 2% concentration of CuO in refrigerant R134a compared to pure R134a refrigerant under constant heat flux condition (35-36^{o}C).

7. Maximum condenser temperature drop is 17.85% (7.54^{o}C) for 10 LPH and 19% (8.06^{o}C) for 15 LPH at 1% concentration of CuO in refrigerant R134a compared to pure refrigerant R134a under constant heat flux condition (35-36^{o}C).

8. Maximum evaporator temperature drop is 10.34% (4.27^{o}C) for 10 LPH and 13.6% (4.27^{o}C) for 15 LPH at 1% concentration of CuO in refrigerant R134a compared to pure R134a refrigerant under constant heat flux condition (35-36^{o}C).

9. Freezing capacity of the refrigeration system increases when nanorefrigerant (R134a + CuO) is used. Freezing capacity is maximum (increases by 18.27%) at 1.25%

concentration for 10 LPH and also at 15 LPH this is maximum (increases by 22%) at 1.25 % concentration of CuO in R134a.

10. The minimum power consumption of the compressor decreases by 13% for 10 LPH and 10% for 15 LPH at 1% volume concentration of CuO in refrigerant R134a at constant heat flux condition. The minimum power consumption of the compressor decreases by 21% for 10 LPH and 41% for 15 LPH at 1.25% volume concentration of CuO in R134a under varying heat flux.

11. The coefficient of performance of the refrigeration system increases by 19.3% for 15 LPH and 20% for 10 LPH at 1.25 volume concentration of CuO in R134a refrigerant when the nanorefrigerant is used instead of conventional pure refrigerant.

7.2 Challenges & future Scope

Based upon the experimental investigation for CuO-R134a nanofluid, it is proposed that the following areas may be considered for further investigations:

1.The nanofluid can be used as a nanorefrigerant in air conditioner and refrigerator.

2. There are number of refrigerants other than R134a can be used to investigate performance.

3. System can be tried for different flow rates, at different evaporator loads and boundary conditions in different concentrations and kinds of nanoparticles with shapes and sizes.

4. Nanorefrigerant results increase in oil viscosity and thermal conductivity which thereby also decreases the compressor and pumping power requirement and higher heat transfer.

5. There are other parameters like surfactants, pH value, sonication time, hybrid transformer oil etc. which also effect the performance of nanorefrigeration system, need to be investigated.

6. The theoretical study the performance of nanorefrigerant R134a is very limited and further investigation is required to predict more accurate behavior with nanorefrigerant R134a.

7. Development of new mechanisms and comparison of these models predications with experimental data will provide theoretical explanation the performance enhancement of nanorefrigerant R134a.

REFERENCES

Bobbo, S., (2010), Influence of nanoparticles dispersion in POE oils on lubricity and R134a solubility. *International Journal of Refrigeration*, Vol.33, pp. 1180-1186.

Bi, S., Shi L. and Zhang, L., (2007), Performance study of a domestic refrigerator using R134a/mineral oil/nano-TiO_2 as working fluid. *ICR07*-Issue2, pp.346.

Bi,S., Shi L. and Zhang L., (2008), Application of nanoparticles in domestic refrigerators. *Applied Thermal Engineering*, Vol. 28, pp.1834-1843.

Bi, S., Guo, K., Liu, Z., (2011), Performance of a domestic refrigerator using TiO_2-R600a nanorefrigerant as working fluid. *Energy Conversion and Management*, Vol. 52, pp. 733-737.

Brinkman, H.C., (1952). The viscosity of concentrated suspensions and solution. *The Journal of Chemical Physics*, Vol.20, pp. 571–581.

Baustian, J.J., Pate, M.B., Bergles, A.E., (1988), Measuring the concentration of a flowing oil–refrigerant mixture, *ASHRAE Transactions*, Vol. 94, No. 1, pp167–177.

Chandrasekar, M., Suresh, S., (2009), A review on the mechanisms of heat transport in Nanofluids, *Journal of Heat Transfer Eng*, Vol. 30, Issue 14, pp. 1136-1150.

Cheng, L.X., Bandarra, E.P., and Thome, J.R., (2008), Nanofluid two-phase flow and thermal physics: a new research frontier of nanotechnology and its challenges. *J Nanosci Nanotechnol* Vol. 8, Isse7, pp.3315-3332.

Choi, S. U. S., (1995), Developments and applications of non-Newtonian flows. Refrigeration Systems, *International Refrigeration and Air Conditioning Conference*. Paper 1145.

Changwei, P., Yong, T. K., (2012), Stability and Thermal Conductivity Characteristics of Nanofluids (H_2O/CH_3OH + NaCl + Al_2O_3 Nanoparticles) for CO_2 Absorption Application, *International Refrigeration and Air Conditioning Conference at Purdue*, pp. 216.

Eiyad, A.N., (2008), Application of nanofluids for heat transfer enhancement of separated flows encountered in a backward facing step, *International Journal of Heat and Fluid Flow* Vol.29, pp. 242–249.

Elena, V., Timofeeva, W., Yu, D.M., France, Singh, D., Jules, L., (2011), Nanofluids for heat transfer: an engineering approach Timofeeva et al. *Nanoscale Research Letters* Vol.6, pp.182.

Guo-liang, D., (2007), Recent developments in simulation techniques for vapour-compression refrigeration systems, *International Journal of Refrigeration*. Vol.30, pp.1119-1133.

Hao, P., (2010), Nucleate pool boiling heat transfer characteristics of refrigerant/oil mixture with diamond nanoparticles. *International Journal of Refrigeration*, Vol.33, pp. 347-358.

Henderson, L.,(2010), Experimental analysis on the flow boiling heat transfer of R134a based nanofluids in a horizontal tube. *IJHMT* , Vol. 53, pp. 944-951.

Hamilton, R.L., Crosser, O.K, (1962), Thermal conductivity of heterogeneous two-component systems. *Industrial and Engineering Chemistry Fundamentals*, Vol. 1, Issue 3, pp. 187–191.

Jensen, M.K., Jackman, D.L., (1984), Prediction of nucleate pool boiling heat transfer coefficients of refrigerant–oil mixtures. *Journal of Heat Transfer*, Vol. 106, pp. 184–190.

Jwo, (2009), Effect of nano lubricant on the performance of Hydrocarbon refrigerant system. *J. Vac. Sci. Techno. B*, Vol.27, Issue 3, pp. 1473-1477.

Juan, C. V., Frank, C., José, A., (2010), A Numerical Study on the Application of Nanofluids in Refrigeration Systems, *International Refrigeration and Air Conditioning Conference at Purdue*, pp.2495.

José, A.R., Ricardo, F.P.T., (2012) , A Simulation Model for the Application of Nanofluids as Condenser Coolants in Vapor Compression Heat Pumps, *International Refrigeration and Air Conditioning Conference at Purdue*, pp.2531.

Kabelac, S., Kuhnke, J.F., (2006), Heat transfer mechanisms in Nanofluids--experiments and theory. *Annals of the Assembly for International Heat Transfer Conference* ,Vol.13.

Kristen, H.,(2010), Flow boiling heat transfer of R134a based nanofluids in a horizontal tube. *IJHMT*, Vol.53, pp 944-951.

Kedzierski, M.A., Kaul, M.P., (1993), Horizontal nucleate flow boiling heat transfer coefficient measurements and visual observations for R12, R134a, and R134a/ester lubricant mixtures. In: Proceedings of the 6th *International Symposium on Transport Phenomena in Thermal Engineering*, Vol. 1, pp. 111–116.

Kumar, D., Elansezhian , R., (2012), Experimental Study on Al_2O_3-R134a Nanorefrigerant in Refrigeration System, *International Journal of Modern Engineering Research*, Vol. 2, Issue. 5, pp-3927-3929.

Li, Y.J., Zhou, J.E., Tung, S., Schneider, E., Xi, S.Q., (2009), A review on development of nanofluid preparation and characterization, *Powder Technology*, Vol.196, Issue 2, pp. 89-101.

Lixin, C., Lei, L., (2013), Boiling and two-phase flow phenomena of refrigerant-based nanofluids: Fundamentals, applications and challenges, *International Journal of Refrigeration* Vol.36, pp.421-446.

Lixin, C., (2009), Nanofluid Heat Transfer Technologies, *Recent Patents on Engineering*, Vol.3, Issue 13.

Lee, K., Hwang, Y.J., Cheong, S., Kwon, L., Kim, S., Lee, J.,(2009), Performance evaluation of nano-lubricants of fullerene nanoparticles in refrigeration mineral oil. *Curr Appl Phys*. Vol.9, pp.128–31.

Murshed, S.M.S., Leong, K.C., Yang, C.,(2008), Thermophysical and electrokinetic properties of Nanofluids, critical review. *Application Thermal Engineering* ,Vol. 28,Issue17-18,pp.2109-2125.

Mahbubul, I.M., Saidur, R., (2012), Investigation of viscosity of R123-TIO_2 nanorefrigerant, International Journal of Mechanical and Materials Engineering , Vol. 7, Issue 2,pp. 146-151.

Navid, B., Komalangan, K., Nariman, B., (2012), Numerical Study on Application of CuO-Water Nanofluid in Automotive Diesel Engine Radiator, *Modern Mechanical Engineering*, Vol. 2, pp-130-136.

Ozerinc, S., Kakac, S., Yazicioglu, A.G., (2010), Enhanced thermal conductivity of nanofluids: a state of the art review, *Journal of Microfluid* Nanofluid, Vol. 8, Issue 2, pp.145-170.

Prasher, R., Song, D., Wang, J.L., Phelan, P.,(2006), Measurements of nanofluid viscosity and its implications for thermal applications. *Appl Phys Lett* , Vol. 89, pp.133108-133110.

Pawel, K.P., Jeffrey, A.E. and David, G.C., (2005), Nanofluids for thermal transport, *Materials Today*, pp. 36-44.

Peng, H., Ding, G., Haitao, H.,(2011), Influences of refrigerant-based nanofluid composition and heating condition on the migration of nanoparticles during pool boiling. Part I: Experimental measurement, *International Journal of Refrigeration*, Vol.34, pp.1823-1832.

Pak, B.C., Cho, Y.I., (1998), Hydrodynamic and heat transfer study of dispersed fluids with submicron metallic oxide particles. *Experimental Heat Transfer*, Vol. 11, Issue 2, pp. 151–170.

R. Reji Kumar ,K. Sridhar , M. Narasimha, (2010), Heat transfer enhancement in domestic refrigerator using R600a/mineral oil/nano-Al_2O_3 as working fluid, *International Journal of Computational Engineering*, Vol. 03,Issue 4.

Subramani, N.,., Prakash, M.J., (2011), Experimental studies on a vapour compression system using nanorefrigerants, *International Journal of Engineering, Science and Technology*, Vol.3, Issue 9, pp. 95-102.

Serdar, C., Sainath, N., Karthik, B.,(2010), Experimental Analysis of a Stirling Refrigerator Employing Jet Impingement Heat Exchanger and Nanofluids, *International Refrigeration and Air Conditioning Conference at Purdue*, pp- 2334.

Singh, E., Timofeeva, W. ,Yu, J., Routbort, D., France, D. and Cepero, J.M., (2009), An investigation of silicon carbide-water nanofluid for heat transfer applications, *Journal of Applied Physics vol*. 105, pp.64306.

Shengshan, B., (2011), Performance of a Domestic Refrigerator using TiO_2-R600a nano-refrigerant as working fluid, *Int J of Energy Conservation and Management*, Vol. 52,pp.733-737.
Yu, W., France, D.M., Routbort, J.L., and Choi, S.U.S.,(2008), Review and comparison of nanofluid thermal conductivity and heat transfer enhancements. Heat *Transfer Engineering*, Vol.29, Issue5, pp.432-460.

Trisaksri, V., Wongwises, S.,(2007), Critical review of heat transfer characteristics of Nanofluids. *Renew Sustain Energy Rev* , Vol. 11, Issue3, pp.512-523.

Yu, W., France, D.M., Timofeeva, E.V., Singh, D., Routbort, J.L., (2010), Thermo-physical property-related comparison criteria for nanofluid heat transfer enhancement in turbulent flow. *Application Physical Lett* ,Vol. 96, pp.213-1093.

Wen, D.S., Lin, G.P., Vafaei, S., Zhang, K.,(2009), Review of Nanofluids for heat transfer applications. Particuology ,Vol. 7, Issue2, pp.141-150.

Wang, X.Q., Mujumdar, A.S.,(2007), Heat transfer characteristics of Nanofluids: a review. *Int J Thermal Scinice* ,Vol. 46, Issue1, pp.1-19.

ANNEXTURE-I

Cost Estimation of components and parts of setup system:

S. No.	Description of Item	Qty	specification	Cost
1	CuO Nanopowder	10gm	20µm	4000
2	Copper pipe	9 meter	¼ Inch	750
3	Soldering material			100
4	Voltmeter	1		100
5	Compressor	1	165 Liter compressor	2500
6	Condenser	1	Tube& fin type for 165 Liter compressor	500
7	Filter	1		50
9	Rota meter	1		4050
10	Expansion Valve	1	Hand operated for 165 Liter compressor	500
11	Evaporator	7.5 meter	¼ inch	650
12	Heater	1	2000 watt	300
13	Rubber pipe	1	20 feet	100
14	Digital Temp. Controller	1		1000
15	Refrigerant charging line	1		300
16	Pressure gauge	1		500
17	Energy meter	2		Lab
18	Main switch	1		500
19	Refrigerant	1500gm	R134a	1200
20	Wiring			500
21	Lubricating Oil	1litre		500
22	Beaker	3(500ml)		500
23	Test Tubes	5		200
24	Board	1		3000
25	Insulation			200
26	valve	6		2000
27	Acetylene gas Cylinder	1		200
28	Flare nut	15	41278	400
29	T and Clamps	15	¼ inch	Lab
30	Nut and Bolt	20		200
31	Stainless Steel Drum	1		600
32	Ampere Meter	1		Lab
33	Miscellaneous			2000
	Total cost (Rs)			27400

ANNEXTURE-II

Constant Heat Flux (Constant Temperature of Evaporator): at (35-36°C)
1-Mass flow rate: 10 LHP
1-Pressure drop in Condenser and Evaporator

Heat Flux Constant	(35-36°C)	Pressure drop in Condenser		
Mass flow rate	10 LPH			
	Concentration	Pr inlet Condenser	Pr outlet Condenser	Δ Pr in Condenser
Pure R134a	0	227.08	215.24	11.84
R134a+CuO(0.25gm)	0.25	231.95	219.68	12.27
R134a+CuO(0.5gm)	0.5	231.11	218.4	12.71
R134a+CuO(0.75gm)	0.75	225.34	212.32	13.02
R134a+CuO(1gm)	1	228.07	214.8	13.27
R134a+CuO(1.25gm)	1.25	236.07	222.68	13.39
R134a+CuO(1.5gm)	1.5	241.15	227.72	13.43
R134a+CuO(1.75gm)	1.75	234.31	220.92	13.39
R134a+CuO(2gm)	2	244.24	230.98	13.26

Heat Flux Constant	(35-36°C)	Pressure drop in Evaporator		
Mass flow rate	10 LPH			
	Concentration	Pr inlet Evaporator	Pr outlet Evaporator	Δ Pr in Evaporator
Pure R134a	0	27.52	18.6	8.92
R134a+CuO(0.25gm)	0.25	27.28	18.64	8.64
R134a+CuO(0.5gm)	0.5	26.23	17.76	8.47
R134a+CuO(0.75gm)	0.75	25.34	17	8.34
R134a+CuO(1gm)	1	24.18	15.96	8.22

R134a+CuO(1.25gm)	1.25	26.02	17.88	8.14
R134a+CuO(1.5gm)	1.5	25.57	17.48	8.09
R134a+CuO(1.75gm)	1.75	25.68	17.64	8.04
R134a+CuO(2gm)	2	25.16	17.16	8

2-Temperature drop in Condenser and Evaporator

Heat Flux Constant	**(35-36˚C)**	**Temperature drop in Condenser**		
Mass flow rate	**10 LPH**			
	Concentration	Temp inlet Condenser	Temp outlet Condenser	∆ T in Condenser
Pure R134a	0	87.68	52.98	34.7
R134a+CuO(0.25gm)	0.25	87.44	52.2	35.24
R134a+CuO(0.5gm)	0.5	87.8	51.66	36.14
R134a+CuO(0.75gm)	0.75	87.02	50.94	39.03
R134a+CuO(1gm)	1	82.98	40.74	42.24
R134a+CuO(1.25gm)	1.25	83.86	42	41.86
R134a+CuO(1.5gm)	1.5	86.28	45.8	40.48
R134a+CuO(1.75gm)	1.75	86.98	46.6	40.38
R134a+CuO(2gm)	2	87.88	46.52	41.36

Heat Flux Constant	(35-36°C)	Temperature drop gain in Evaporator		
Mass flow rate	10 LPH			
	Concentration	Temp. outlet Evaporator	Temp. inlet Evaporator	∆ T in Evaporator
Pure R134a	0	33.2	1.03	32.17
R134a+CuO(0.25gm)	0.25	32.96	-0.18	32.78
R134a+CuO(0.5gm)	0.5	32.02	-1.52	33.52
R134a+CuO(0.75gm)	0.75	32.56	-2.02	34.58
R134a+CuO(1gm)	1	29.8	-5.84	35.64
R134a+CuO(1.25gm)	1.25	32	-3.88	35.88
R134a+CuO(1.5gm)	1.5	31	-3.92	35
R134a+CuO(1.75gm)	1.75	31.96	-3.62	35.58
R134a+CuO(2gm)	2	32	-4.44	36.44

3-Power consumption and COP.

Heat Flux Constant	(35-36°C)	Power consumption in Compressor and Heater		
Mass flow rate	10 LPH			
	Concentration	E consumption in Compressor	E consumption in Heater	C.O.P
Pure R134a	0	920	800	0.86956
R134a+CuO(0.25gm)	0.25	900	820	0.91111
R134a+CuO(0.5gm)	0.5	860	805	0.93604
R134a+CuO(0.75gm)	0.75	820	810	0.9878
R134a+CuO(1gm)	1	740	800	1.08108
R134a+CuO(1.25gm)	1.25	820	870	1.06097

R134a+CuO(1.5gm)	1.5	860	840	0.976744
R134a+CuO(1.75gm)	1.75	870	720	0.82758
R134a+CuO(2gm)	2	930	660	0.70967

2-Mass flow rate:15 LPH

1-Pressure drop in Condenser and Evaporator

Heat Flux Constant	**(35-36°C)**	**Pressure drop in Condenser**		
Mass flow rate	**15 LPH**			
	Concentration	Pr inlet Condenser	Pr outlet Condenser	∆ Pr in Condenser
Pure R134a	0	232.57	219.68	12.89
R134a+CuO(0.25gm)	0.25	237.92	224.6	13.32
R134a+CuO(0.5gm)	0.5	226.56	212.8	13.76
R134a+CuO(0.75gm)	0.75	216.11	202.04	14.07
R134a+CuO(1gm)	1	234	219.68	14.32
R134a+CuO(1.25gm)	1.25	245.56	231.12	14.44
R134a+CuO(1.5gm)	1.5	243.12	228.64	14.48
R134a+CuO(1.75gm)	1.75	240.36	225.92	14.44
R134a+CuO(2gm)	2	246.8	232.6	14.2

Heat Flux Constant	**(35-36°C)**	**Pressure drop in Evaporator**		
Mass flow rate	**15 LPH**			
	Concentration	Pr inlet Evaporator	Pr outlet Evaporator	∆ Pr in Evaporator
Pure R134a	0	34.84	25.02	9.82
R134a+CuO(0.25gm)	0.25	35.4	25.88	9.52

R134a+CuO(0.5gm)	0.5	33.94	24.8	9.14
R134a+CuO(0.75gm)	0.75	32.84	24	8.78
R134a+CuO(1gm)	1	33.4	25.02	8.42
R134a+CuO(1.25gm)	1.25	34.76	26.76	8.15
R134a+CuO(1.5gm)	1.5	33.84	25.88	7.94
R134a+CuO(1.75gm)	1.75	33	25.11	7.89
R134a+CuO(2gm)	2	33.8	25.8	8

2-Temperature drop in Condenser and Evaporator

Heat Flux Constant	**(35-36°C)**	**Temperature drop in Condenser**		
Mass flow rate	**15 LPH**			
	Concentration	Temp inlet Condenser	Temp outlet Condenser	∆ T in Condenser
Pure R134a	0	88.92	54.74	34.18
R134a+CuO(0.25gm)	0.25	86.04	50.41	35.63
R134a+CuO(0.5gm)	0.5	85.16	51.8	36.82
R134a+CuO(0.75gm)	0.75	85.32	45.79	39.53
R134a+CuO(1gm)	1	85.92	43.6	42.24
R134a+CuO(1.25gm)	1.25	88	47.92	41.86
R134a+CuO(1.5gm)	1.5	87.12	47.64	40.48
R134a+CuO(1.75gm)	1.75	90.12	49.24	40.88
R134a+CuO(2gm)	2	90.8	48	41.36

Heat Flux Constant	(35-36°C)	Temperature drop gain in Evaporator		
Mass flow rate	15 LPH			
	Concentration	Temp. outlet Evaporator	Temp. inlet Evaporator	∆ T in Evaporator
Pure R134a	0	32.94	5.27	27.67
R134a+CuO(0.25gm)	0.25	32.86	4.88	27.98
R134a+CuO(0.5gm)	0.5	32.74	3.72	29.02
R134a+CuO(0.75gm)	0.75	31.04	1.96	30.08
R134a+CuO(1gm)	1	30.94	-0.2	31.14
R134a+CuO(1.25gm)	1.25	32	0.62	31.38
R134a+CuO(1.5gm)	1.5	31.84	1.34	30.5
R134a+CuO(1.75gm)	1.75	32.88	1.8	31.08
R134a+CuO(2gm)	2	33	1.06	31.94

3-Power consumption and COP.

Heat Flux Constant	(35-36°C)	Power consumption in Comperassor and Heater		
Mass flow rate	15 LPH			
	Concentration	E consumption in Compressor	E consumption in Heater	C.O.P
Pure R134a	0	1020	850	0.83333
R134a+CuO(0.25gm)	0.25	980	840	0.85714
R134a+CuO(0.5gm)	0.5	960	830	0.86458
R134a+CuO(0.75gm)	0.75	930	840	0.903225
R134a+CuO(1gm)	1	920	920	1
R134a+CuO(1.25gm)	1.25	930	960	1.032258
R134a+CuO(1.5gm)	1.5	960	940	0.979166

R134a+CuO(1.75gm)	1.75	930	780	0.838709
R134a+CuO(2gm)	2	1020	630	0.617647

ANNEXTURE-II

Heat Flux varied range(40-25℃) varied Temperature of Evaporator): 40-25℃
1-Mass flow rate:10 LPH
1- Time history in Evaporator.

Time Taken (minutes)	40	39	38	37	36	35	34	33
Pure R134a	0	5	11	16	21	27	32	37
R134a+CuO(0.25gm)	0	5	11	16	21	27	32	37
R134a+CuO(0.5gm)	0	5	11	16	21	27	32	37
R134a+CuO(0.75gm)	0	4	11	16	21	26	31	37
R134a+CuO(1gm)	0	3	9	14	19	24	29	35
R134a+CuO(1.25gm)	0	3	9	11	16	21	26	31
R134a+CuO(1.5gm)	0	3	9	14	19	24	28	33
R134a+CuO(1.75gm)	0	5	13	20	25	31	37	43
R134a+CuO(2gm)	0	6	15	22	29	36	43	51
Time Taken (minutes)	32	31	30	29	28	27	26	25
Pure R134a	44	50	55	63	71	76	84	93
R134a+CuO(0.25gm)	44	50	55	63	71	76	84	92
R134a+CuO(0.5gm)	44	50	55	63	71	76	83	91
R134a+CuO(0.75gm)	44	50	57	65	71	77	84	90
R134a+CuO(1gm)	43	49	54	62	68	75	83	89
R134a+CuO(1.25gm)	39	44	49	57	62	67	75	80

R134a+CuO(1.5gm)	39	44	49	56	61	66	74	78
R134a+CuO(1.75gm)	48	52	64	73	80	87	96	103
R134a+CuO(2gm)	63	71	79	92	102	111	126	136

2- Total time required for all concentration CuO.

Time Taken (minutes)	Total time
Pure R134a	93
R134a+CuO(0.25gm)	92
R134a+CuO(0.5gm)	91
R134a+CuO(0.75gm)	90
R134a+CuO(1gm)	89
R134a+CuO(1.25gm)	80
R134a+CuO(1.5gm)	78
R134a+CuO(1.75gm)	103
R134a+CuO(2gm)	136

3-P ower consumption for all Concentration CuO.

Total Time taken for variation Heat Flux (40-25°C) and Power consumption by Compressor									
mass flow rate	**10 LPH**								
R134a + CuO (gm)	0	0.25	0.5	0.75	1	1.25	1.5	1.75	2
Time Taken (minutes)	93	92	91	90	83	76	78	103	136
Power consumption	230	225	220	210	200	190	210	275	340

2-Mass flow rate:15 LPH

1- Time history in Evaporator

Time Taken (minutes)	40	39	38	37	36	35	34	33
Pure R134a	0	5	11	16	21	27	32	37
R134a+CuO(0.25gm)	0	4	11	16	21	26	31	37
R134a+CuO(0.5gm)	0	3	9	14	19	24	29	35
R134a+CuO(0.75gm)	0	4	11	16	21	26	32	36
R134a+CuO(1gm)	0	4	9	14	19	24	28	33
R134a+CuO(1.25gm)	0	4	9	13	17	21	25	29
R134a+CuO(1.5gm)	0	4	10	15	19	24	28	33
R134a+CuO(1.75gm)	0	3	9	14	19	24	29	34
R134a+CuO(2gm)	0	6	14	21	28	36	43	50
Time Taken (minutes)	32	31	30	29	28	27	26	25
Pure R134a	44	50	55	63	71	76	83	91
R134a+CuO(0.25gm)	44	50	57	65	71	77	84	90
R134a+CuO(0.5gm)	43	49	54	62	68	75	83	88
R134a+CuO(0.75gm)	43	48	53	61	67	72	80	86
R134a+CuO(1gm)	41	46	51	58	64	69	76	81
R134a+CuO(1.25gm)	36	40	44	51	56	59	60	71
R134a+CuO(1.5gm)	39	44	49	58	63	68	76	82
R134a+CuO(1.75gm)	41	46	51	59	65	70	78	85
R134a+CuO(2gm)	59	65	71	79	86	93	103	111

2- Total time required for all concentration CuO.

	Total Time
Pure R134a	91
R134a+CuO(0.25gm)	90
R134a+CuO(0.5gm)	88
R134a+CuO(0.75gm)	86
R134a+CuO(1gm)	81
R134a+CuO(1.25gm)	71
R134a+CuO(1.5gm)	82
R134a+CuO(1.75gm)	85
R134a+CuO(2gm)	111

3-P ower consumption for all Concentration CuO.

Total Time taken for variation Heat Flux (40-25°C) and Power consumption									
mass flow rate	**15 LPH**								
R134a + CuO (gm)	0	0.25	0.5	0.75	1	1.25	1.5	1.75	2
Time Taken (minutes)	91	90	88	86	81	71	74	94	111
Power consumption	310	300	280	240	200	180	220	330	380

3-Compare the Total time Required and Power consumption for mass flow rate (10,15) LPH

Volume Fraction(R134a+CuO%)	0	0.25	0.5	0.75	1	1.25	1.5	1.75	2
Total Time (10 LPH)	93	92	91	90	83	76	78	103	136
Power consumption(10 LPH)	230	225	220	210	200	190	210	275	340
Total Time (15 LPH)	91	90	88	86	81	71	74	94	111
Power consumption(15 LPH)	310	300	280	240	200	180	220	330	380